AN ABSTRACT OF THE THESIS OF

Gary J. DeJong for the Doctor of Philosophy

in Chemistry presented on July 27, 1973

Title: High Intensity Pulsed Hollow Cathode Lamps

Redacted for privacy

Abstract approved:

Edward H. Piepmeier

Time-resolved, line emission wavelength profiles were obtained for a pulsed hollow cathode lamp and a special arc-glow lamp with the use of a piezoelectrically driven interferometer. A computer was used to control the sweep of the interferometer, the pulsing of the source and the acquisition of data. Minor manipulation of the data stored in core facilitated the presentation of intensity vs wavelength emission profiles in a time resolved form. Ten sequential line profiles, each covering 21 μseconds of time, were obtained for the pulsed sources.

This system was used to study a commercial copper hollow cathode lamp driven at 100 Hz with pulse currents of up to 400 mA. Pulses lasted for up to 300 μseconds. Line profiles showed extreme self-reversal of the resonance emission lines after 100 μseconds of time. Variations of line profile with dc background current level and spatial position within the discharge were also investigated. Line widths during the first 21 μseconds of the discharge ranged from 0.0012 nm to 0.0022 nm.

A unique type of capillary bore cathode was also studied. This

bore formed an arc-glow discharge under pulsing conditions similar to those used for the commercial lamp. Pressures ranged from 15 to 26 Torr. The arc-glow was found to enhance both the integrated line intensity and the line profile of the Cu resonance lines when compared to the commercial lamp in the pulsed mode. Line widths in the first 21 μseconds ranged from 0.0012 to 0.0025 nm.

HIGH INTENSITY PULSED HOLLOW CATHODE LAMPS

by

Gary Joel DeJong

A THESIS

submitted to

Oregon State University

in partial fulfillment of

the requirements for the

degree of

Doctor of Philosophy

June 1974

APPROVED:

Redacted for privacy

Associate Professor of Chemistry
in charge of major

Redacted for privacy

Head of Department of Chemistry

Redacted for privacy

Dean of Graduate School

Date thesis is presented July 27, 1973

Typed by Neita DeJong for Gary Joel DeJong

ACKNOWLEDGMENTS

I would like to express my appreciation to Ed Piepmeier for his helpful suggestions during both the research and the writing of this thesis.

I would especially like to thank my loving wife, Neita, for supporting us during the last six years, both financially and emotionally, and my daughter, Amity, for giving me the impetus to put this all together.

TABLE OF CONTENTS

HIGH INTENSITY PULSED HOLLOW-CATHODE LAMPS

Introduction

For many years the hollow cathode emission lamp run at 5-20 mA dc currents has been used as the primary source of atomic line radiation for analytical atomic absorption measurements. Under these conditions the hollow cathode lamp emits line radiation at moderate intensities and narrow line widths on the order of 0.001-0.002 nm (3). The relatively low level of line intensity becomes a problem for atomic absorption measurements in those instances where the absorbance is high, and also when the absorption measurement is made in a very short time span (tens of μseconds) at which point photon shot noise becomes the limiting factor. Both of these handicaps may be minimized with a line source having a line intensity decades greater than the commonly used hollow cathode lamp. Atomic fluorescence, a second form of observing atomic populations, would also benefit greatly from increases in intensities of atomic line emission sources. Research in this area has led to the development and use of microwave discharge lamps (electrodeless discharge lamps), hollow cathode lamps using an auxiliary discharge designed by Walsh (16) and also to the use of an ordinary hollow cathode lamp pulsed at high currents (50-500 mA) for short periods of time (50 μsec - 5 msec) at various pulse rates (10-300 Hz). Dawson and Ellis (8) reported gains for pulsed lamps ranging from 50 to 300 times that of the dc level lamp for various elements. These lamps were pulsed at 300 Hz with on times of 10-40 μsec at currents of up to 600 mA. Prugger, et al. (15) found that a calcium lamp pulsed at

600 mA for 150 μsec showed, using a tilting etalon, little or no self-reversal in the line profile except at power dissipations exceeding those found in normal dc operation. Cordos and Malmstadt (5) reported an increase in relative line intensity of the resonance line for several commercial lamps by the use of an intermittant mode, in which the lamp is pulsed for 10 msec at up to 200 mA for perhaps 20 pulses, with an off time of 100 msec between pulses, ending with a pause of several seconds before resuming the pulsed sequence. This and several other pulsing schemes (12,13) have been used in atomic fluorescence instrumentation because of the increased sample irradiance available. Cordos and Malmstadt also report that the emission line profile apparently shows no self-reversal and based this conclusion on data showing a linearly increasing line intensity with increasing pulse current. Self absorption and reversal is known to be one cause of a nonlinear relationship between intensity and concentration in flame photometry. However, as the results presented in this thesis show, it does not necessarily follow that a linear relationship between intensity and pulse current proves the absence of self absorption or reversal in a hollow cathode lamp where large concentration and temperature gradients exist.

Observation of the line profile may be accomplished by the use of a Fabry-Perot interferometer. A pressure scanning interferometer was used by Davies (7) to study the emission line profile of the copper resonance line doublet at 324.7 nm using an auxiliary discharge type hollow cathode designed by Walsh (16). Davies reported that the

increase in line intensity is accompanied by a significant decrease in self-reversal of the resonance line compared to a normal discharge lamp without the auxiliary electrodes. Bruce and Hannaford (3) used a variable gap Fabry-Perot interferometer to measure the half-width of a calcium hollow cathode lamp at various dc current levels and reported line widths from 0.0092 Å to 0.0154 Å for currents from 5-15 mAdc. In 1963 Cooper and Greig (4) described a Fabry-Perot interferometer capable of rapid scanning (10 μsec) by mounting one of the quartz flats on a piezoelectric ceramic tube and changing the spacing between the mirrors by applying a potential to the tube. A similar instrument allowed Kirkbright and Sargent to observe the thallium 377.6 nm hyperfine structure from a hollow cathode lamp (9) and to also measure the atomic line half-width of the calcium atoms excited in a flame.

For atomic absorption measurements the emission line from the primary source should be considerably narrower than the absorption line width for best results. Yasuda (19) has shown a decrease in calcium absorbance in a flame due to self-reversal of the resonance line in the hollow cathode lamp, affecting both the slope and the linearity of the calibration curve. Extreme self-reversal could also cause a decrease in the expected fluorescence emission in an atomic fluorescence analysis using a pulsed hollow cathode. This study was conducted in an effort to see to what extent these phenomena occur in a pulsed lamp for pulsed sources such as laser plumes, and to determine how results might be improved.

Time-resolved line profiles have not been obtained for a pulsed hollow cathode lamp. These profiles would be important for analytical

work involving such a pulsed emission source. Changes in the line shape with time could cause discrepancies in the analytical calibration curve if great care is not taken to make the measurement at the same point in time on each pulse. Also, any attempt to study variations within an atomic reservoir with time using the pulsed lamp could be greatly distorted by changes in the line shape emitted from the hollow cathode lamp.

A commercial piezoelectrically driven Fabry-Perot interferometer was used by this author in conjunction with a PDP-11/20 minicomputer for time resolved studies of a pulsed hollow cathode lamp. Both commercial and demountable lamps were pulsed at 100 Hz with currents of up to 400 mA and pulse durations of 300 μseconds.

Experimental

Accurate measurement of an intensity vs wavelength profile of an atomic spectral line is possible only if the spectral bandwidth of the measuring instrument is negligible with respect to the half-width of the intensity profile. Large spectrographs can be used to observe line profiles when used in high orders but are usually limited both in the resolution obtained and in the low level of light resulting from the use of the high orders. A second and increasingly popular method of profile measurement is the use of a Fabry-Perot interferometer. This interferometer allows extremely high resolving powers and has high transmittance for use with relatively low levels of light.

A Fabry-Perot interferometer, Figure 1, ideally consists of two perfectly plane and parallel reflecting surfaces, each with reflectance R, transmittance T and absorbance A. The incident light beam is divided by multiple reflections into an infinite number of parallel rays forming sharp interference fringes at the focal plane of a lens placed directly behind the interferometer. The intensity of the central fringe ideally varies with wavelength according to Airy's formula (4):

$$A(\nu) = \frac{T^2}{(1-R)^2} \left\{ 1 + \frac{4R}{(1-R)^2} \sin^2 \pi \nu \Delta \right\}^{-1} \qquad (1)$$

where $\nu = 1/\lambda$, Δ (optical retardation) = 2nd cos i, λ = wavelength, n = refractive index, i = angle of incidence, and d is the separation between the reflecting surfaces. Transmission maxima occur when $\Delta = m\lambda$ where m is the order of interference. When the refractive index

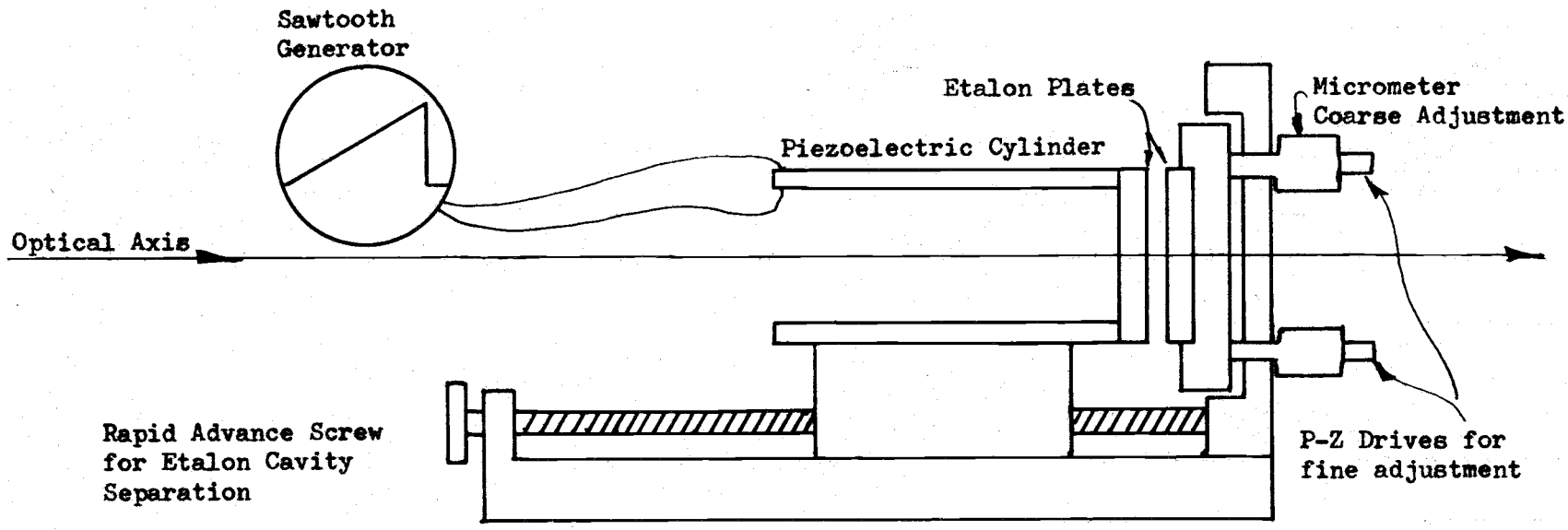

Figure 1. Schematic diagram of a piezoelectrically driven scanning Fabry-Perot interferometer.

is close to unity, as in air, and the beam is perpendicular to the surfaces (cos i = 1), then Δ is essentially equal to 2d, twice the spacing of the reflecting surface. At constant Δ, a change of order by $\pm$ 1 corresponds to a change of wavelength of $\pm \Delta\lambda$, where $\Delta\lambda = -\lambda^2/\Delta$, since $\Delta\lambda$ ususally is much smaller than λ. The quantity $\Delta\lambda$, is known as the free spectral range. To scan a line profile photoelectrically, the central fringe is observed through an aperture placed at the focal plane of the lens, while the optical retardation is changed linearly by either variation of the refractive index n or the physical separation of the parallel plates d.

For cos i = 1, and n = 1, m λ = 2d in each spectral range. For constant m and small relative changes in d, $\Delta\lambda/\lambda = \Delta d/d$. Therefore during a scan each time d changes by one-half wavelength, the order of m changes by one and the scan of the free spectral range is repeated over approximately the same wavelength region.

The optical resolution is determined by the finesse N, given by

$$N = \Delta\lambda / \Delta\lambda_i \qquad (2)$$

where $\Delta\lambda_i$ is the instrumental half-width and $\Delta\lambda$ is defined as above.

There are three important contributions to the final instrument finesse:

I) The reflection finesse N_R due to the shape of the Airy function

$$N_R = \frac{R^{1/2}}{1 - R} \qquad (3)$$

II) Surface defects finesse N_D, causing the plates to be neither parallel nor planar at all points.

III) The scanning finesse, N_F, due to the finite aperture located at the focal plane of the lens following the interferometer.

A good approximation to the final instrumental finesse is given by (4)

$$\frac{1}{N^2} = \frac{1}{N_R^2} + \frac{1}{N_D^2} + \frac{1}{N_F^2} \qquad (4)$$

where the variables are defined as above. Since the instrumental width is $\Delta\lambda/N$, there are N information points in each free spectral range which can be used for defining the line profile. A value of N = 20 is usually considered adequate. Our instrument has shown a value of N as high as 40.

The experimental system used in this research had as its heart a Tropel Model 242 piezoelectric scanning Fabry-Perot interferometer equipped with quartz plates having a reflectance of 97% for the wavelength range of 300 to 330 nm, giving a theoretical reflection finesse N_R limit of 98 in this region. Gross plate separation was controlled with a rapid advance 40 pitch screw which moved the scanning mirror and its mount. The plate separation was read on a mm scale engraved on the interferometer platform and had a vernier scale allowing readings to 0.05 mm. Total mirror separation was adjustable from 0.05 to 125 mm. Parallelness of the fixed mirror relative to the scanning mirror was controlled with two coarse micrometer screws for initial adjustment and piezoelectric drives driven by 0-700 volt variable supplies for

fine adjustment. In the commercial model of the interferometer the reflecting plates are held in place by an O-ring around the circumference of the plate in one case, and a retaining ring in the other. This retainment was modified by removing the O-rings and simply gluing the plates to their respective mounts to reduce vibration of the plates and increase instrumental stability. The entire table upon which the instrumentation was mounted was isolated from the floor by a double layer of carpet and foam rubber. The vacuum pump used with the demountable hollow cathode lamp was placed on an isolation table which in turn was also isolated from the floor with foam-backed carpet. The interferometer was mounted on a 17" x 6" steel platform ½ inch thick with its optical axis coincident with the optical axis of the Heath Model EU-700 monochromator and the Heath Model EU-701 photomultiplier housing. The use of the monochromator as a variable band-pass filter is necessitated by the very small free spectral range (FSR) of the interferometer. If lines outside the one FSR of interest are allowed to enter the cavity, orders of interference will be superimposed and the fringe pattern becomes very complex. The photomultiplier used was an RCA 1P28A which has excellent uv sensitivity.

Figure 2 shows the configuration of the optical components used in the assembly of the apparatus. The emission from the hollow cathode lamp was focused by the use of the parabolic folding mirrors onto the entrance slits of the monochromator. A 1.00 mm pinhole was placed just in front of the slit to allow only the radiation from a 1.00 mm area of the cathode to enter the monochromator by use of 1-to-1 imaging.

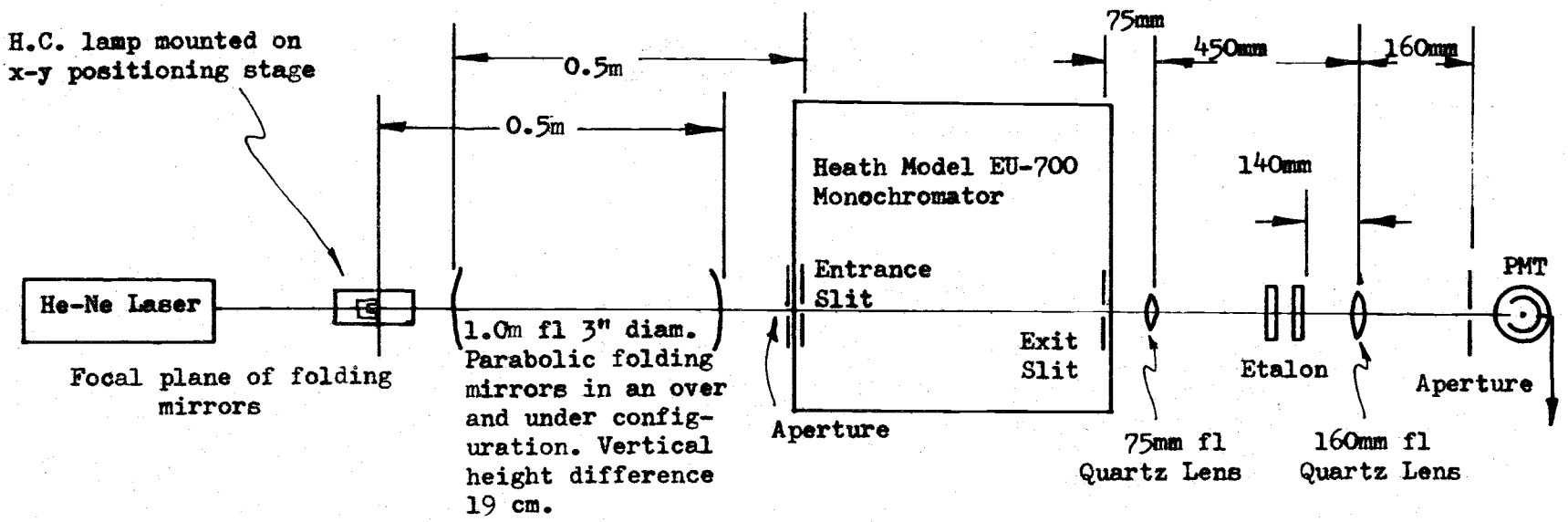

Figure 2. Schematic of optical system.

Immediately after the monochromator a plano-convex Suprasil quartz lens of focal length 75 mm was used to collimate the divergent light from the exit slits into the free aperture of the interferometer. After passing through the interferometer, the light was focused by a double-convex Suprasil quartz lens of focal length 160 mm onto the scanning aperture, an aluminum sheet with a 0.50 mm aperture, and hence into the detector.

The interferometer was equipped with magnetic feet which held it to the 17-inch long steel platform positioned behind the monochromator. The lens L_1, with the curved face toward the slits, was mounted on a magnet which allowed easy movement when desired, yet maintained the necessary stability for alignment. The 17-inch platform was covered by a black Plexiglas housing with openings for the drive cables and a removable portion to allow access to the coarse parallel adjustment. The focusing lens L_2, double convex, and the scanning aperture were enclosed in a second 8-inch long Plexiglas box and were each fastened to a separate x-y positioner made from modified microscope stages to allow fine positioning for alignment.

The hollow cathode lamp was mounted on a mobile x-y platform with position resolution of 0.01 mm. Two 3" diameter parabolic mirrors with 1 meter focal length were mounted on aluminum braces which allowed vertical and horizontal movement as well as a provision for 3-point mounting and adjustment for the mirrors.

The positions of the folding mirrors and hollow cathode lamp were determined by backlighting of the monochromator with a diffuse

light source, in this case a P111 photographic enlarger bulb mounted on the monochromator. The apertures of the two folding mirrors were filled by the slit image and the hollow cathode lamp cathode was mounted in the plane of the slit image focused by the folding mirrors. A quartz optical flat and the 1.00 mm aperture were then placed in front of the entrance slits so that they were perpendicular to the optical axis. A He - Ne laser was then mounted and adjusted so that all of the reflections from the parabolic mirrors and the optical flat were superimposed on the exit aperture of the laser beam, and all of the reflections on the mirrors and optical flat were coincident. This was taken to be true optical alignment for all components positioned on the entrance side of the monochromator.

The monochromator was then set to allow the 632.6 nm laser radiation to pass through the monochromator into the interferometer enclosure. Again, the optics following the monochromator were adjusted so that the beam passed through the center of the plates and such that all reflections were coincident on the exit slit. This provided a good initial optical alignment along the optical axis for all those components positioned behind the quartz flat.

Fine Adjustment of the Interferometer Cavity

The laser was replaced by a Ca hollow cathode lamp and the monochromator adjusted to the 422.6 nm Ca line. Adjustment of the interferometer cavity was done coarsely by eye, using a first-surface mirror at 45° behind the rear aperture of the interferometer and visually

observing the light pattern obtained with the Ca 422.6 nm line. When the mirrors are not parallel, moderately bright, closely spaced concentric arcs are seen against a somewhat less bright background. If the alignment is extremely bad, no arcs will be seen, and the collimating lens must be removed. One or more images of the exit slit will be seen when looking into the cavity. If more than one image is seen, it is necessary to bring all of the images to coincidence by the use of the coarse micrometer adjustments of the stationary interferometer flat. Replacement of the collimating lens in its original position should produce the closely spaced arcs. Once obtained, the coarse adjustments are gently manipulated to increase the spacing between the arcs until finally a pattern of concentric, bright circular fringes is obtained. At this point the alignment is as good as can possibly be obtained by hand. For further tuning, photoelectric detection and piezoelectric (p-z) adjustment are necessary.

To finely adjust the interferometer the 324.7 nm line of a Cu hollow cathode lamp in the dc mode with a current of 10-15 mA may be used. The photocurrent generated by the detector is monitored directly on a Tektronix type 531A oscilloscope with 1 MΩ , 20 pf termination. The interferometer is caused to scan by connecting the p-z drive to the 150-volt sawtooth output of the 531A oscilloscope, driving the interferometer over 3 to 4 free spectral ranges during one oscilloscope sweep (Figure 3). Typical settings include a photomultiplier voltage of 700 vdc, oscilloscope time base of 100 msec/division and sensitivity of 0.2 v/division, monochromator slit width 1000 μm.

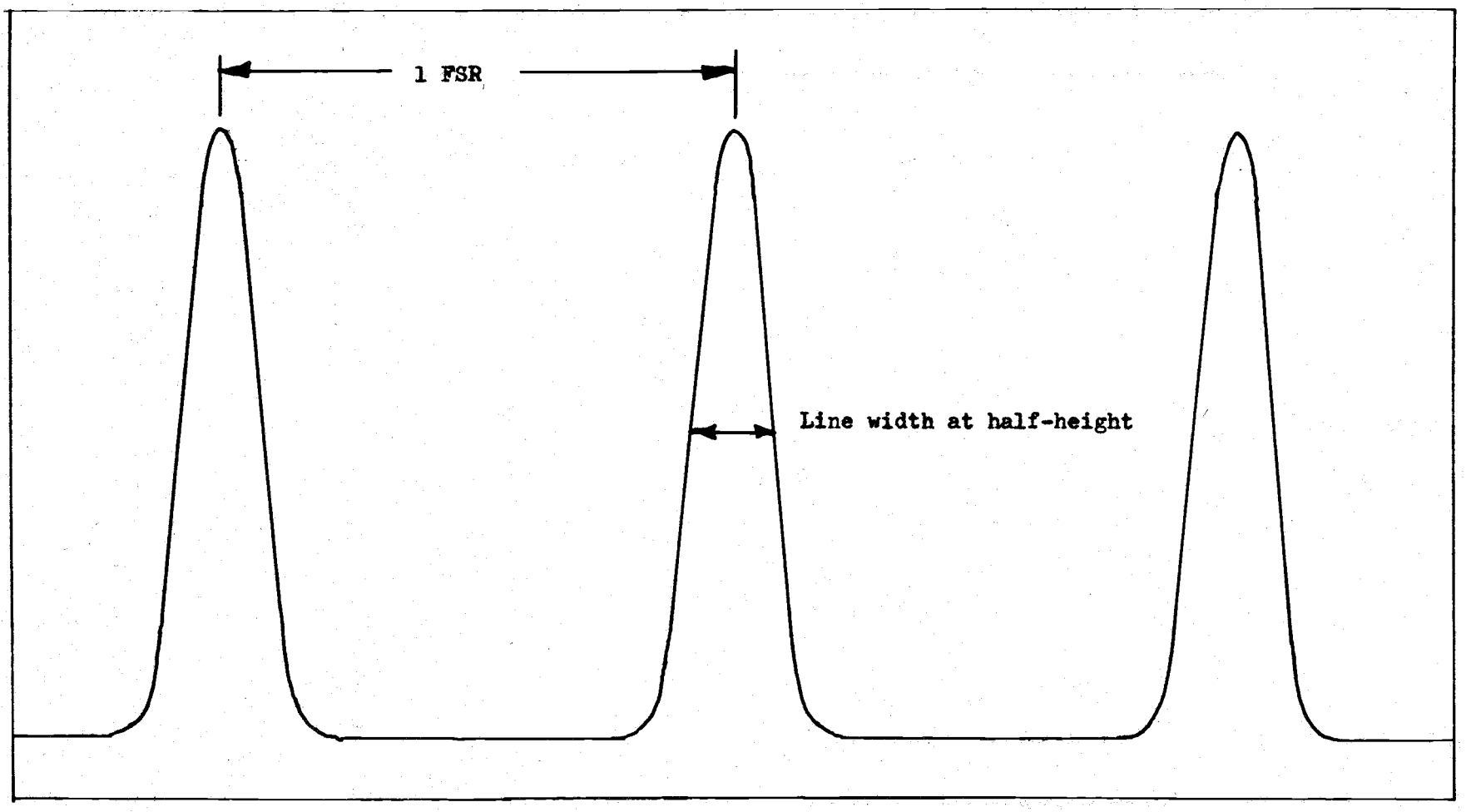

Figure 3. The three peaks seen in an interferometer scan of one line (Ag 328.0nm) in a scan covering about 3 free spectral ranges (FSR). Lamp current is 10 mA DC, one free spectral range covers 0.00918 nm. Scan observed on x-y recorder.

The voltage controls on the variable voltage supply are then varied until the line profile of the highest peak is at its largest magnitude and narrowest width, with the baseline remaining flat. If narrowest width and maximum intensity do not coincide, it is necessary to make fine adjustments to both the focusing lens and scanning aperture following the interferometer. At best alignment, sharp, clean peaks with a flat baseline are obtained.

The interferometer was found to be extremely sensitive to changes in the ambient air temperature and a one-inch thick styrofoam insulating encasement was placed around the interferometer and scanning aperture housings with aluminum foil placed around it in an attempt to desensitize the interferometer. The attempt was only partly successful and the interferometer was found to be stable for only a few hours a week during cool weather and not at all during warm weather. This was attributed to the lack of temperature control inside the laboratory. During those periods when the interferometer was stable and data was taken, the resolution was checked between each run and adjusted, if necessary.

Interferometer Calibration

The calibration of the interferometer mirror spacing scale was facilitated with the use of a sodium hollow cathode lamp (Perkin-Elmer No. 1970) and scanning the doublet with wavelengths of 330.2988 nm and 330.2369 nm in a dc mode, with currents of 10-15 mA (Figure 4). True mirror spacings were calculated from the equation

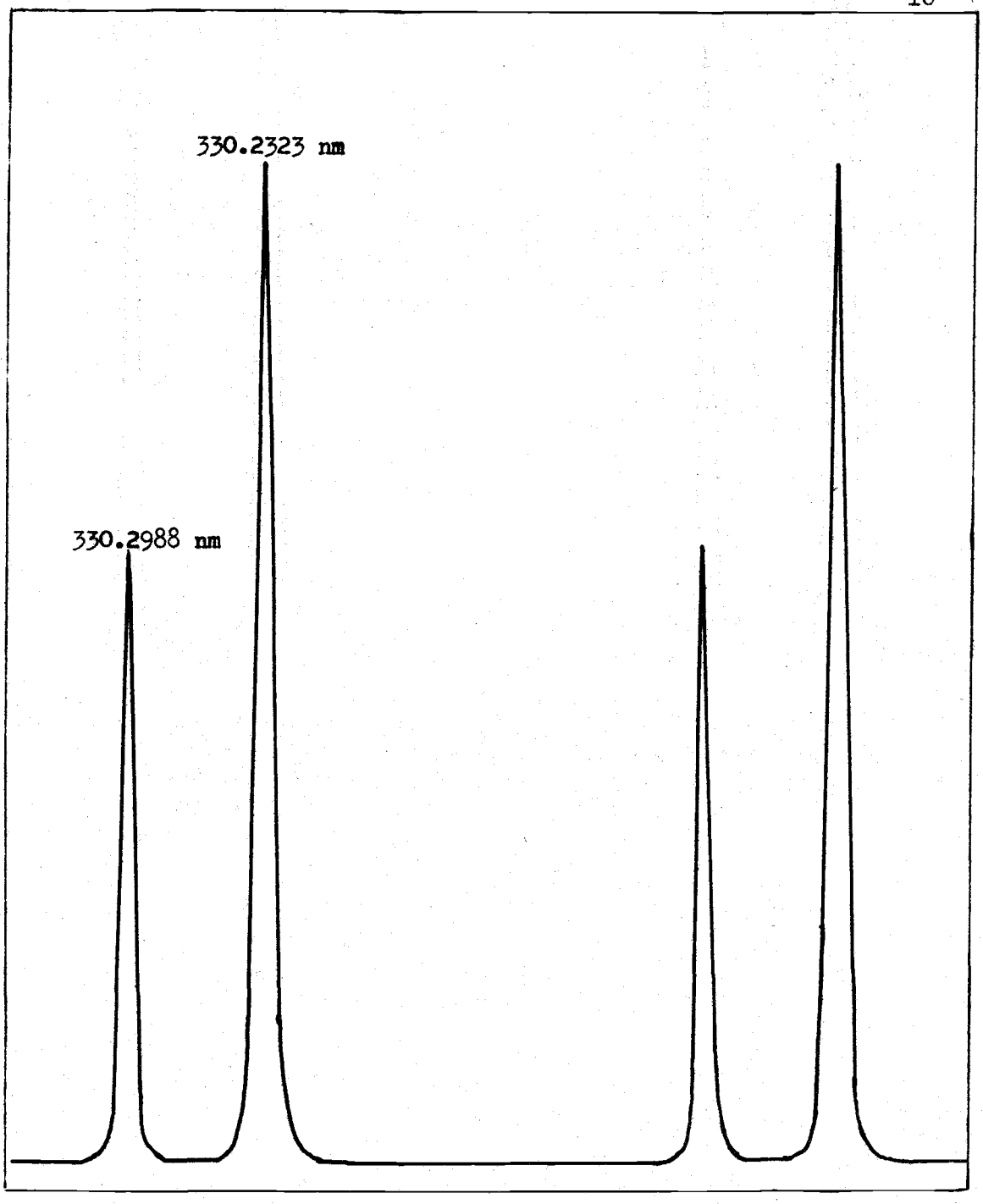

Figure 4. Interferrogram with mirror spacing of 0.14 mm of the Sodium doublet used to calibrate the interferometer, showing ability to resolve two closely spaced lines. Lamp current was 15 mA DC, recorded on x-y recorder.

$$d = \lambda^2/2n\Delta\lambda \qquad (5)$$

where λ is the wavelength, n is the refractive index of the medium between the mirrors (taken to be 1.00 for air) and $\Delta\lambda$ is the free spectral range calculated from

$$\Delta\lambda = [\lambda_1 - \lambda_2](X/X_{12}) \qquad (6)$$

where λ_1 = 330.2988 nm, λ_2 = 330.2369 nm, X is distance in chart divisions corresponding to one free spectral range as measured on the recorder readout and X_{12} is the distance in chart divisions between the doublets on the chart readout. Table 1 shows the results of these measurements and calculations, indicating a scale zero offset error of 0.26 mm.

Table 1. Cavity reading, calculated cavity spacing, and offset.

d_r (scale reading) mm	d_c (calc spacing) mm	$d_r - d_c$
0.30	0.05	0.25
0.40	0.16	0.24
0.50	0.23	0.27
0.60	0.33	0.27
0.70	0.41	0.29
0.80	0.53	0.27
0.90	0.03	0.27

Ave $d_r - d_c = 0.26 \pm 0.01$ mm

The finesse was determined by making the spacing between the mirrors very small ($<$0.1 mm) so that the free spectral range would be large relative to the true line width, causing the measured line half-width to be the instrumental half-width. Using Equation 2 the

finesse was found to be 40 ± 5 for this particular instrumental configuration. De Galan (6) states that the finesse should equal or exceed a value of 25 for satisfactory line profile studies.

Experimental Procedures

Control of the experiment and data acquisition was accomplished by the use of a PDP-11/20 minicomputer. Minor manipulation of the data enabled outputting of the data in a time-resolved form. The PDP-11/20 computer was equipped with a KA11 central processor with 8K of core, PC11 High Speed Paper Tape Reader and Punch, KW11-P programmable real-time clock, AD01-D multichannel analog-to-digital (A/D) converter, and an AA11-D digital-to-analog (D/A) conversion system. Two D/A channels out and two A/D channels for input were used to tie the computer to the instrumentation. The A/D inputs of the computer can be used to monitor and store positive voltages of up to 9.99 volts. Because of this the photocurrent from the detector was amplified and inverted with two McKee-Pederson operational amplifiers in the configuration shown in Figure 6 with an RC time constant of 5 μseconds prior to sensing it with channel 2 of the A/D which has a conversion time of 22 μseconds per conversion to 10-bit integer. If the data is taken from the A/D converter prior to the conclusion of the conversion, the added precision given by the last one or two bits will be lost.

Channel Ø of the A/D was used to monitor the condition of the sweep of the 531A oscilloscope by measuring the output of a 10:1 voltage divider placed on the output of the (+)-gate of the oscilloscope.

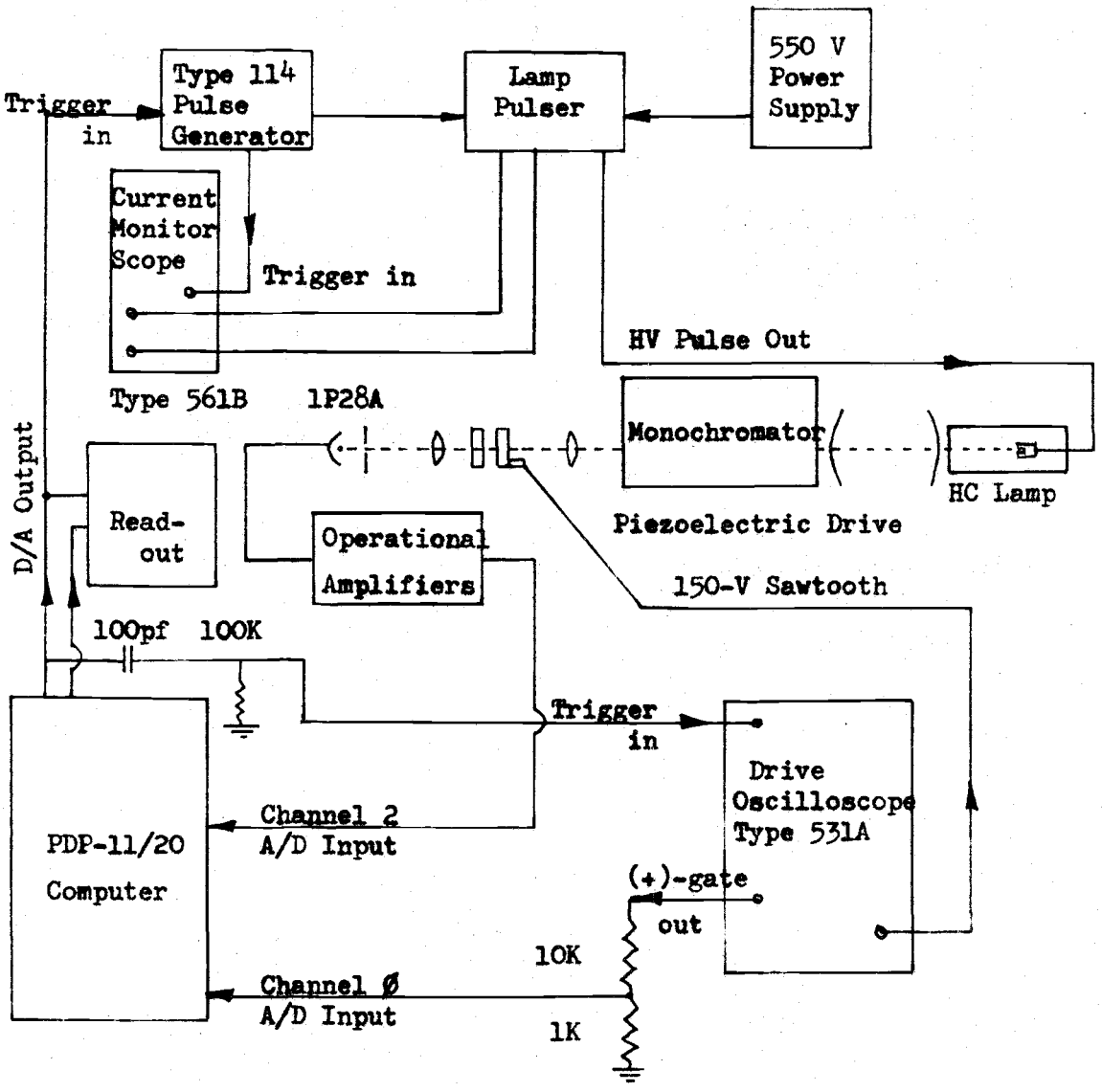

Figure 5. Schematic diagram of complete instrumental configuration.

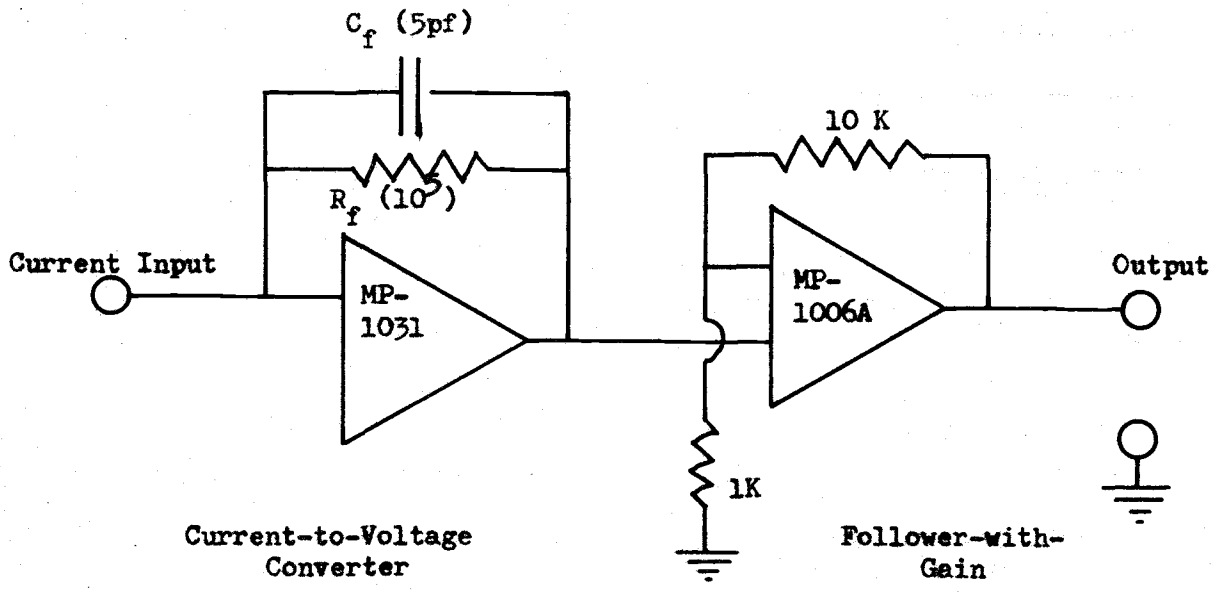

Figure 6. Schematic of operational amplifier circuit.

Channel Y on the D/A output was used to trigger both the sawtooth of the 531A oscilloscope and a Tektronix 114 pulse generator.

A Tektronix 114 triggerable pulse generator provided a pulse of variable duration, set typically at 300 μseconds, to the high voltage pulser which drove the hollow cathode lamp. The high-voltage pulser, Figure 7, was a modified version of the pulser of Dawson and Ellis (8) and allowed independent setting of both the dc level in the hollow cathode lamp and the current of the pulse. The power supply was a Fluke model 407 high voltage power supply capable of supplying 550 V at 500 mA continuously. The pulse current was observed with a Tektronix type 561B dual trace oscilloscope by monitoring the voltage drop across a 100-Ω resistor in series with the hollow cathode lamp.

Sequence of Events During an Experiment

For the running of a single experiment, typical instrument settings were as follows: Tektronix 531A sweep setting, 5 sec/sweep; PMT voltage, 700 VDC, amplifer gain, 10^5; RC time constant, 5 μseconds; pulse current, 300 mA; pulse duration, 300 μsec; total number of interferometer scans, 64. After these settings had been made, control was given to the PDP-11/20 which then commenced the experiment and acquired the desired data. During this time the computer first tests the (+)-gate of the 531A oscilloscope to see if the voltage is zero, indicating that the oscilloscope is not sweeping and is in a triggerable state. If the (+)-gate is non-zero, the computer waits until it has reached the zero state. When it becomes zero, a pulse of +10 volts is sent out of the computer on D/A channel Y to the external trigger inputs of

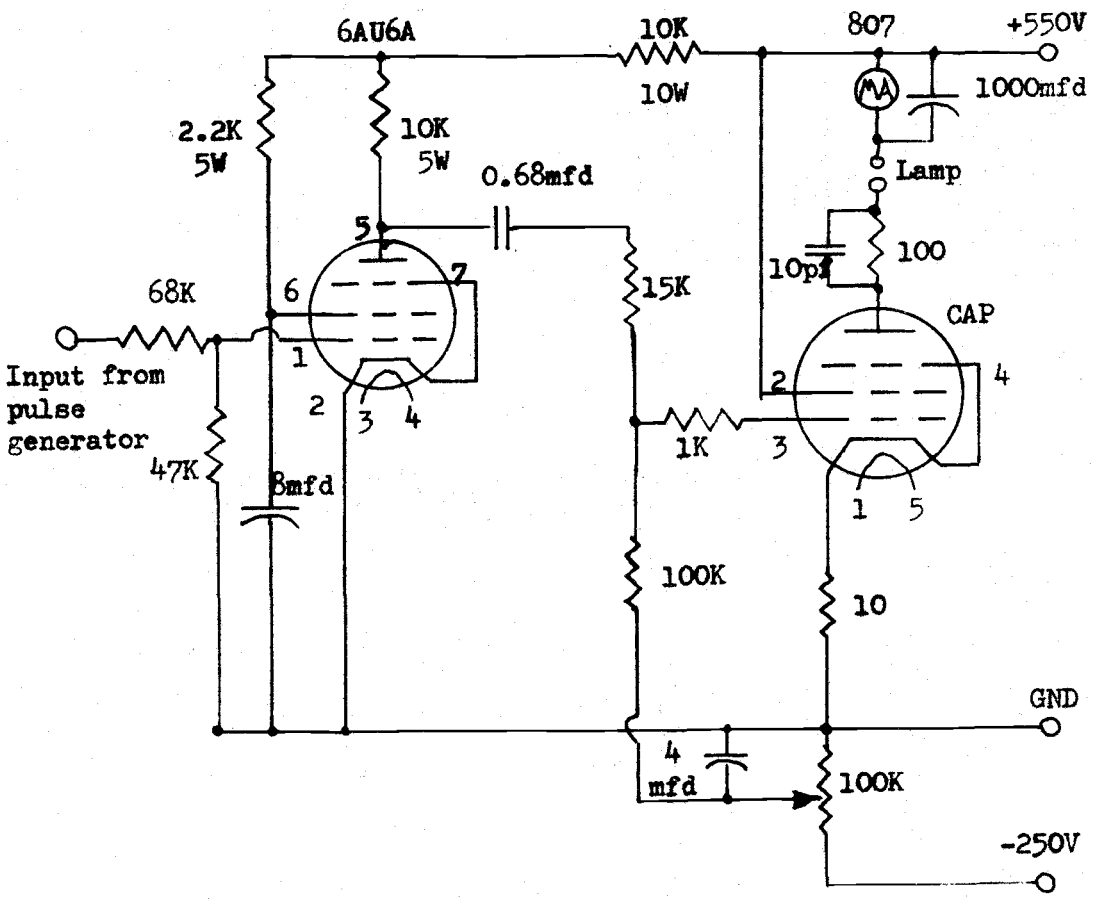

Figure 7. Schematic diagram of the high voltage pulser used to drive the hollow-cathode lamp.

the 631A oscilloscope and the 114 pulse generator. This initiates a pulse of light 300 μseconds long from the hollow cathode lamp and simultaneously starts the sweep of the 531A oscilloscope and its accompanying sawtooth ramp. It is this ramp voltage which drives the interferometer through a few (3-4) spectral ranges during the one 531A oscilloscope sweep.

Twenty-one μseconds after sending out the trigger, the computer starts the conversion on the A/D input connected to the operational amplifier circuit and measures and stores the photocurrent signal 10 successive times during 210 μseconds and places these values in 10 consecutive addresses in core. After a 10-msecond delay, a second trigger pulse is sent out to the 531A oscilloscope and the 114 pulse generator. The oscilloscope is still sweeping and ignores the trigger. The pulse generator sees the trigger and pulses the lamp for 300 μseconds for the second time. Ten measurements of the photocurrent are again taken by the computer and stored in the ten consecutive words of core following the first ten. This sequence is repeated until 500 pulses are generated and 5000 words of core are filled, all during one sweep of the 531A oscilloscope (i.e., one interferometer scan). The computer now returns to monitor the (+)-gate of the 531A oscilloscope and waits for the scan to end. This constitutes one scan.

When the (+)-gate returns to zero, the sequence begins a second time with a trigger pulse sent to the 531A and the 114 pulse generator. The new datum for each point is added to the corresponding datum from the previous scan already stored in that word of memory. This, in

effect, reduces random noises by point averaging over the several scans. The scan sequence is repeated n times (typically 64), with n set in the computer by the operator prior to the execution of the experiment.

The computer now has made n 5-second interferometer sweeps and contains 5000 data points taken on 500 pulses. Data taken for a few pulses is shown in Figure 8, where A_1 is the first point taken for the first of the 500 pulses, A_2 the second point, A_3 the third, etc. Similarly, the next 499 pulses are each broken up into 10 data points. During one pulse, the interferometer has scanned over only 0.05% of one free spectral range. With a finesse of 40, a scan must be longer than 2.5% of the free spectral range before it is significant. Thus it can be assumed for simplicity that the interferometer spacing is essentially identical for all 10 of the points taken during one hollow cathode pulse. The data can now be outputted in the following manner. The first data point is A_1, the second, B_1, the third C_1, and so forth (Figure 8), to data point number one of pulse number 500. The entire set of 500 points covers the 5-sec interferometer scan, giving an interferometer scan which shows the line profile as it appears between 0 to 21 μseconds after the initiation of the pulse. By outputting A_2, B_2, C_2, etc., a scan is constructed for the line profile as it appears between 21 to 42 μseconds after pulse initiation. Doing the same for the remaining points on each pulse, we now have 10 sets of line profile data, each separated in time by 21 μseconds, i.e., time resolved line profiles for a pulsed hollow cathode lamp.

In practice, the profiles were plotted on a Varian model 80 X-Y

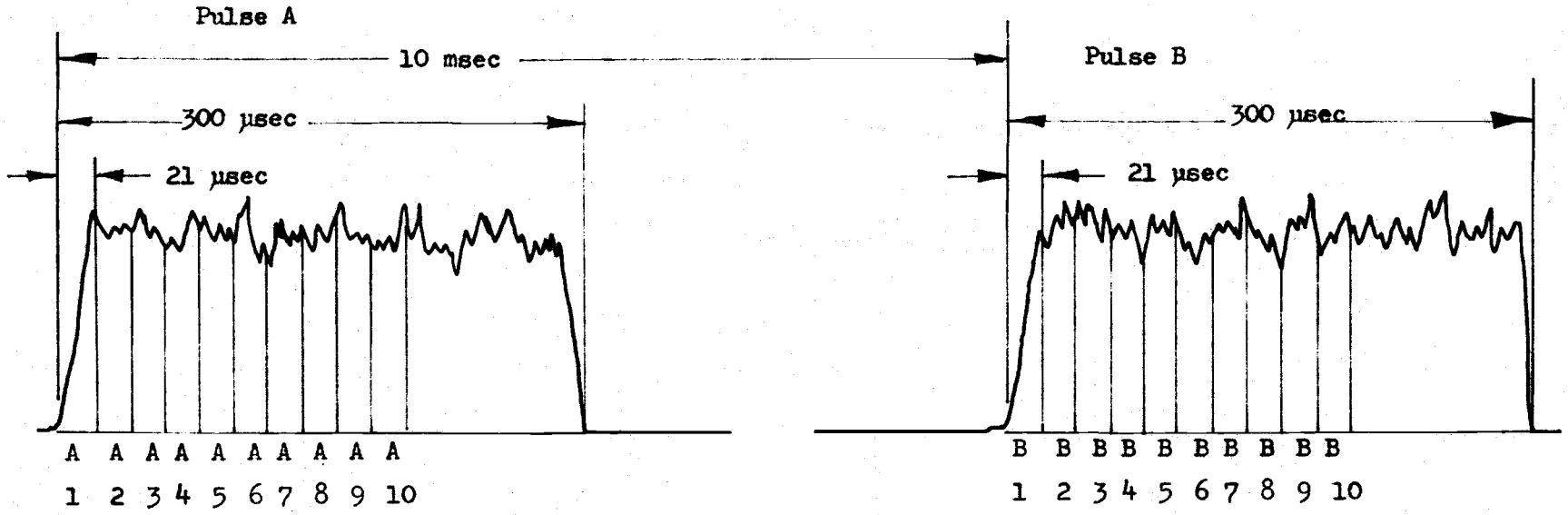

Figure 8. First two lamp pulses of a sequence of 500 pulses showing the 10 pieces of data taken from each pulse.

recorder using channel X of the computer as the time axis incrementor and channel Y as the signal axis. A schematic of the entire instrumental configuration is shown in Figure 5. A flow chart of the program and the PAL-11A mnemonics are included in the appendix.

A Demountable Discharge Lamp

In order to try to build a discharge lamp to be optimized specifically for pulsed operation, a demountable lamp was built which would allow the fitting and trial of various electrode configurations, Figure 9. Windows were 1" diameter quartz plates to allow studies into the UV and were adhered to the surface of the lamp body with Apiezon W silicon to form a vacuum seal. A simple vacuum manifold (Figure 10) was constructed with a Swaglok needle valve for control of the Argon filler gas. The vacuum manifold (Figure 10) was equipped with ballast tanks to reduce erratic flow caused by the pulsing nature of the vacuum pump and the pressure regulator on the Argon tank. The pressure in the system was monitored on both sides of the demountable lamp with Gilmont micrometer manometers. Pressure drop between the manometers (across the lamp) was found to be negligible. The vacuum pump was mounted on an isolation table, and carpet and foam isolation was used under the legs of the isolation table as well. Tungsten wire electrodes were introduced into the system via Ace glass electrode holders. The copper electrodes of interest were fastened to the tungsten electrode by a crimped copper tube to give good mechanical and electrical properties. The copper electrodes were cleaned with a

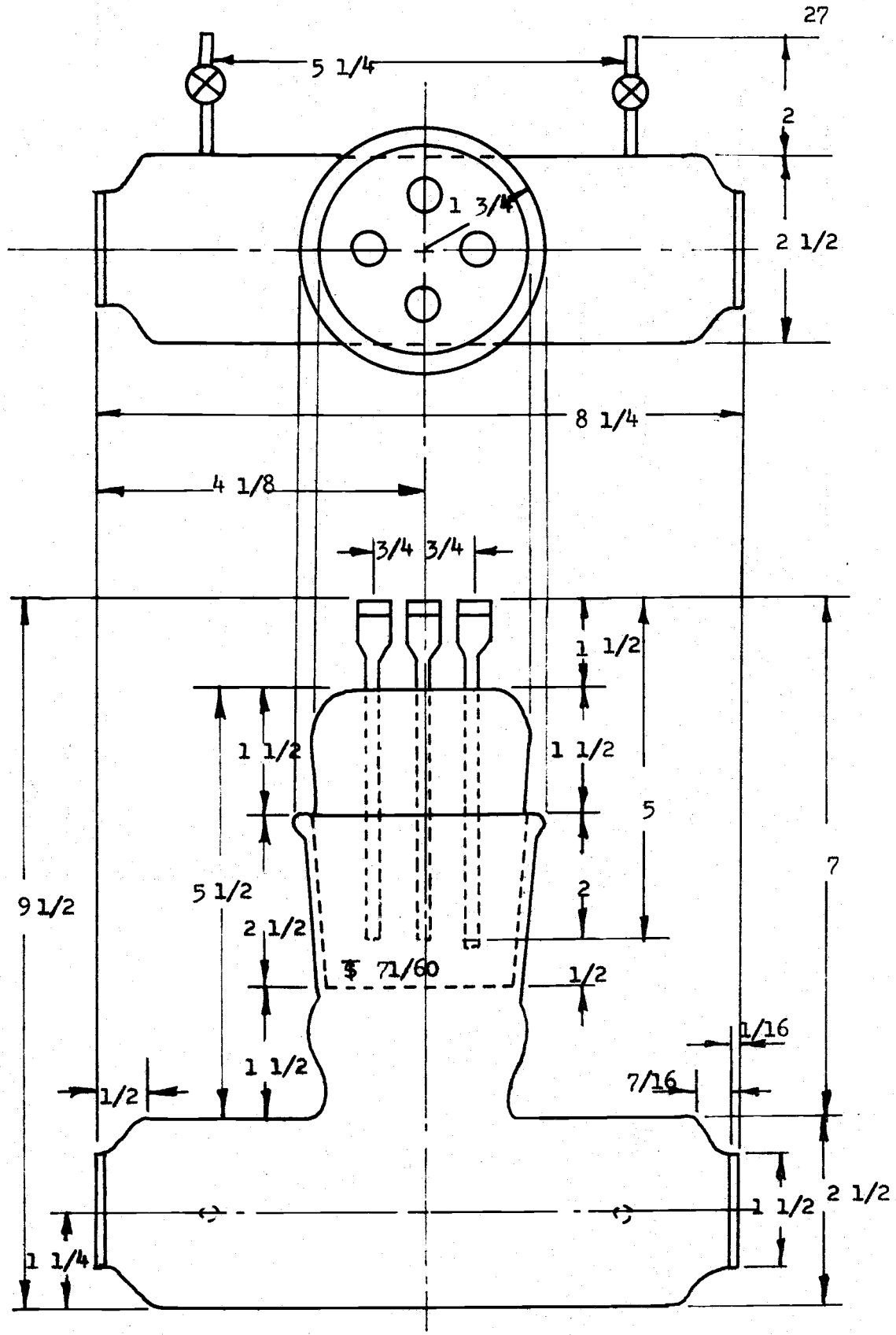

Figure 9. Demountable lamp. All dimensions in inches.

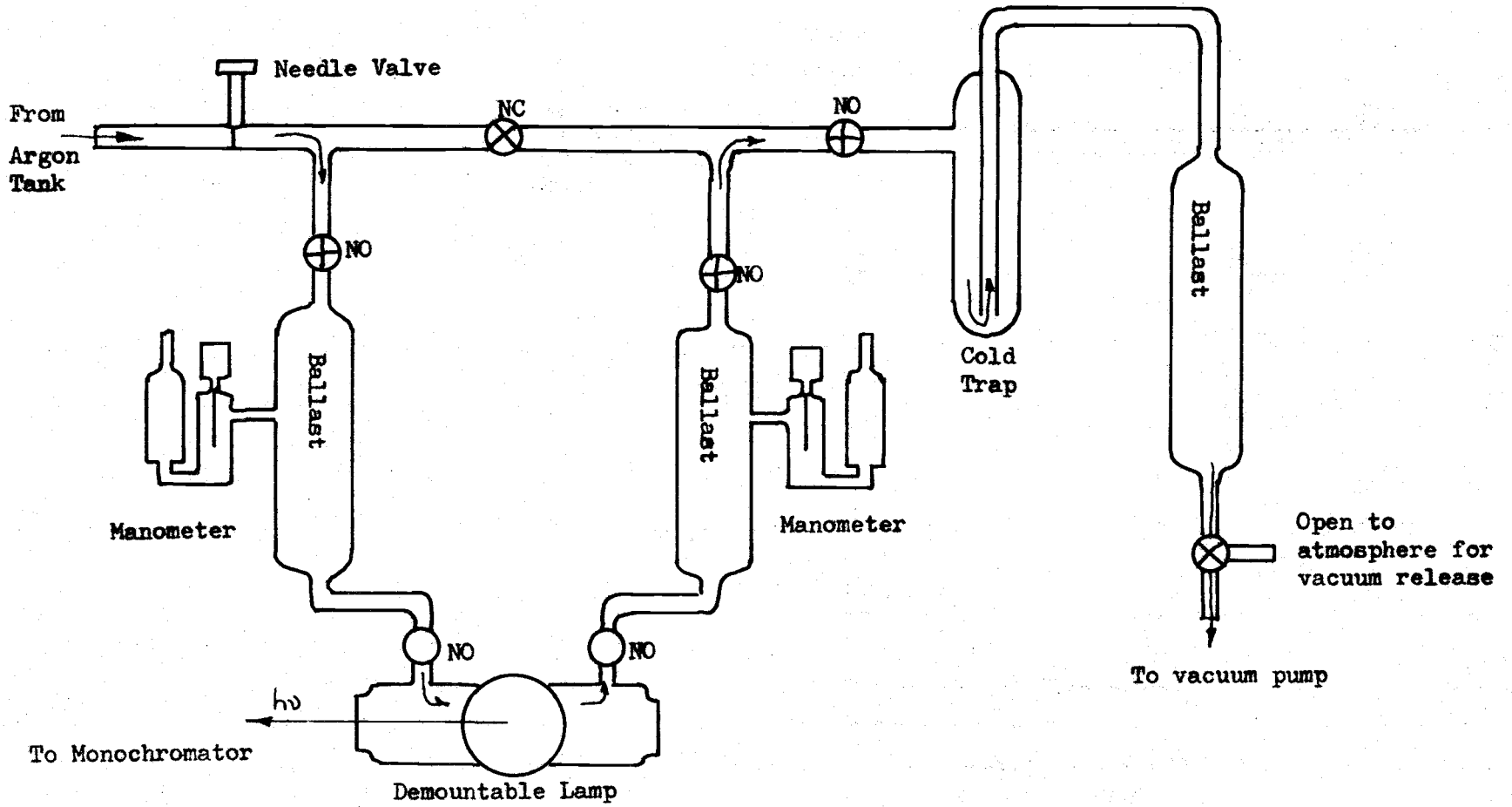

Figure 10. Block diagram of vacuum system and direction of Argon flow.

wire brush and rinsed in 2.0 M HCl and distilled H_2O prior to being placed in the discharge lamp. The assembled lamp was then pumped down to about 3-4 torr, flushed with Argon and pumped down, repeating the flushing about 3 times before any attempt was made to start the discharge in the lamp. A 0.3 mm aperture at the monochromator was used with the lamp to do spatial resolution of the pulsed discharge.

THE GLOW DISCHARGE

The electrical discharge within a hollow cathode lamp that contains an inert gas at low pressure is known as a glow discharge. There are three types of glow discharges that may be visually distinguished from each other. They are the normal glow, the abnormal glow, and the arc. The normal glow discharge is typified by operation at current density values from 0.1 to 1.0 mA/cm^2, depending upon the size and shape of the electrodes. Several different glow regions within the lamp may be distinguished when operating at pressures of about 1.0 Torr and using the parallel plate electrode configuration (10). (The regions are not normally distinguishable in a normal hollow cathode because of the bright cathode glow region). The regions of brightness correspond to regions of high energy and high electric field. In the dark regions the energy of the ions falls to that of the ambient gas; consequently ionization and excitation are considerably less in these regions (11).

As the current increases, the glow region at the cathode increases in size until the entire cathode is covered with the glow. Then at higher current densities, "hot spots" or regions of higher intensity (and current density) are formed near the cathode surface. This is known as the condition of abnormal glow. If the current density continues to increase, the "hot spots" collapse to one small region on the surface of the cathode and an arcing condition of very high current density ensues.

In the normal glow condition, space charge regions are established within the lamp as the ions and electrons drift toward the cathode and

the anode, respectively. The potential drop across the positive space charge is known as the cathode fall. The space charge and the glow region at the cathode very closely coincide. It is this normal glow which predominates in the commercial hollow cathode lamp under the usual 5-15 mA dc current conditions. This may be true under the high current pulsed conditions used in these experiments since the hot spots which are characteristic of the abnormal glow were not observed during pulsed operation.

Discharges operating at moderate to high current density values (0.1 to several hundred mA/cm^2) create high energy ions which cause a sputtering of the cathode material from the cathode surface as they impact. This creates a cloud of atomic vapor of the cathodic material above the surface of the cathode. For a given current the amount of atomic vapor which is sputtered from the cathode surface depends upon the kinetic energy of the impacting ion, the pressure of the inert gas, and the metal itself. Silver, for example, has a greater sputtering rate than copper (17), and argon is a better sputtering agent than neon (17). The sputtered atoms in the cathodic vapor emit lines that are characteristic of free atoms. Resonance lines are usually more intense than other lines, making these lamps very useful in analytical atomic spectroscopy.

The atoms that are sputtered from the cathode may also diffuse into other parts of the lamp. At moderate dc levels (20-40 mA) the atomic vapor clouds in the cooler regions may cause severe self-reversal of the emission lines of the excited atoms that are in the more energetic regions near the cathode (1). Self-reversed lines may cause difficulties

since the wavelengths of most intense emission from the lamp may not coincide with the wavelength of maximum absorption in the sample vapor.

EXPERIMENTAL RESULTS AND DISCUSSION

Commercial Hollow-Cathode Lamp

Interferometry measurements were conducted on a commercial Westinghouse Cu hollow-cathode lamp No. 23042 used in pulsed atomic absorption measurements of laser plumes. The wavelength of primary interest was the Cu 324.75 nm resonance line because of its isolation from other interfering lines and its wide use in both atomic absorption and atomic fluorescence measurements.

With a lamp current of 10 mA dc and an etalon spacing of about 1 mm the 324.75 nm Cu(I) emission line showed up as an unsymmetrical doublet. By increasing the separation of the etalon plates in small increments and scanning the emission line after each increase, it was possible to optimize the separation for good wavelength resolution and yet unambiguously identify the doublet in each free spectral range. The etalon cavity spacing which gave the best results was 5.74 nm $\pm$ 0.05 nm. Two free-spectral-ranges (FSR) for this spacing are shown in Figure 11, along with the important instrumental parameters. Several scans of the 324.75 nm lines gave a peak separation of 0.0040 nm $\pm$ 0.0001 nm, which agrees well with the 0.0038 nm reported by Brix and Humbach (2). They reported that this splitting is due to interaction between the electron moment and the nuclear magnetic moment, I, which is 3/2 for both of the Cu isotopes. The peaks are each formed from groups of six hyperfine lines, three from each isotope, which have splittings much less than the Doppler width of the lines, and are hence unresolvable. The ratio of these two lines (peak intensity ratio, or

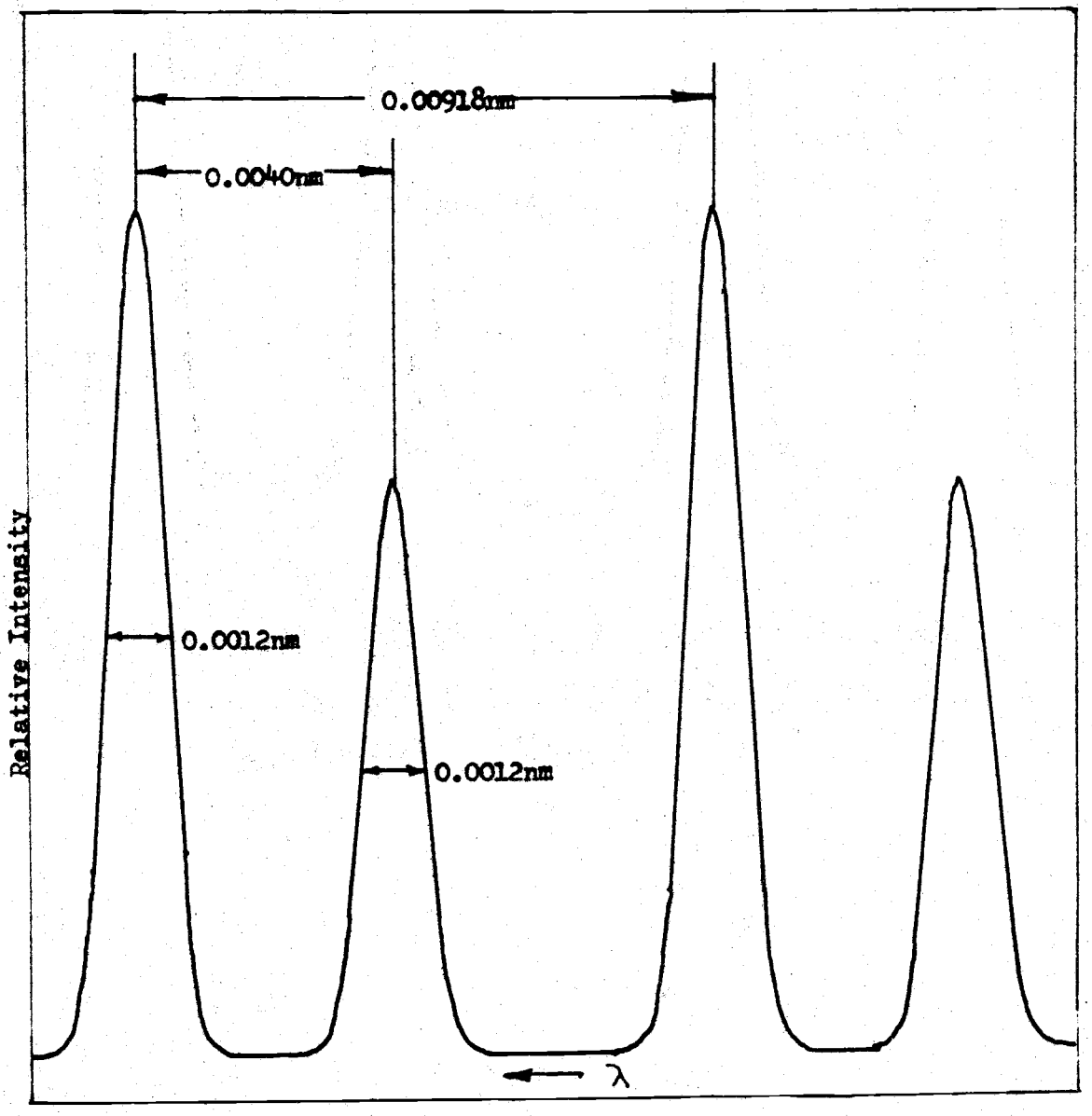

Figure 11. Two free spectral ranges of the Cu 324.7 nm doublet with an etalon mirror spacing of 5.74 mm. One free spectral range is equal to 0.00918 nm.

PIR) is 5/3 or 1.67 (7) with no absorption. Deviations from this ratio may be used as a measure of line self-absorption. The highest PIR observed for the lamp at 10 mA dc current level was 1.48, indicating the presence of some self-absorption even at these low intensity levels.

A plot of line-width at half-height (known hereafter simply as line-width) vs dc current level for the major emission line was constructed to allow comparison with later measurements on the same lamp in the pulsed mode (Figure 12). The minor line was found to behave in a similar way to the major line in both the dc and pulsed modes. The increase of line-width with dc current, shown in Figure 12, is apparently caused by increased self-abosrption at higher currents and the start of self-reversal at currents above 15 mA dc. Doppler broadening increases only as the square root of temperature and is therefore probably a less significant contribution to the increase in line-width. Most literature sources quote values of 0.001 to 0.002 nm (13, 19) as the line-width for hollow cathode lamps driven in the 5-20 mA dc current range. These values agree well with those plotted in Figure 12.

All of the data for the commercial lamp in the 300 μsecond pulse mode was obtained by superimposing (by digital addition) 64 sweeps and time resolving the output as described in the Experimental section. Shot noise was a problem since short periods of time were being observed. Averaging the results from 64 sweeps helped to reduce the effects of shot noise by a factor of 8. To check this method, a single scan for a lamp driven at 10 mA dc was recorded directly on the x-y plotter without the use of the computer. The computer was then used to make

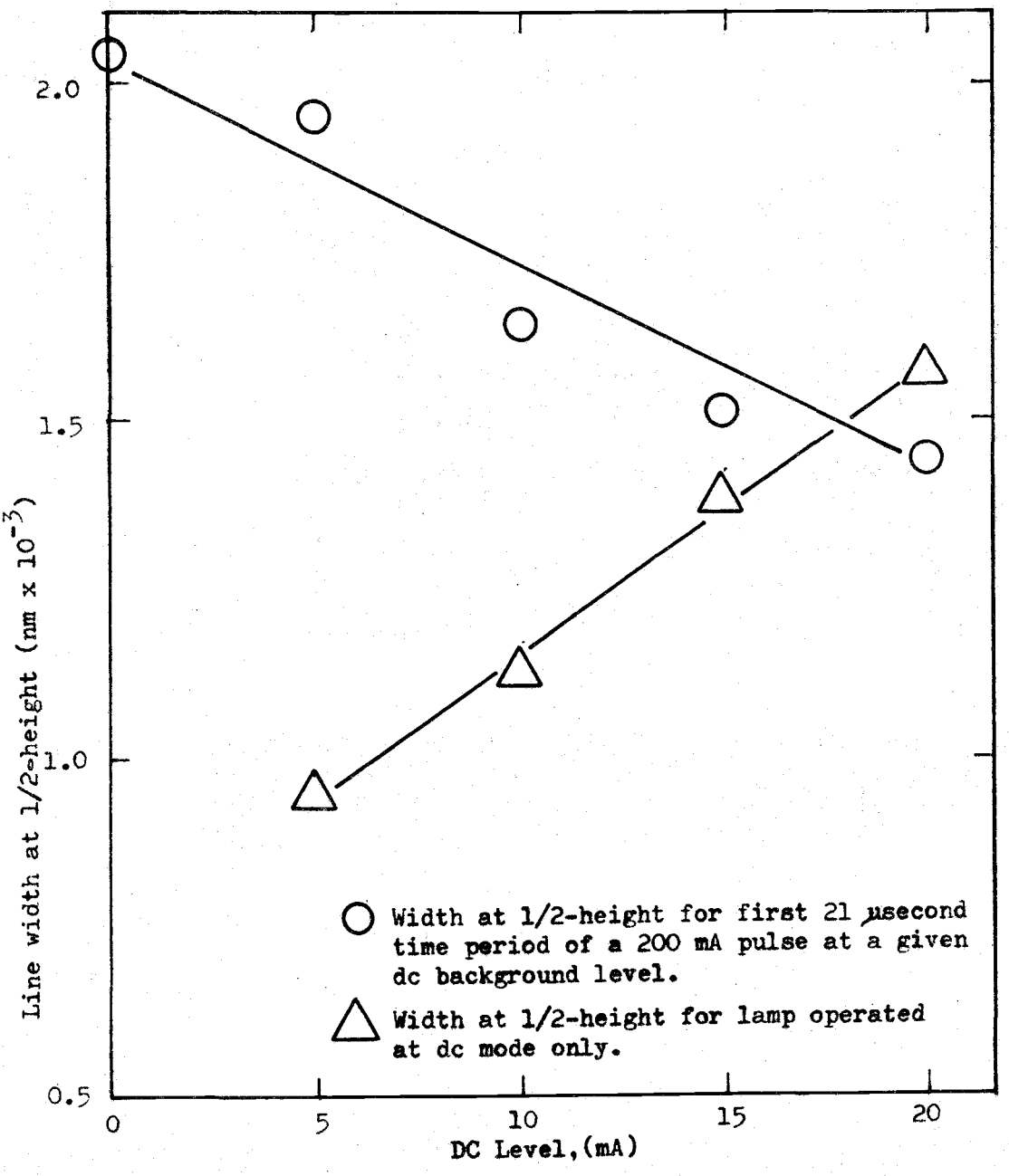

Figure 12. Line-width of the major emission line at 324.7 nm vs lamp dc current level (no pulse) and line-width during the first 21-μsecond time period for 200 mA lamp pulse superimposed on various dc background current levels.

64 scans over the same lines under identical lamp conditions. The time resolved output was then compared to the line profile obtained without the computer. Figure 13 shows this comparison. The profiles are nearly identical, indicating that there is little or no distortion of the line profile during either the taking of the data or the plotting of the data in its time resolved form.

A second method of comparing the line profile from the computer with a more directly obtainable profile was also used. This involved comparing the line profile observed on an oscilloscope for a pulse of 21-μseconds duration with the profile produced by the computer for the first 21 μseconds of a 300-μsecond long pulse. Pulse current for both cases was 400 mA with a 1.0 mA dc background current. Again, the results were essentially identical.

Figures 14 through 17 each show time resolved line intensity vs wavelength profiles for the commercial hollow cathode lamp under various dc background conditions with current pulses of various levels superimposed on the dc level of the lamp. Each figure shows five profiles separated in time. Each profile covers 21 μseconds of time, and the profiles are given sequentially from left to right. The time periods covered are 0-21 μseconds, 21-42 μseconds, 42-63 μseconds, 63-84 μseconds and 84-105 after the start of the pulse. The small crosses in the figures are placed the same distance above the baseline for each profile and spaced horizontally to be equivalent to a wavelength difference of 0.0040 nm (the spacing between the hyperfine lines), and are placed at the center of emission intensity for a normally driven (10 mA dc) lamp.

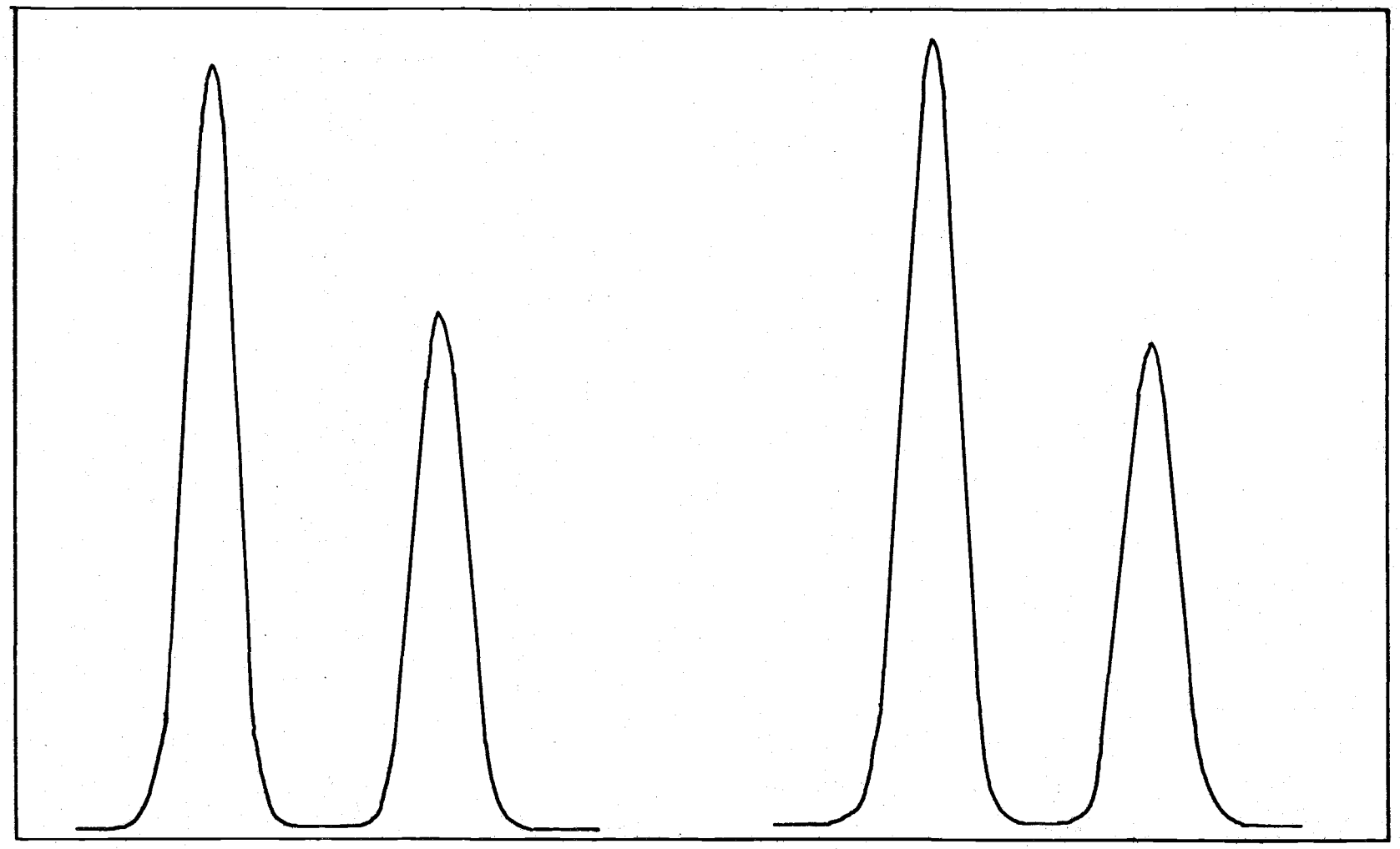

Figure 13. Comparison of Cu 324.7 nm doublet of a hollow cathode lamp at 10 mA dc obtained with a single scan on the x-y recorder (left) and 64 computer scans (right).

Each profile is one FSR long and shows the two hyperfine lines of copper. Where there appears to be more than two lines in a single FSR, this is due to the combination of peak broadening and strong self-reversal of the resonance radiation.

The instrumental parameters controlling the relative intensity are given in the caption of each figure. These are the photomultiplier power supply voltage (PMT), the feedback resistance in the operational amplifier (R_f), the slit-width (SW), slit height (SH), and recorder scale (R_s). These parameters were manipulated for each lamp condition to try to allow maximum use of the 10-bits in the A/D converter. Hence, the relative intensities from one figure to the next may not be directly comparable unless all of the instrumental parameters are the same. The feedback capacitance (C_f) is also given in each caption.

Variation of Line Profile with Pulse Current

Figures 14 through 17 show the change in line profile with time for pulse currents ranging from 125 to 400 mA with a continuous background dc level of 10 mA in the lamp. All of the intensities shown on these figures are directly comparable. Note that for all of the pulse levels both hyperfine lines show definite self-reversal by the third time period. The ratio of line intensities in the first time period also varies from 1.25 to unity as the pulse current increases. This self-reversal and the decrease in intensity ratio are caused by the atomic Cu vapor diffusing from the excitation region into the cooler outer regions where the fraction of excited atoms dramatically decreases.

Figure 14. Time resolved line profiles of the Cu(I) 324.7 nm emission lines in the commercial hollow cathode lamp. Pulse current = 125 mA, dc background current level = 10mA.

R_f= 10^5

C_f= 50pf

SW= 600 μm

SH= 3.0 mm

PMT= 750 VDC

Scale= 1.0 V/inch

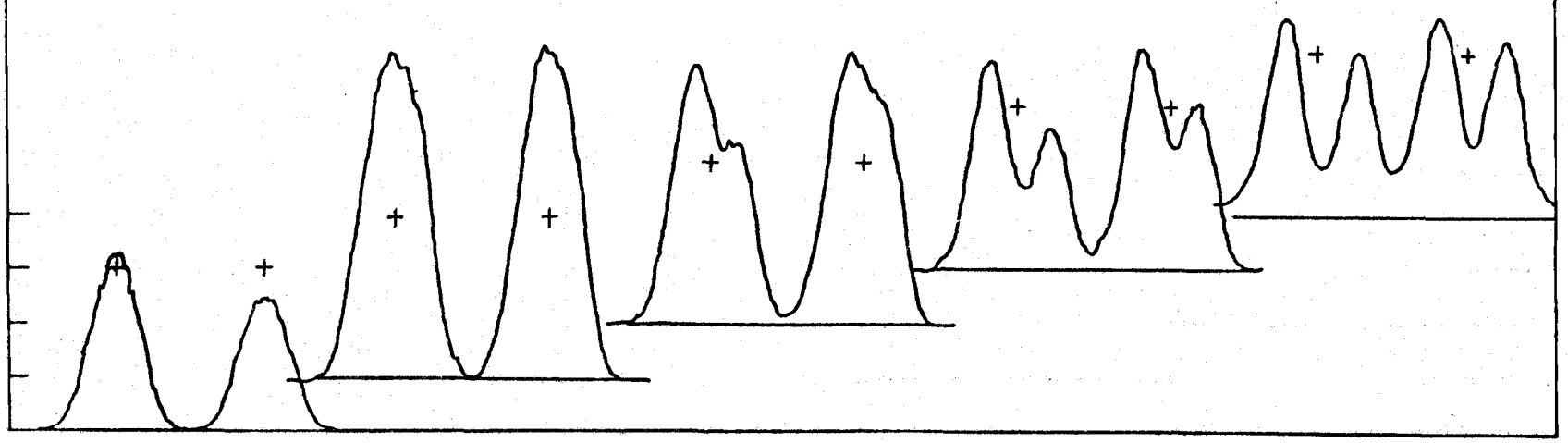

Figure 15. Time resolved line profiles of the Cu(I) 324.7 nm emission lines in the commercial hollow cathode lamp. Pulse current = 220 mA, dc background current level = 10 mA.

$R_f = 10^5$

$C_f = 50$ pf

SW = 600 μm

SH = 3.0 mm

PMT = 750 VDC

Scale = 1.0 V/inch

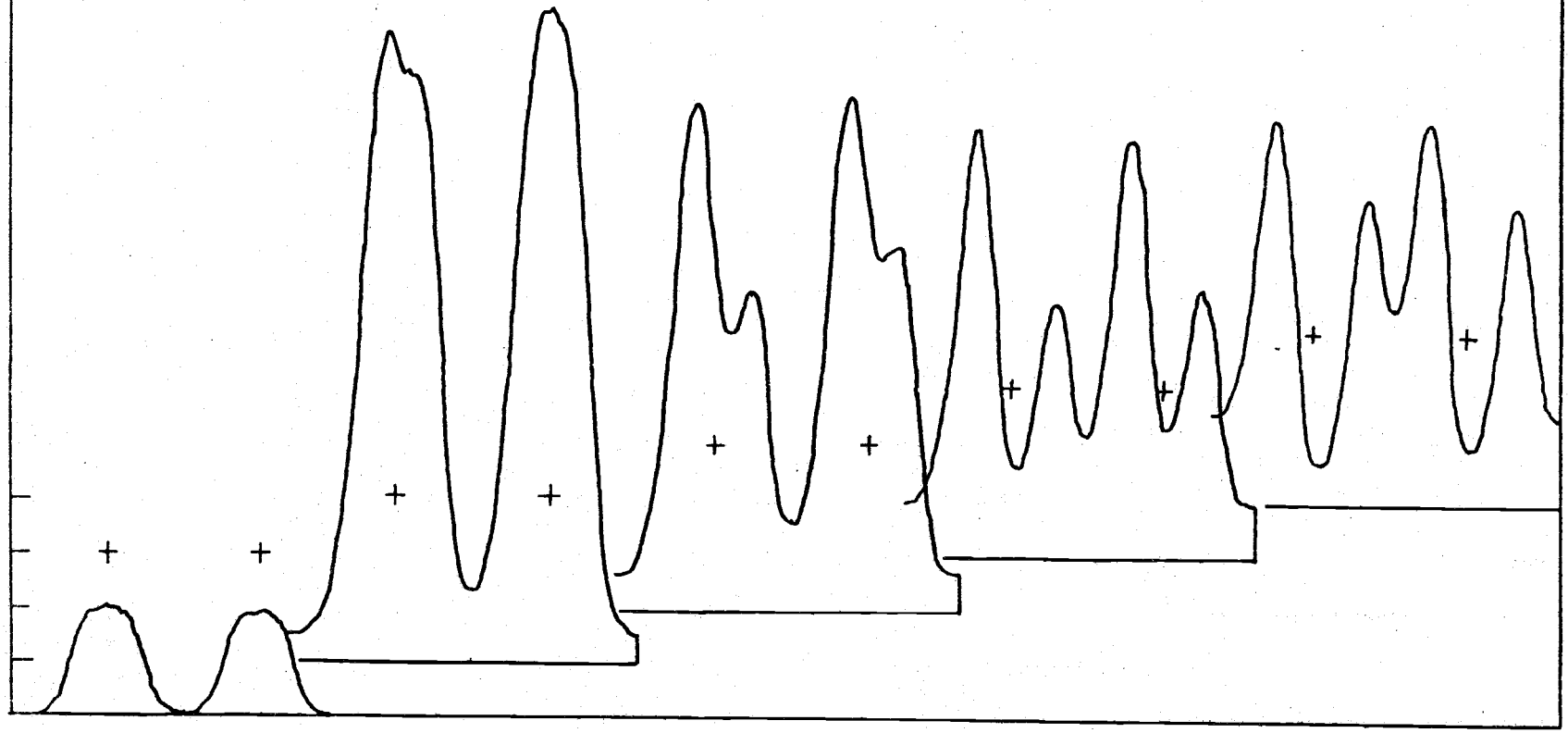

Figure 16. Time resolved line profiles of the Cu(I) 324.7 nm emission lines in the commercial hollow cathode lamp. Pulse current = 300 mA, dc background current level = 10 mA.

$R_f = 10^5$

C_f = 50 pf

SW = 600 μm

SH = 3.0 mm

PMT = 750 VDC

Scale = 1.0 V/inch

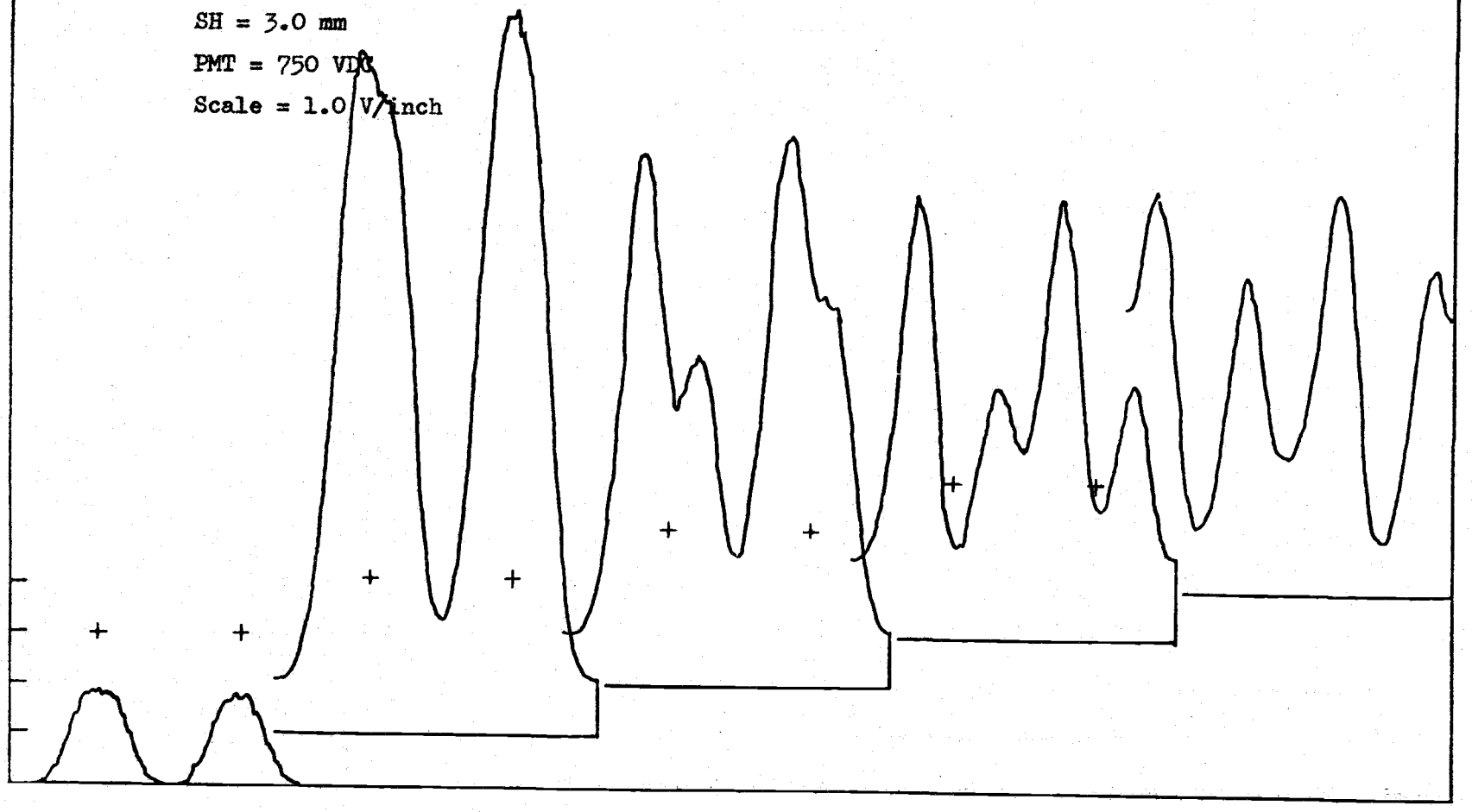

Figure 17. Time resolved line profiles of the Cu(I) 324.7 nm emission lines in the commercial hollow cathode lamp. Pulse current = 400 mA, dc background current level = 10 mA.

$R_f = 10^5$

$C_f = 50$ pf

SW = 600 μm

SH = 3.0 mm

PMT = 750 VDC

Scale = 1.0 V/inch

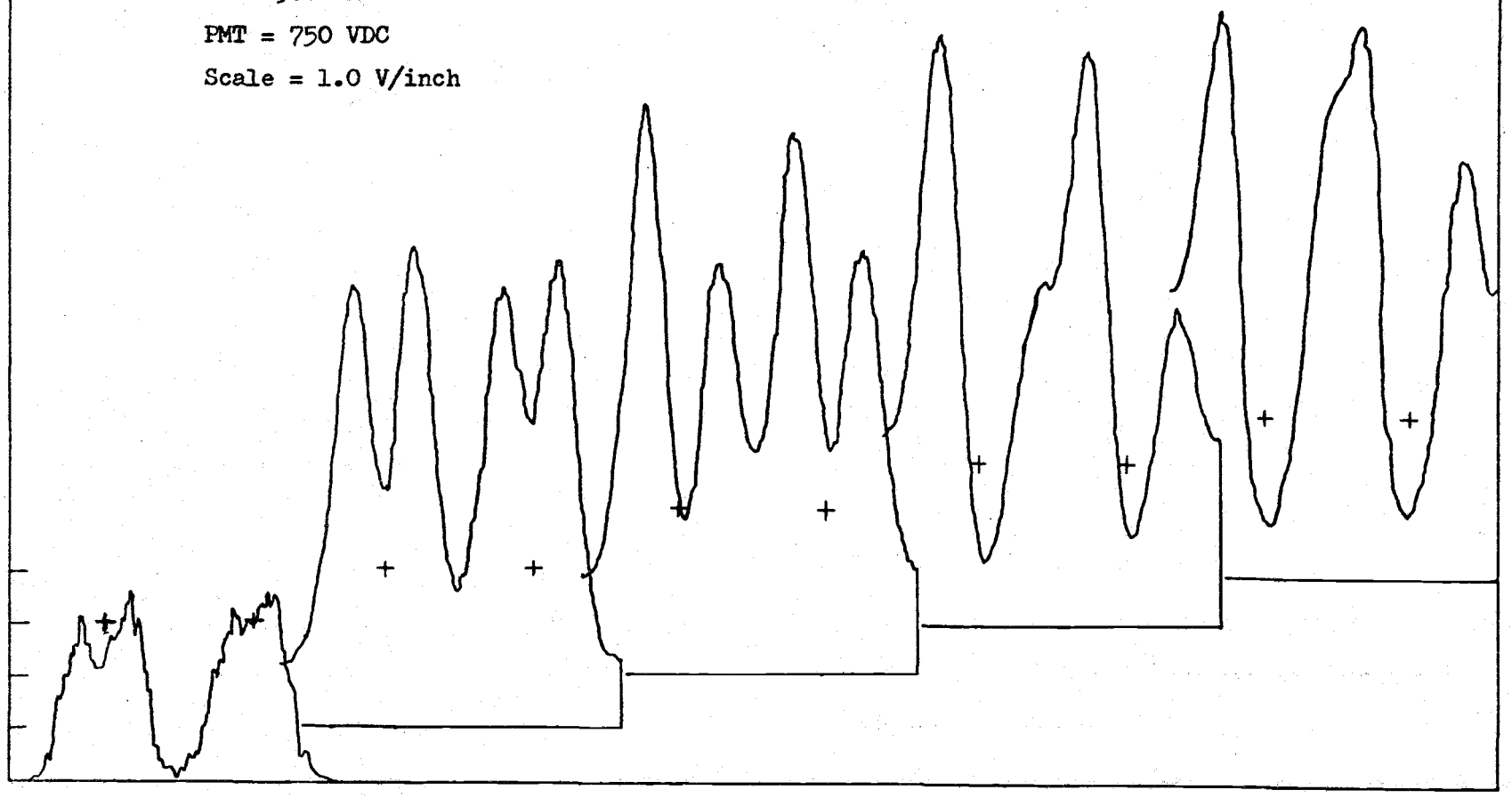

This cooler vapor absorbs the radiation emitted by the Cu atoms remaining in the excitation region of the cathode, causing first the decrease in intensity ratio and then, as the absorption increases, the self-reversal.

A close look at the figures will show that while the 400 mA pulse shows self-reversal immediately, it is not until the third time period that reversal appears at all in the 125 mA pulse, and the reversal is not severe until the fourth time period. At long time periods (0.5 mseconds) reversal is severe for both the 125 and 400 mA pulses. This may be due to the fact that the higher currents can cause greater sputtering from the cathode surface, increasing more quickly the number of absorbing atoms between the region of greatest intensity and the detection system.

The glowing region just outside the cathode of the lamp was visually observed to become brighter during the pulsing mode. Observations in a darkened room showed the glow region outside the cathode to increase in dimension along the axis of the tube with increasing pulse current. At 400 mA the length of the glow reached about 30 mm, compared to the 1-3 mm glow region seen in a 10 mA dc driven lamp.

Close observation of a self-reversed peak shows that the absorption is greater on the uv side of the emission line, causing an unsymmetrically absorbed line. Care must be taken in gauging the intensity of the wings of the lines since the overlap of the wing of one line with that of another, causes an apparent increase in intensity.

Measurements on the lamp in the dc mode and the pulsed mode were

made of the major line on a storage oscilloscope with moderately reversed lines having baseline resolution (the wings were not overlapped). It was observed within an experimental error of 0.0002 nm that the corresponding wings of the two emission lines (one from the pulsed mode and one from the dc mode) were not shifted with respect to each other. The absorption peak was found to be shifted toward the uv with respect to the peak of the dc level emission line by 0.00045 nm. The distance of this shift was about equal in magnitude to the minimum resolvable wavelength interval of the interferometer. This shift, if attributed to the Doppler effect, is equivalent to a stationary emitting and a stationary detector with an absorbing region moving toward the detector with a relative velocity of 4×10^4 cm/sec. This could be due to a relatively stationary emitting region within the cathode cup with most of the absorption due to atoms moving out of the cup into the cooler regions of the discharge. The actual shift would be somewhat less than the observed shift because the true absorption maximum and the apparent absorption peak do not coincide unless the 100% transmittance baseline is horizontal. In the hypothetical case of an absorbing region moving away from the emitting region, the 100% transmittance baseline is the shape of the emission line profile coming from the emission region.

Figure 18 indicates the increase in line width for the first time period with pulse current with a 10 mA dc background level. This appears to be mainly due to self absorption broadening since the increase in line width is also accompanied by a decrease in the ratio of the peak intensities of the hyperfine lines (Figure 18).

All of the above mentioned measurements were made on a 3.0 mm

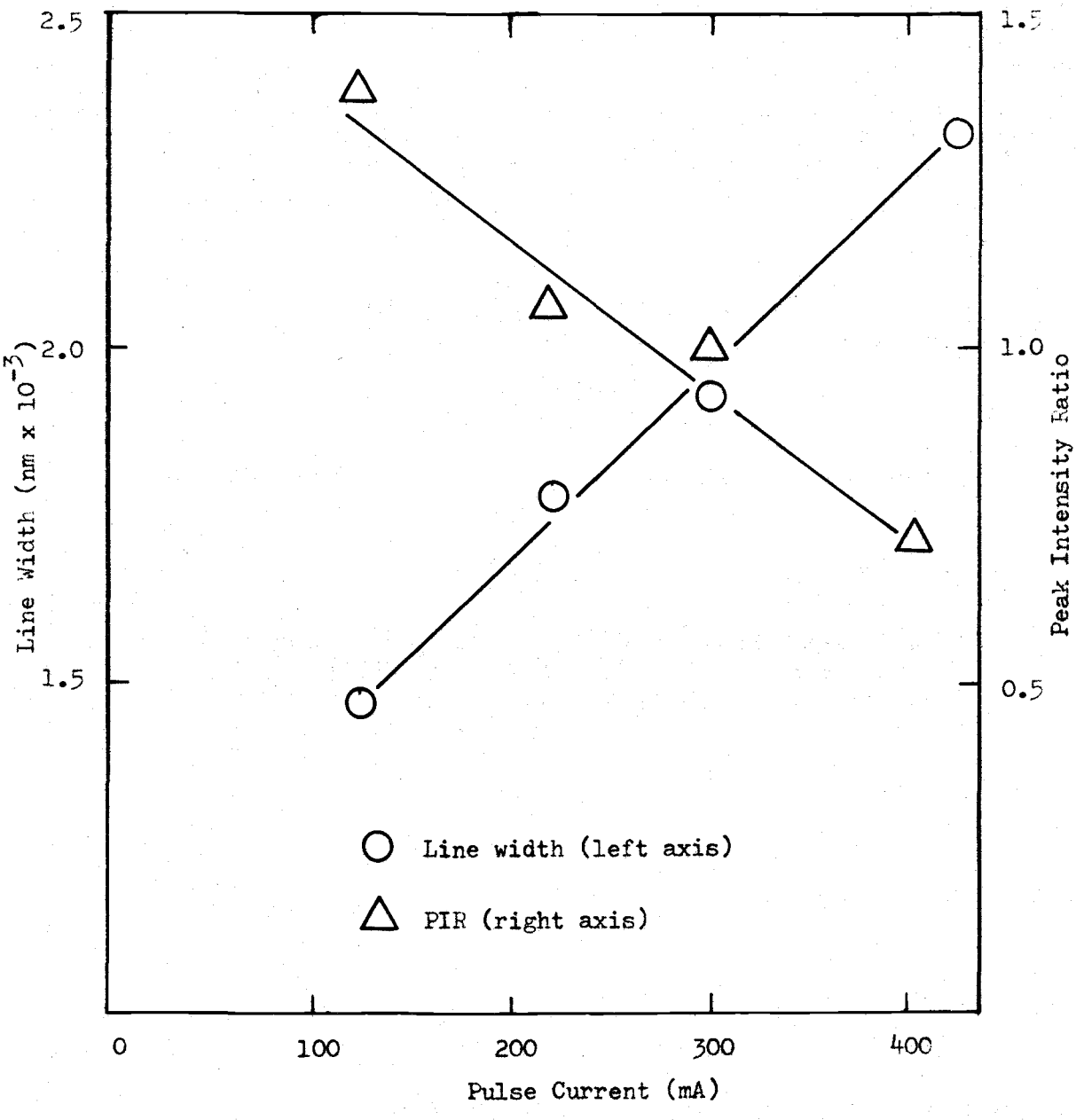

Figure 18. Line width (left axis) and peak intensity ratio (right axis) vs pulse current at a 10 mA dc background level for the first 21 μseconds of a pulse in the commercial hollow cathode lamp.

high by 0.60 mm wide cross-section of the cathode image. A 1.00 mm diameter aperture was placed at the entrance slit of the monochromator to allow better spatial resolution of the glow region. The remainder of the data concerning the commercial Cu lamp was obtained using the 1.00 mm entrance aperture.

Variation of Profile with DC Background Current Level

The next five figures (19 through 23) show variation of line profile and intensity for a pulse amplitude of 200 mA on top of various dc background levels (1-20 mA). The intensity scales are the same for these five figures. In all cases except at 1.0 mA dc, the first 21 μseconds shows no self-reversal, increasing to only moderate reversal after 42 μseconds. During the 21-42 μsecond time period the degree of self-reversal appears to decrease with increasing dc level. This may be attributed to the growth (increase in depth) of the excitation region with dc level accompanied by a corresponding decrease in the optical depth of the absorbing cloud, causing reduced self-reversal. In all cases the self-reversal is extreme after 100 μseconds.

A plot of the hyperfine peak intensity ratio for the first 21-μsecond interval is shown in Figure 24a for background current levels from 0 to 20 mA and a pulse current of 200 mA. Figure 12 shows a plot of line width during the first 21 μseconds of a 200-mA pulse for the major hyperfine line with various dc background levels. As the background dc current level increases, the half-width is seen to decrease and the peak intensity ratio increases. This is due to reduction in self

Figure 19. Time resolved line profiles of the Cu(I) 324.7 nm emission lines in the commercial hollow cathode lamp. Pulse current = 200 mA, dc background current level = 1.0 mA.

$R_f = 10^6$

$C_f = 5$ pf

SW = 1000 μm

PMT = 600 VDC

Scale = 1.0 V/inch

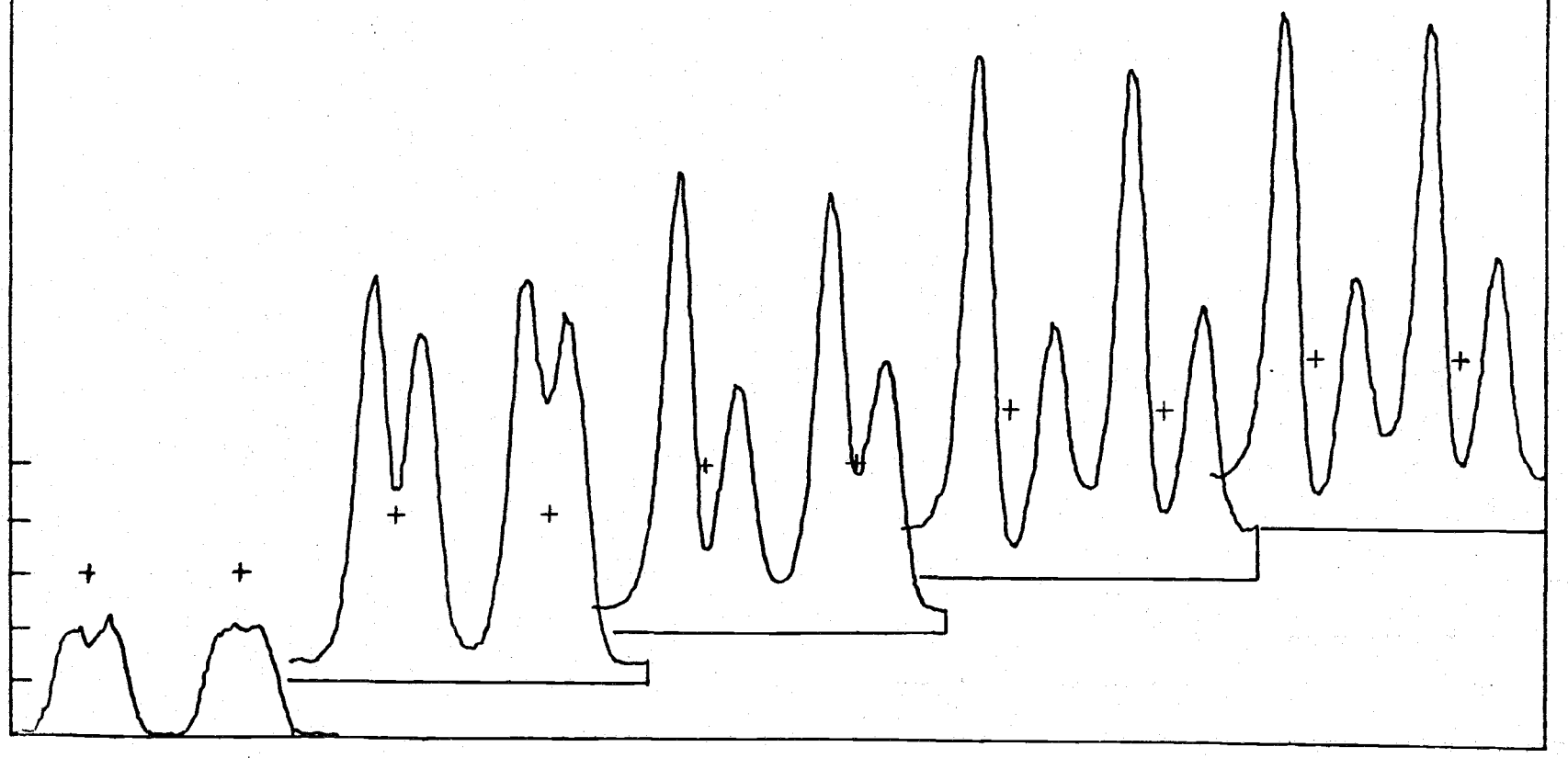

Figure 20. Time resolved line profiles of the Cu(I) 324.7 nm emission lines in the commercial hollow cathode lamp. Pulse current = 200 mA, dc background current level = 5 mA.

$R_f = 10^6$

$C_f = 5$ pf

SW = 1000 μm

PMT = 600 VDC

Scale = 1.0 V/inch

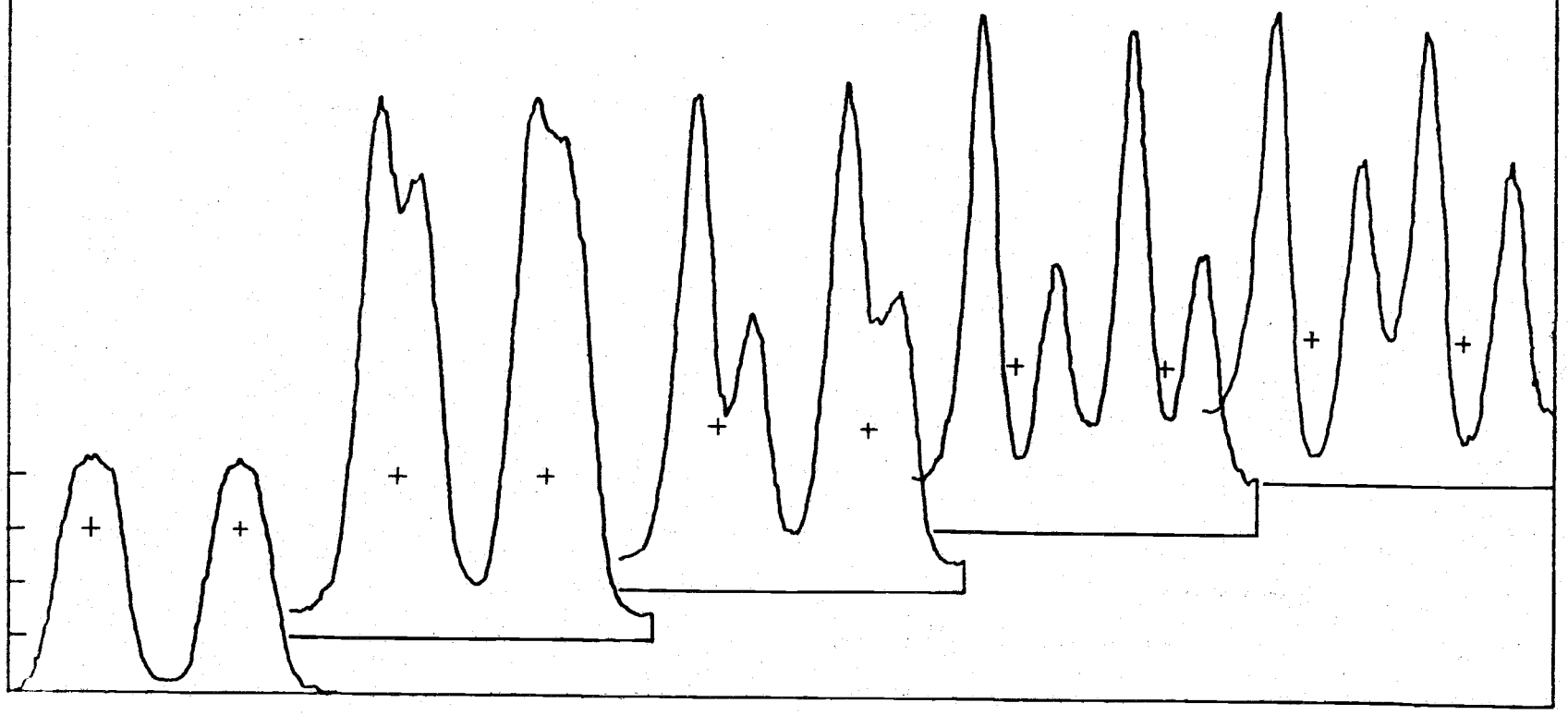

Figure 21. Time resolved line profiles of the Cu(I) 324.7 nm emission lines in the commercial hollow cathode lamp. Pulse current - 200 mA, dc background current level = 10 mA.

$R_f = 10^6$
$C_f = 5$ pf
SW = 1000 μm
PMT = 600 VDC
Scale = 1.0 V/inch

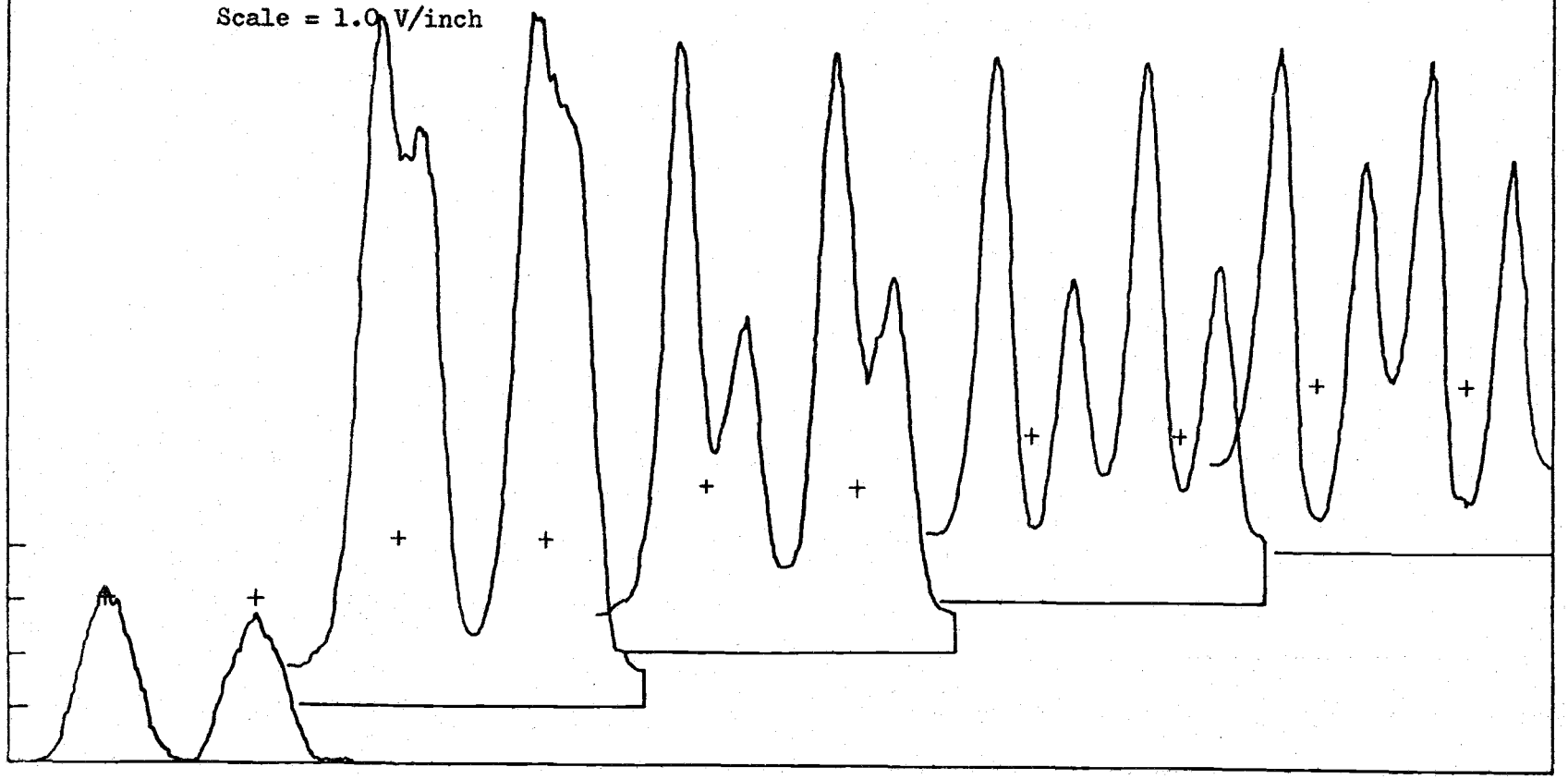

Figure 22. Time resolved line profiles of the Cu(I) 324.7 nm emission lines in the commercial hollow cathode lamp. Pulse current = 200 mA, dc background current level = 15 mA.

$R_f = 10^6$

$C_f = 5$ pf

SW = 1000 μm

PMT = 600 VDC

Scale = 1.0 V/inch

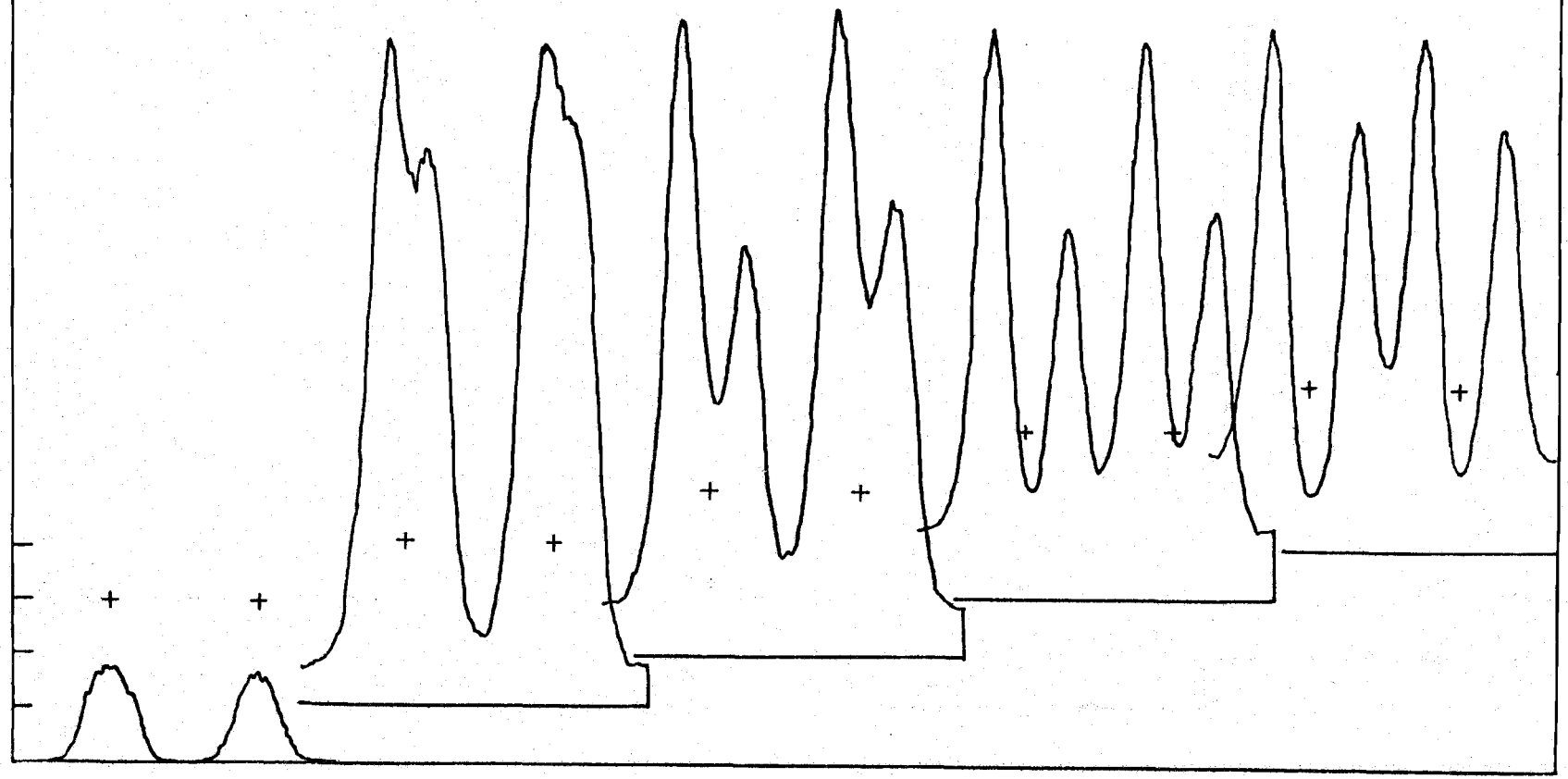

Figure 23. Time resolved line profiles of the Cu(I) 324.7 nm emission lines in the commercial hollow cathode lamp. Pulse current = 200 mA, dc background current level = 20 mA.

$R_f = 10^6$

$C_f = 5$ pf

SW = 1000 μm

PMT = 600 VDC

Scale = 1.0 V/inch

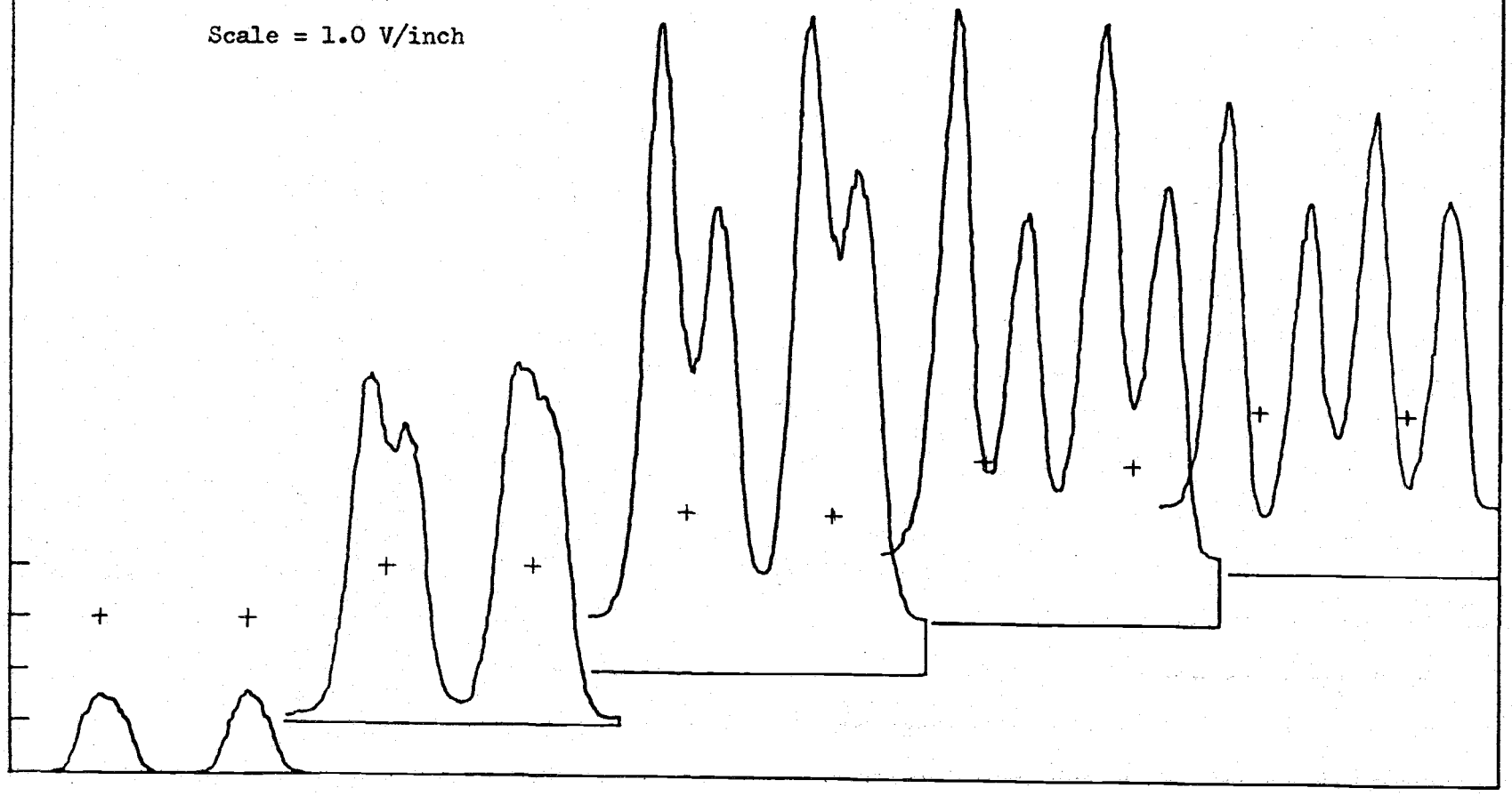

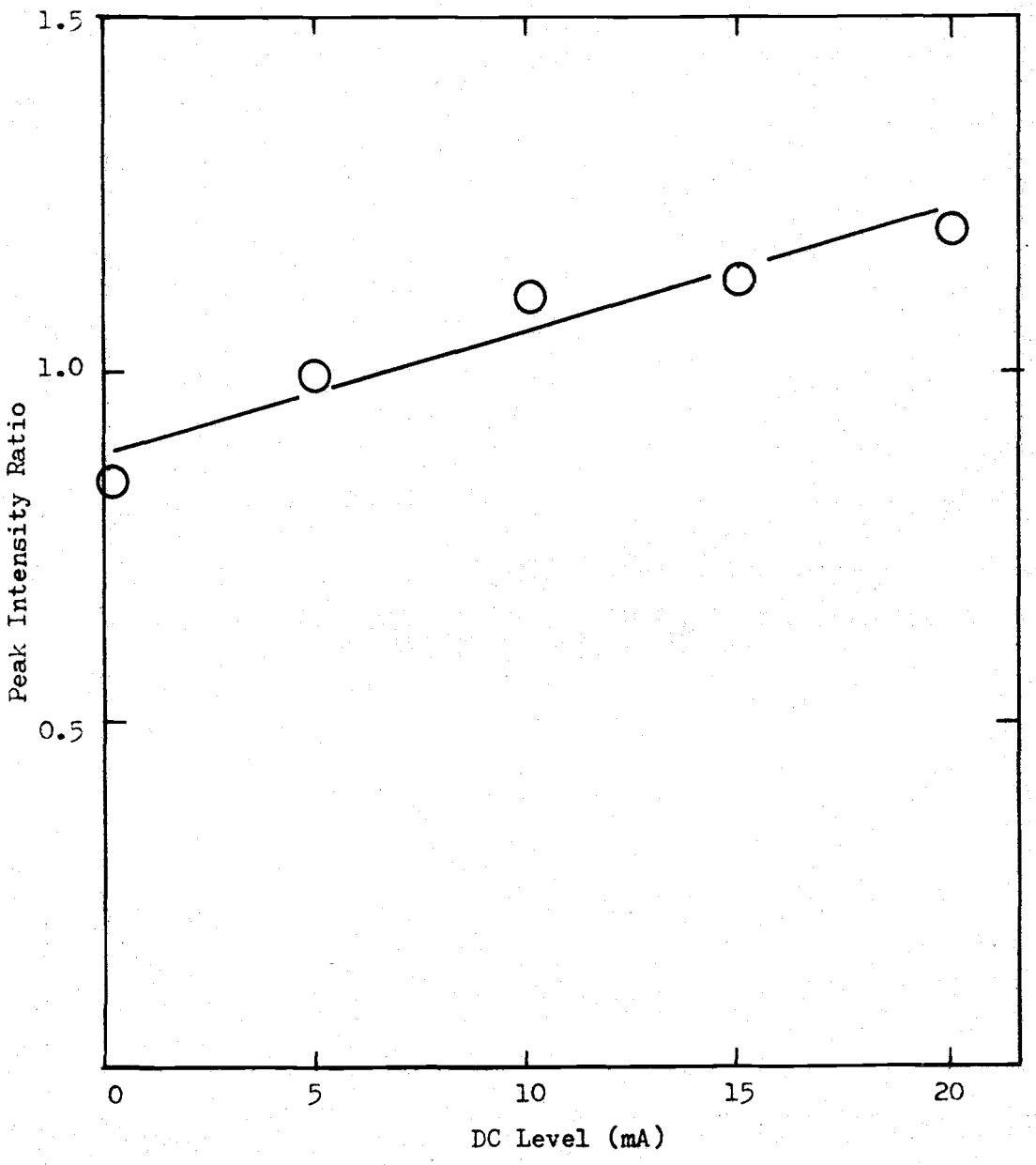

Figure 24a. Peak intensity ratio vs dc background current level for a commercial Cu lamp pulsed at 200 mA.

absorption with increasing background current.

It may also be seen from Figures 19 through 23 that the peak intensity (highest point on the self-reversal line) during the second time period increases with the background dc current up to 10 mA dc. It then levels off and decreases at 20 mA dc, with the third time period showing an increase in peak intensity.

Monitoring of the current pulse at various dc background levels showed a marked increase in pulse rise time (5% to 95%) from 5 μseconds at 1-mA dc background current to 30 μseconds at 20-mA dc background current. This may be due in part to the space charge which is set up within the lamp under dc conditions. The space charge provides a fixed voltage profile and ion distribution within the lamp that tends to stabilize the lamp against change prior to the pulse discharge. As the dc current level increases, the size of the space charge (and the visual glow region) also increases, giving the lamp greater stability. Thus, at higher dc current levels (caused by application of higher voltages to the lamp) the stabilizing effect of the space charge may be causing a greater delay in the onset of the current flow and hence a delay in the increase in peak intensity seen in the time resolved profiles. This delay in reaching maximum current will also delay the increased sputtering associated with it, and hence also delay the onset of self-reversal seen at high sputtering rates.

Spatial Resolution of Emission Region

Figures 24b through 29 show the line profiles observed at the center 1.00 mm of the emission image and the edge 1.00 mm of the emission image for three pulse levels (125 mA, 225 mA, and 400 mA). The intensity scale for each pair of Figures is the same. The most notable new information is that in all three cases the reversal of the emission line is more severe at the edge of the discharge than at the center of the discharge. This indicates that the copper vapor is more concentrated at the edge where it is originally introduced by sputtering than it is in the center. The profiles for a 10 mA dc level discharge are identical at the edge and center of the discharge, as shown in Figure 30. This indicates uniform excitation and diffusion phenomena across the area of observation.

Pulse Durations Longer than 300 μseconds

Cordos and Malmstadt (5) reported a linear relationship between pulse current and integrated intensity for this type of copper hollow cathode lamp. This linear relationship was duplicated in this research for both 300 μsecond and 5 msecond long pulses, Figure 31. This was accompanied by monitoring the current pulse generated at the photomultiplier on an oscilloscope with the interferometer removed from the system.

Cordos and Malmstadt used an "intermittant" pulse mode in which the lamp was pulsed at 10 Hz for 5-10 mseconds for about 2 seconds with a pause of 15 seconds between each series of pulses. They reported that

Figure 24b. Time resolved line profiles of the Cu(I) 324.7 nm emission lines at the center 1.00 mm of the discharge in the commercial hollow cathode lamp. Pulse current = 125 mA, dc background current level = 5.0 mA.

$R_f = 10^5$

$C_f = 50$ pf

SW = 1000 μm

PMT = 700 VDC

Scale = 0.2 V/inch

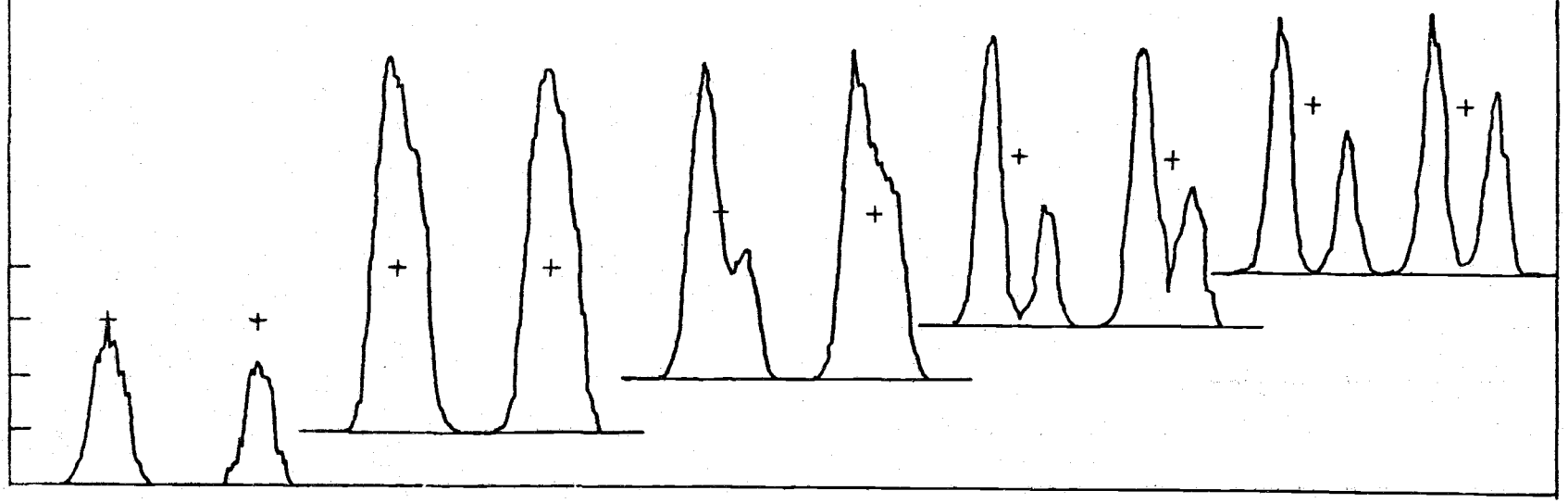

Figure 25. Time resolved line profiles of the Cu(I) 324.7 nm emission lines at the edge 1.00 mm of the discharge in the commercial hollow cathode lamp. Pulse current = 125 mA, dc background current level = 5 mA.

$R_f = 10^5$

C_f = 50 pf

SW = 1000 μm

PMT = 610 VDC

Scale = 0.5 V/inch

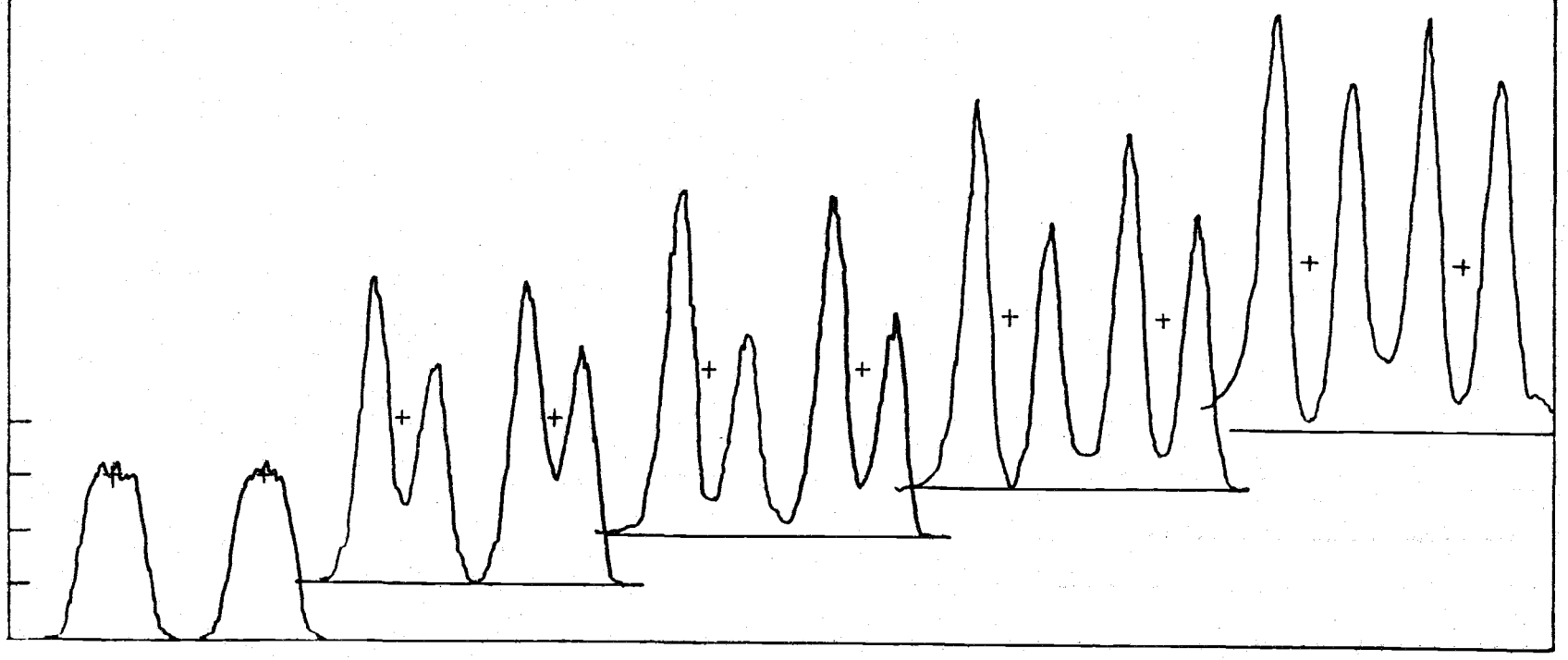

Figure 26. Time resolved line profiles of the Cu(I) 324.7 nm emission lines at the center 1.00 mm of the discharge in the commercial hollow cathode lamp. Pulse current = 225 mA, dc background current level = 5 mA.

$R_f = 10^6$

$C_f = 5$ pf

SW = 1000 μm

PMT = 600 VDC

Scale = 1.0 V/inch

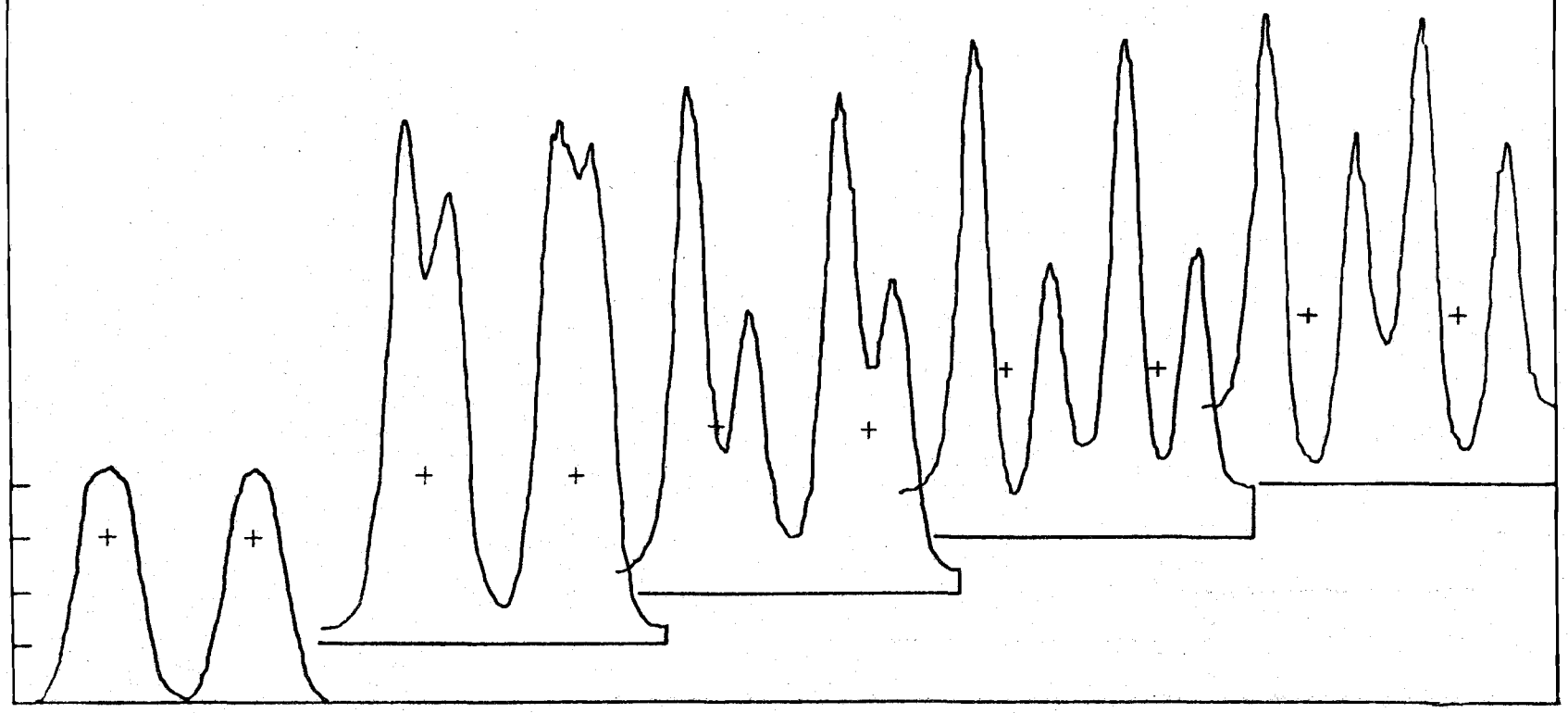

Figure 27. Time resolved line profiles of the Cu(I) 324.7 nm emission lines at the edge 1.00 mm of the commercial hollow cathode lamp. Pulse current = 225 mA, dc background current level = 5 mA.

$R_f = 10^6$

$C_f = 5$ pf

SW = 1000 μm

PMT = 600 VDC

Scale = 1.0 V/inch

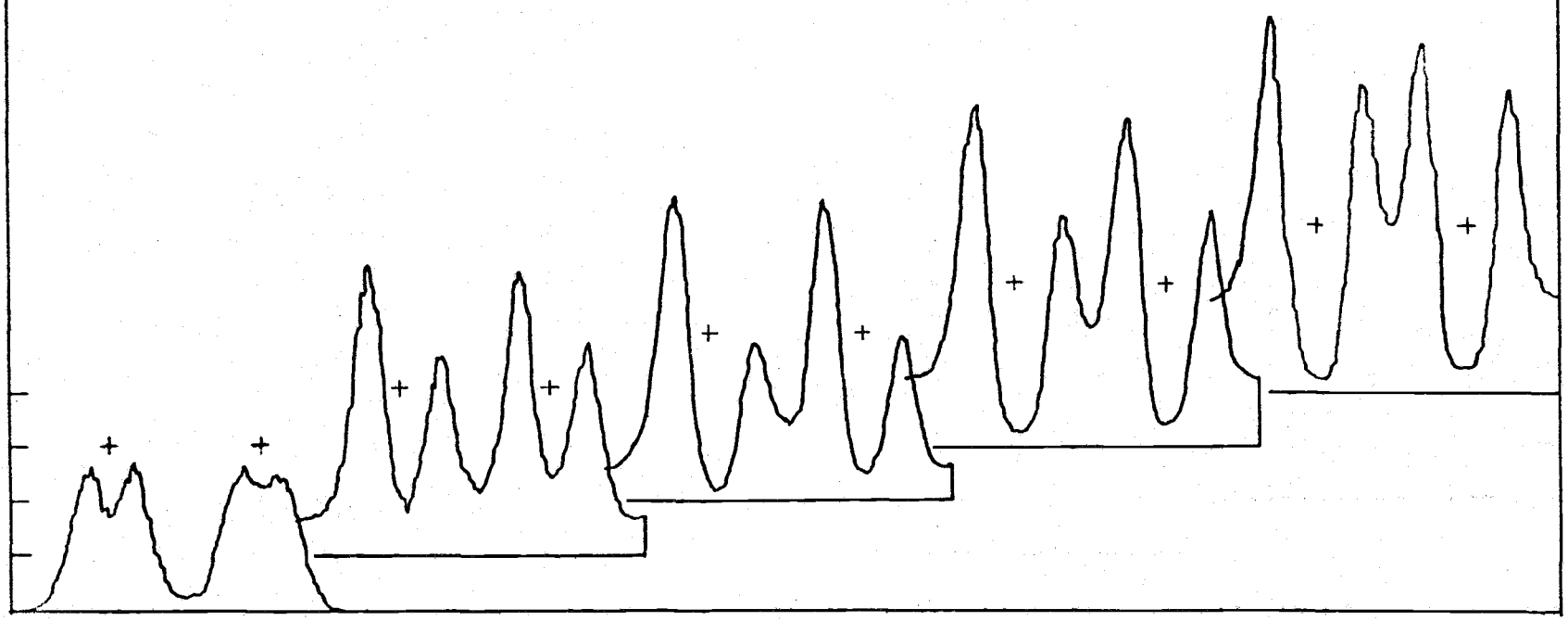

Figure 28. Time resolved line profiles of the Cu(I) 324.7 nm emission lines at the center 1.00 mm of the discharge in the commercial hollow cathode lamp. Pulse current = 400 mA, dc background current level = 5 mA.

$R_f = 10^6$

$C_f = 5$ pf

SW = 1000 μm

PMT = 570 VDC

Scale = 1.0 V/inch

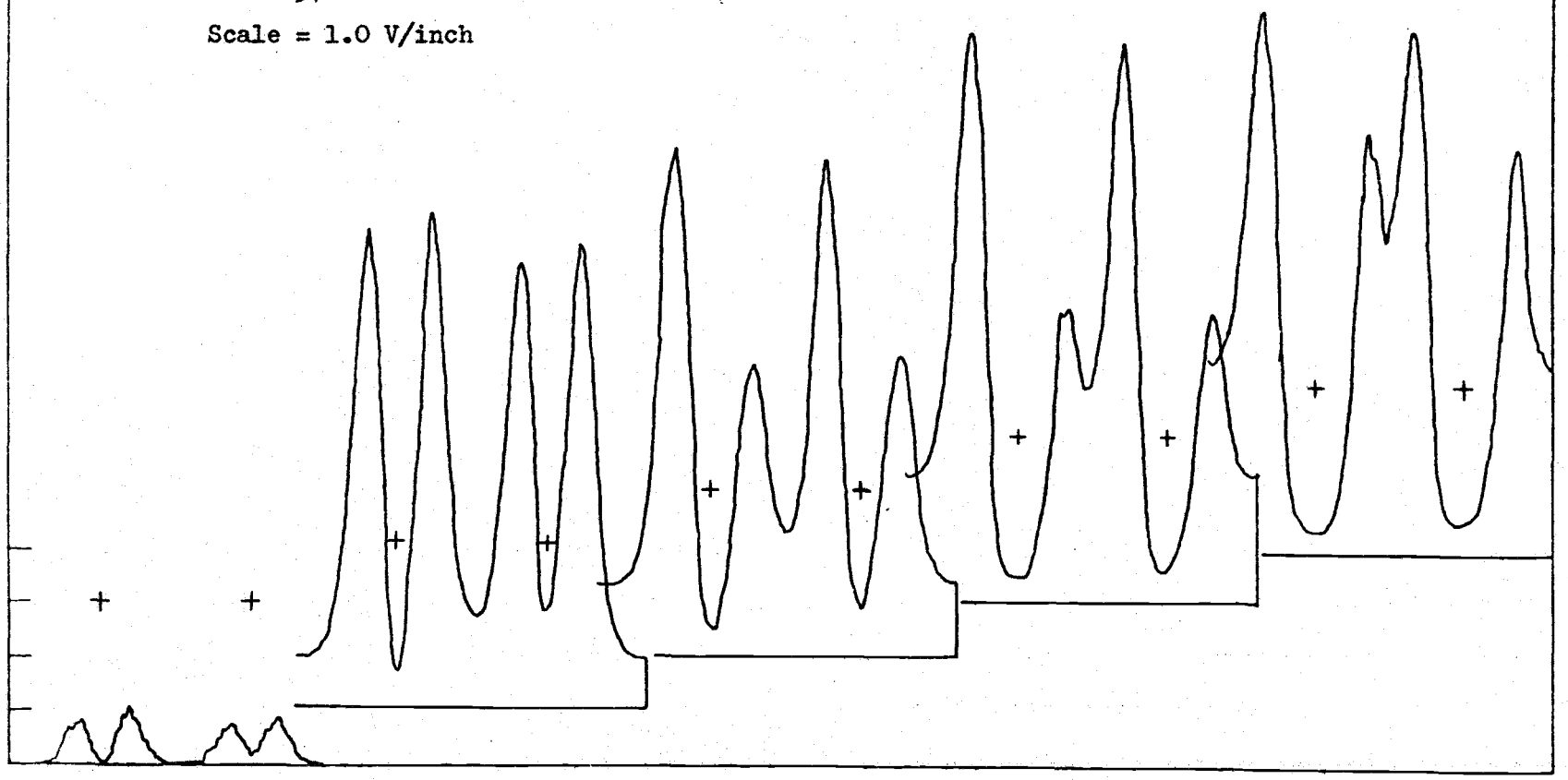

Figure 29. Time resolved line profiles of the Cu(I) 324.7 nm emission lines at the edge 1.00 mm of the discharge in the commercial hollow cathode lamp. Pulse current = 400 mA, dc background current level = 5 mA.

$R_f = 10^6$

$C_f = 5$ pf

SW = 1000 μm

PMT = 570 VDC

Scale = 1.0 V/inch

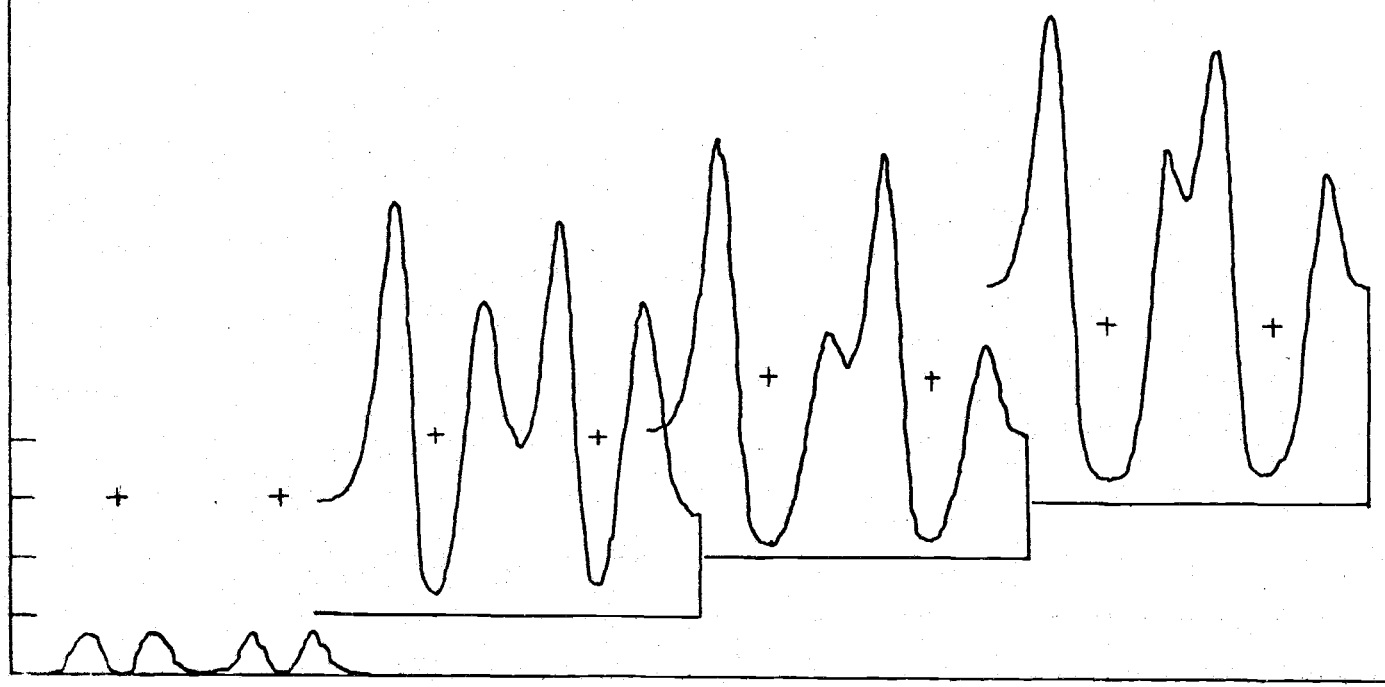

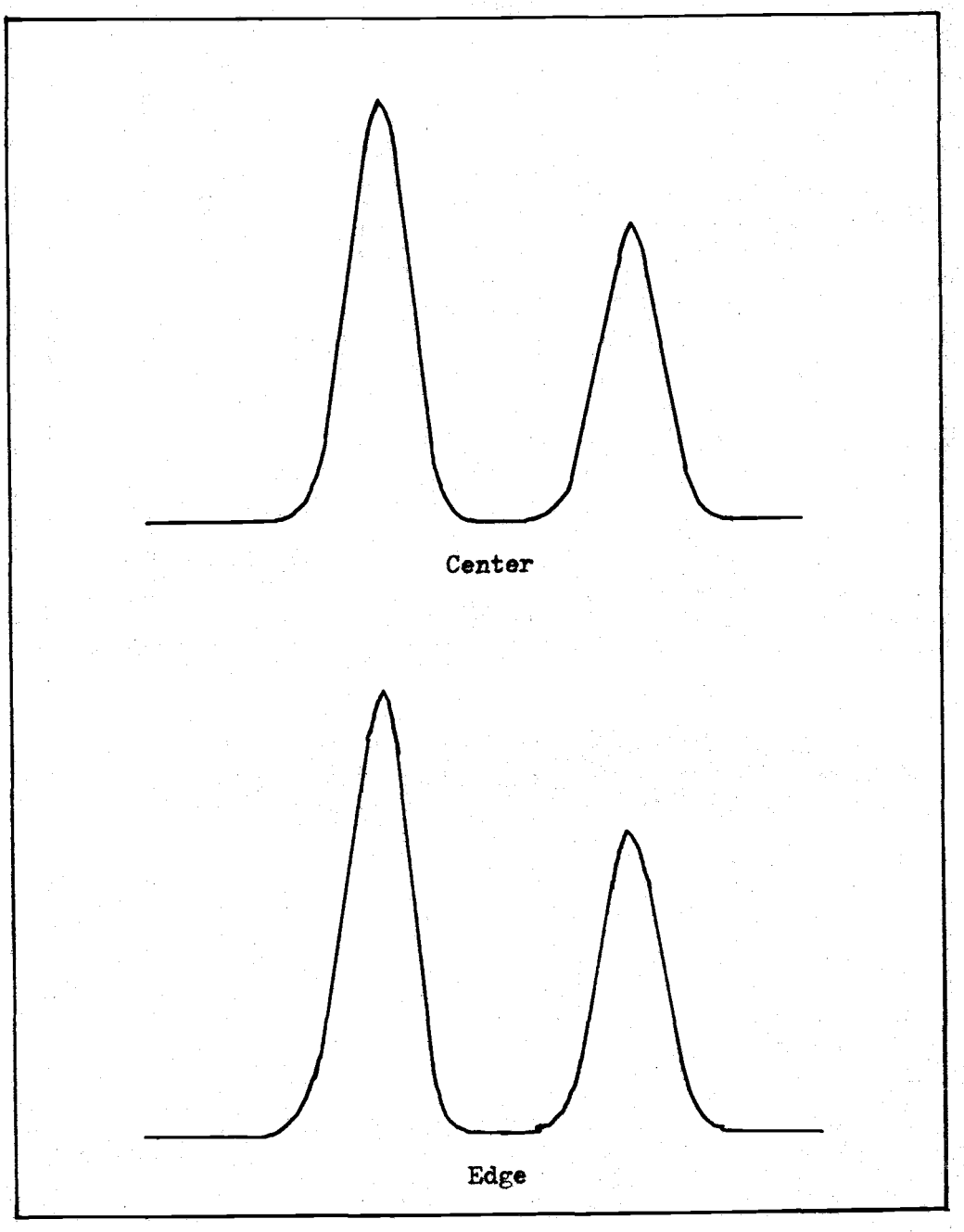

Figure 30. Copper 324.7 nm doublet at center 1.00 mm and edge 1.00 mm of the discharge region in the commercial hollow cathode lamp at a 12.0 mA dc current level.

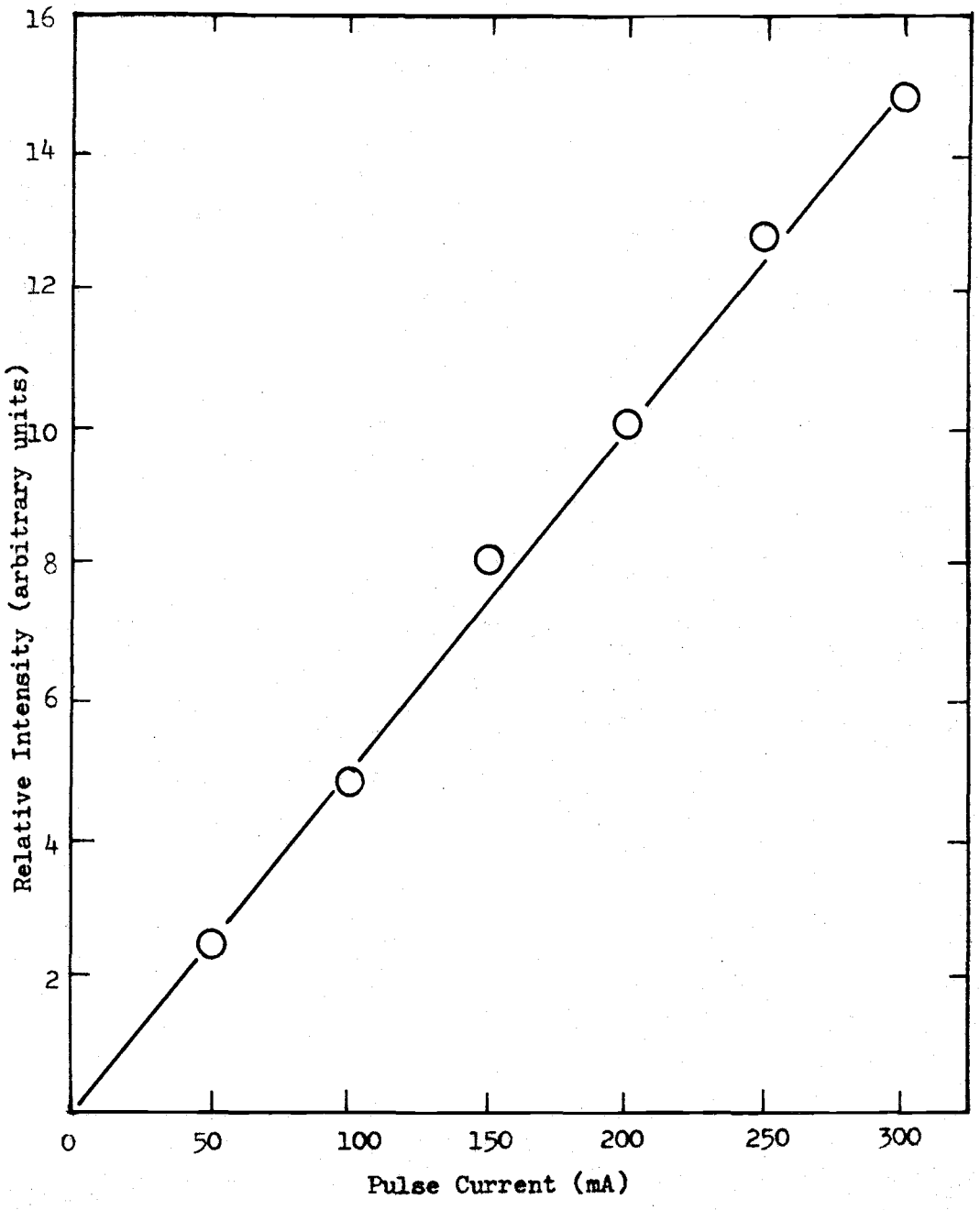

Figure 31. Relative integrated Cu intensity vs pulse current for the commercial hollow cathode lamp.

Figure 32. Time resolved line profiles of the Cu(I) 324.7 nm emission lines. Pulse duration was 5 mseconds, line profiles are 0.5 mseconds apart. Pulse = 100 mA, dc = 0.0 mA.

$R_f = 10^5$

$C_f = 50$ pf

SW = 1000 μm

PMT = 720 VDC

Scale = 1.0 V/inch

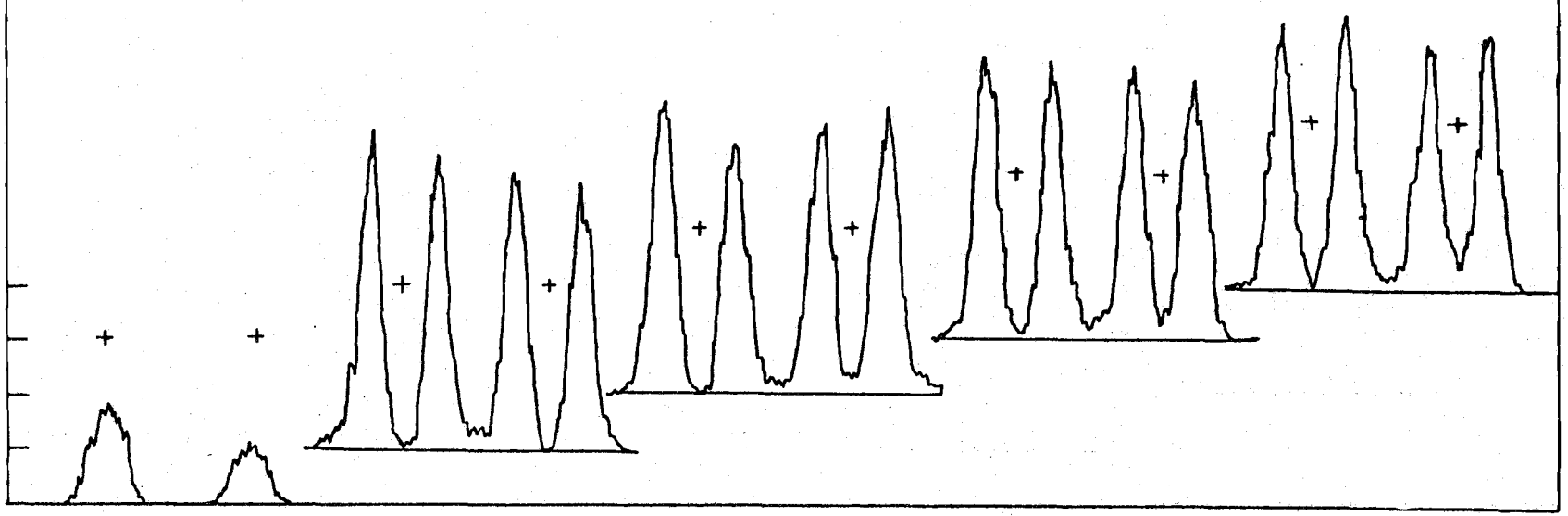

Figure 33. Time resolved line profiles of the Cu(I) 324.7 nm emission lines. Pulse duration was 5 mseconds, line profiles are 0.5 mseconds apart. Pulse current = 150 mA, dc background current level = 0 mA.

$R_f = 10^5$

$C_f = 50$ pf

SW = 1000 μm

PMT = 720 VDC

Scale = 1.0 V/inch

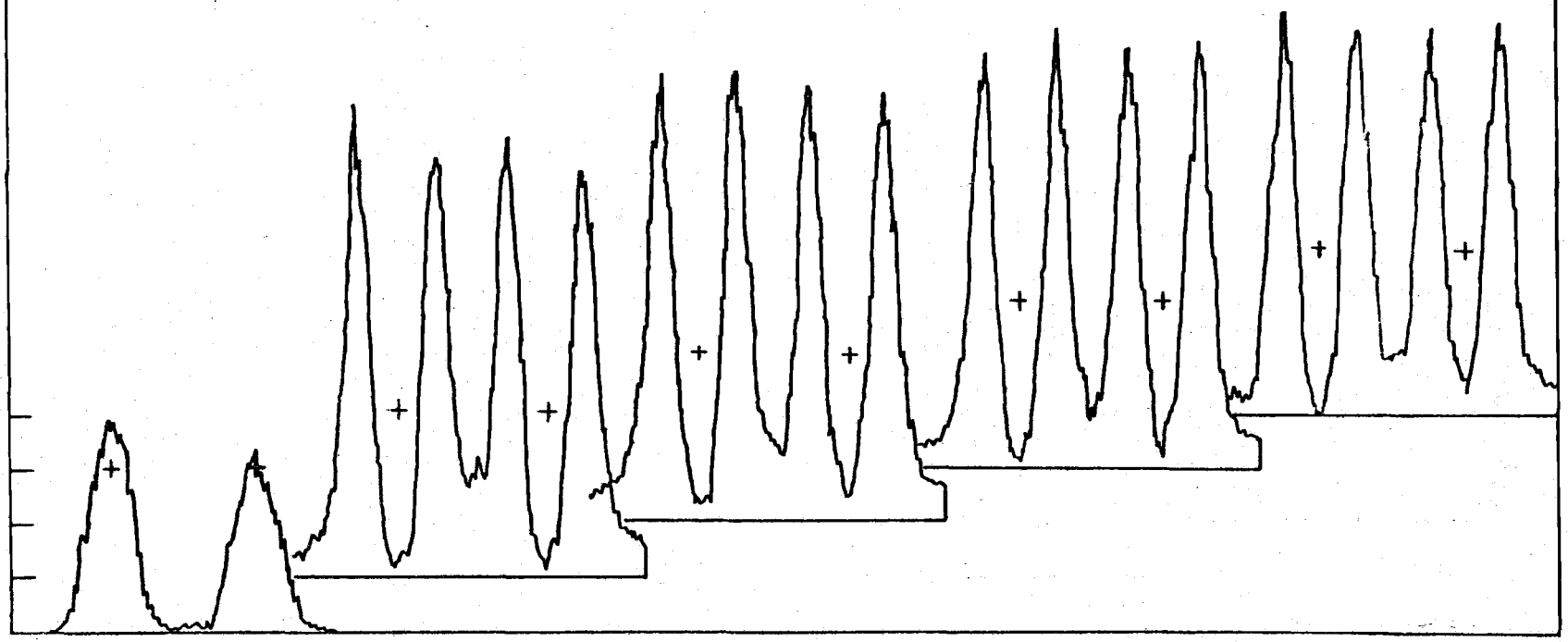

Figure 34. Time resolved line profiles of the Cu(I) 324.7 nm emission lines. Pulse duration was 5 mseconds, line profiles are 0.5 mseconds apart. Pulse current = 200 mA, dc background level = 0 mA.

$R_f = 10^5$

$C_f = 50$ pf

SW = 1000 μm

PMT = 720 VDC

Scale = 1.0 V/inch

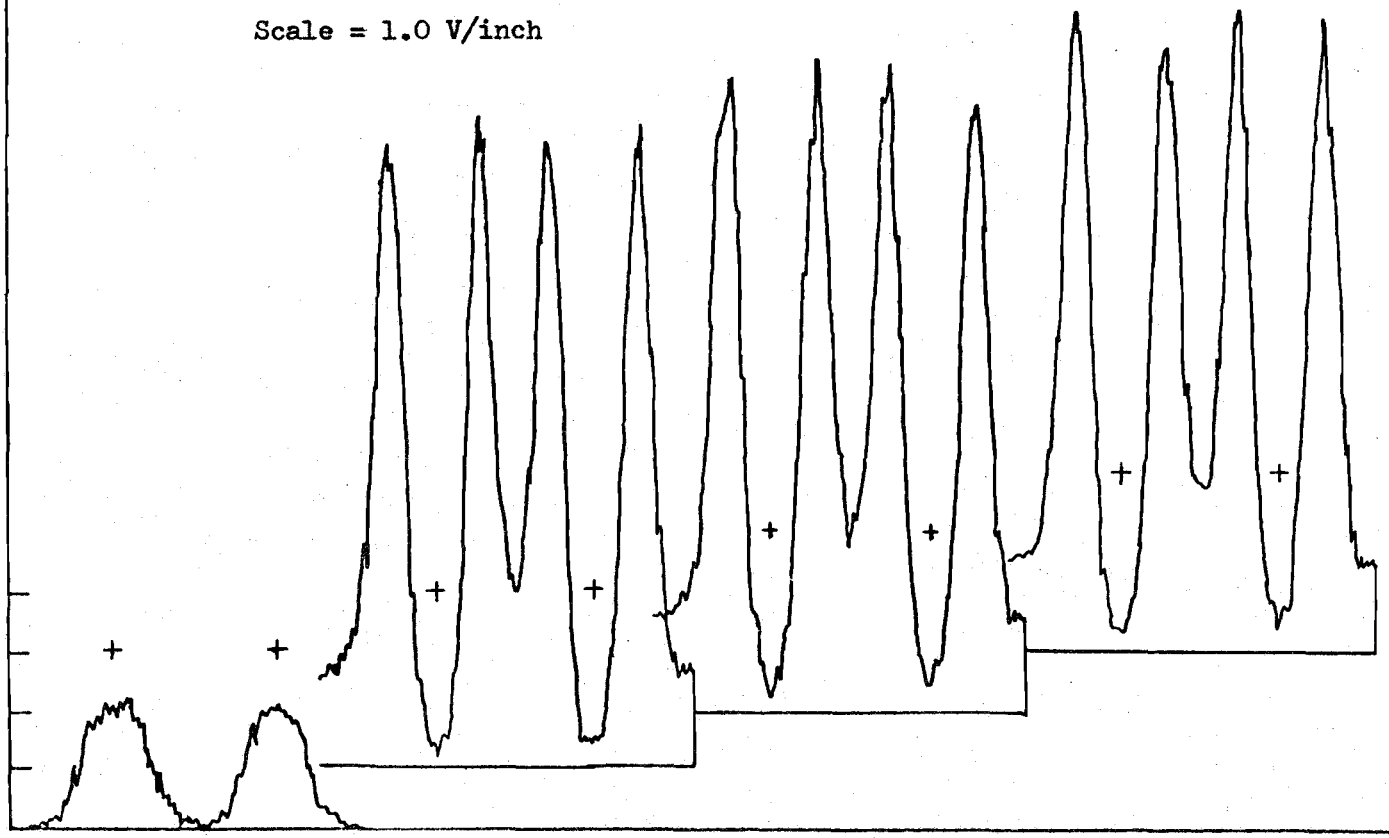

this linear relationship led them to believe that no self-reversal of the line occurred. This hypothesis was tested in this research by modifying the computer program to collect and output a line profile (21 μseconds long) at each 0.5-msecond interval during a 5-msecond pulse. To shorten the experiment to a reasonable length, only 4 scans were superimposed. Other instrumental parameters were the same as those used before on the shorter pulses (see data on the Figures). The time resolved outputs for the pulse levels of 100 mA, 150 mA, and 200 mA are shown in Figures 32, 33, and 34, respectively. All of the scans have directly comparable intensity scales. Note that in all cases extreme self-reversal is seen 0.5 mseconds after the initiation of the pulse.

Two of these pulse levels, 150 mA and 200 mA, were studied during the first 210 μseconds of the 5-msecond pulse using the computer routine for the 300-μsecond pulses but modified for 10 Hz operation. Only four scans were superimposed for each output rather than the normal 64 to shorten each run to 250 seconds to minimize the influence of interferometer drift. The results are shown in Figure 35 for 150 mA and 36 and 37 for 200 mA. Intensity scales for these profiles are the same as for those of Figures 32 through 34. These profiles taken during the first 210 μseconds show that the reversal starts early in the pulse (as seen for the short 300-μsecond pulses) and reaches a steady state (no change in intensity or profile with time) after about 100 μseconds for the 150-mA pulse and after 200 μseconds for the 200-mA pulse.

Thus, while the time and wavelength integrated intensity for a

Figure 35. Time resolved line profiles of the Cu(I) 324.7 emission lines. Pulse duration was 5.0 mseconds, line profiles taken sequentially each 21 μseconds. Pulse current = 150 mA, dc background current level = 0 mA.

$R_f = 10^5$

$C_f = 50$ pf

SW = 1000 μm

PMT = 720 VDC

Scale = 1.0 V/inch

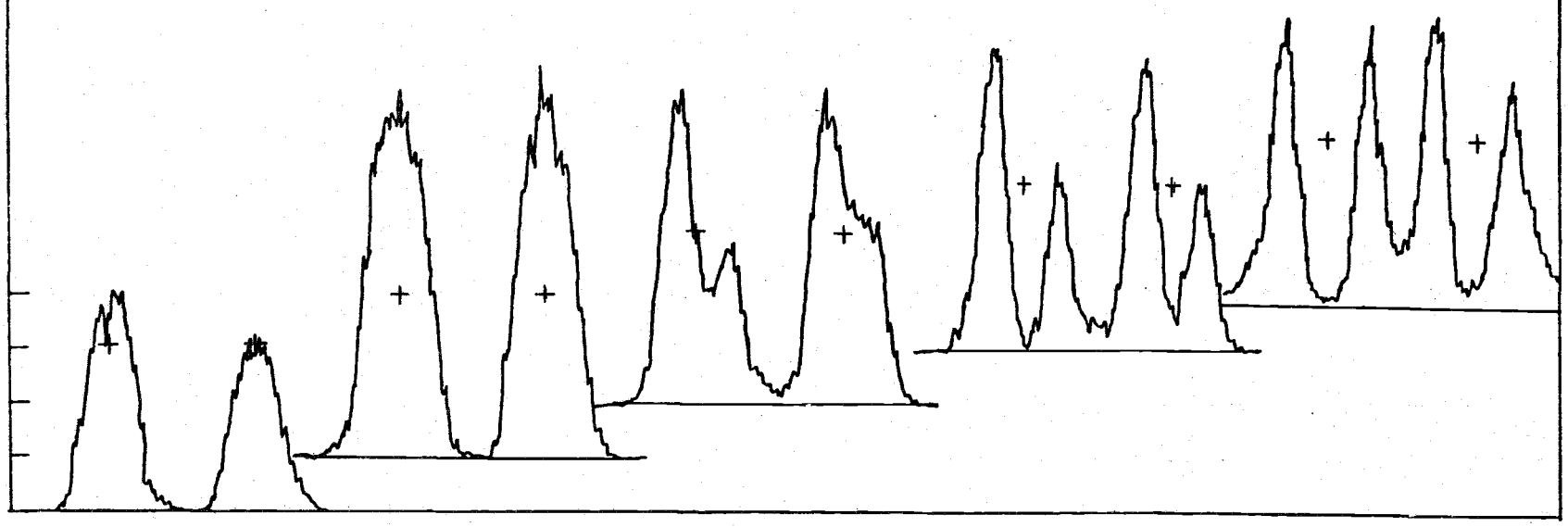

Figure 36. Time resolved line profiles of the Cu(I) 324.7 emission lines. Pulse duration was 5.0 mseconds, line profiles taken sequentially each 21 μseconds. Time periods 1 through 5. Pulse current = 200 mA, dc background current level = 0 mA.

$R_f = 10^5$

$C_f = 50$ pf

SW = 1000 μm

PMT = 720 VDC

Scale = 1.0 V/inch

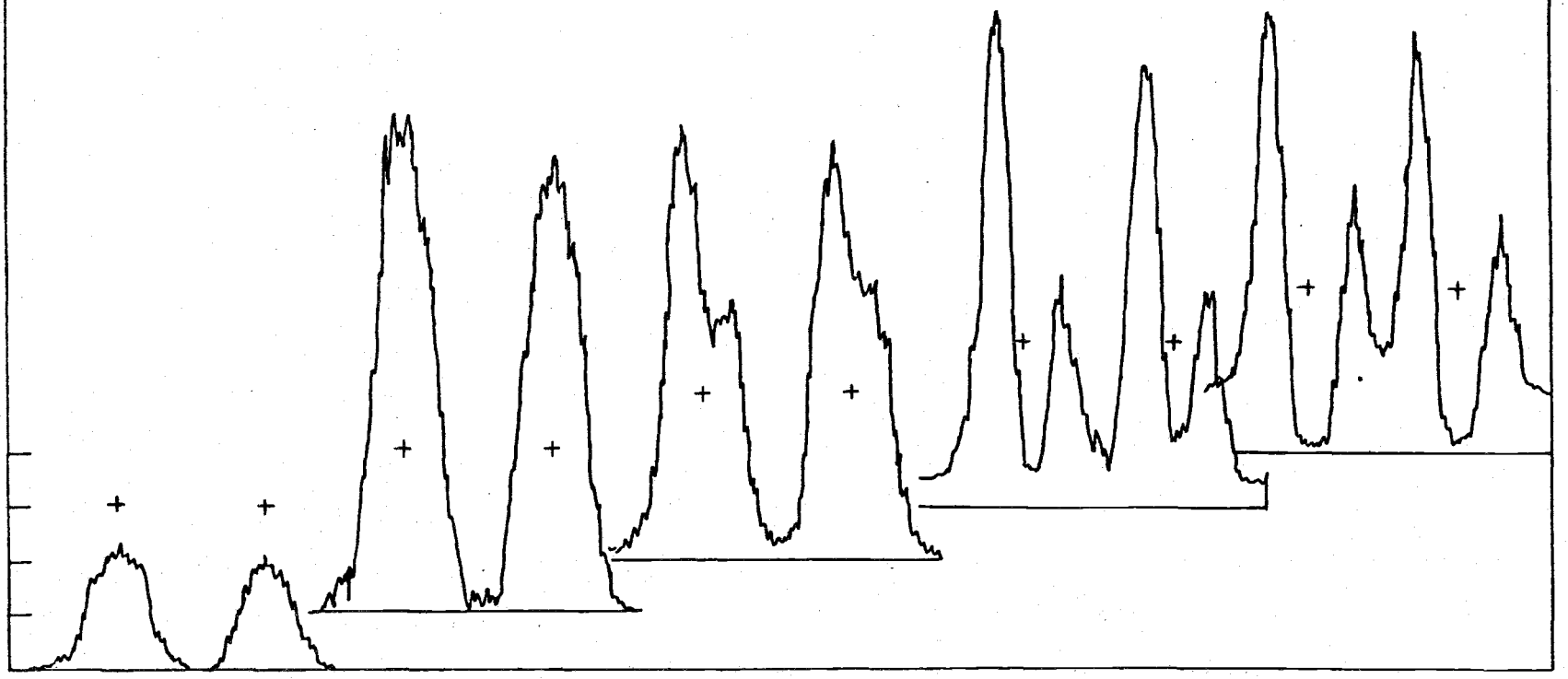

Figure 37. Time resolved line profiles of the Cu(I) 324.7 emission lines. Pulse duration was 5.0 mseconds, line profiles taken sequentially each 21 μseconds. Time periods 6 through 10. Pulse current = 200 mA, dc background current level = 0 mA.

$R_f = 10^5$

C_f = 50 pf

SW = 1000 μm

PMT = 720 VDC

Scale = 1.0 V/inch

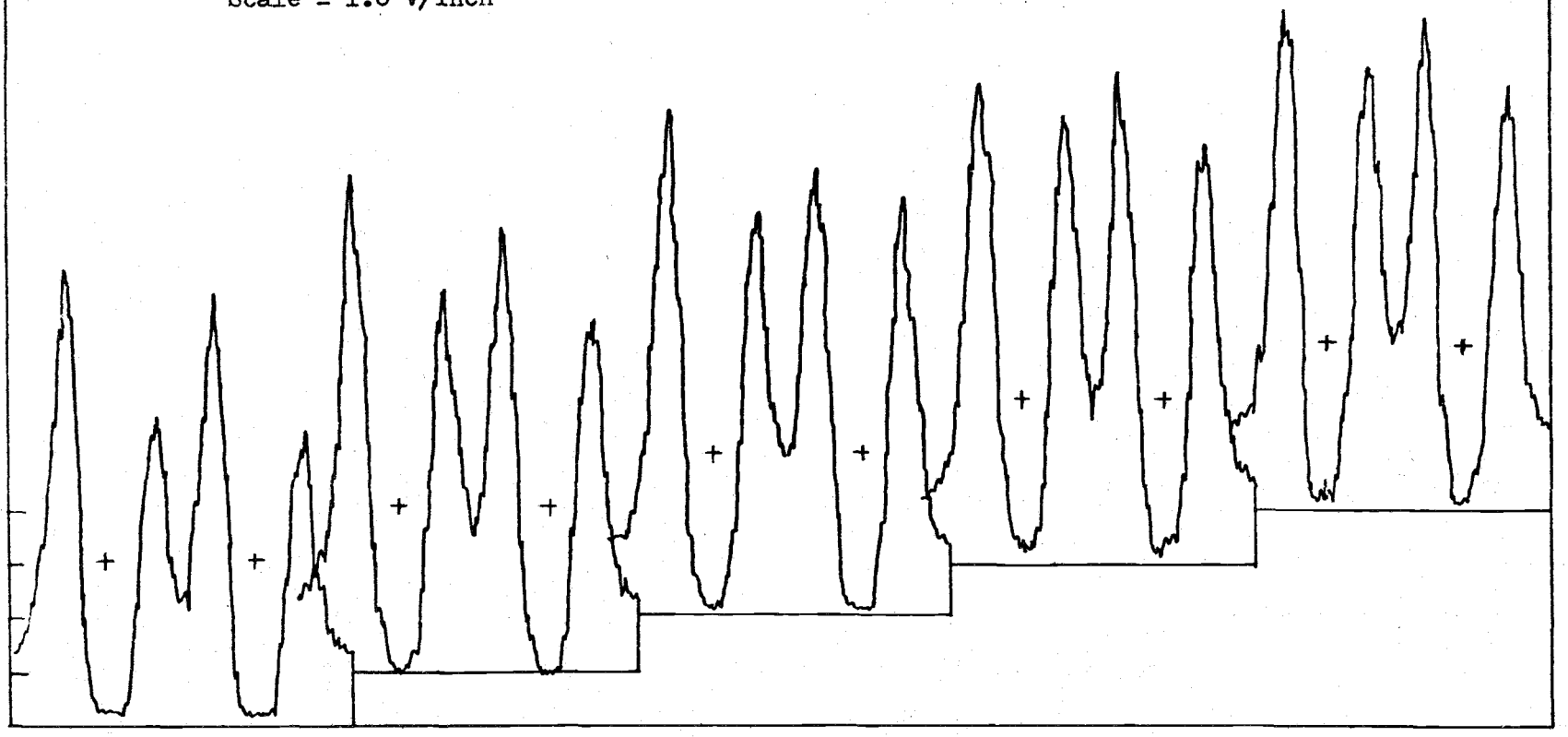

pulse does increase with pulse current, there remains strong self-reversal in the Cu doublet even for long pulses at low pulse rates, indicating that great care must be taken in the interpretation of data for pulsed systems in which there are large concentration and energy gradients, and where one parameter, such as lamp current, may change not only the sampling rate but also the shape or size of the discharge regions.

A Short Comparison with a Silver Lamp

To demonstrate the influence that concentration has upon self-reversal, a brief study of a silver hollow cathode lamp was made. Figure 38 shows the 328.07 nm line of silver in a Westinghouse No. 22806B silver hollow cathode lamp driven in the pulsed mode at 200 mA with a 5 mA dc background level. Silver has a higher sputtering rate than copper under low pressure conditions (13) and is a heavier atom that diffuses more slowly. Therefore silver would be expected to have a higher concentration in the lamp than copper under similar conditions. Since the transition probability for the silver line is only 20% less than the copper line, the increased concentration would be expected to be accompanied by stronger self-reversal. Figure 38 shows this to be so. Additional evidence for the increased concentration was the observation of a heavy silver plating on the walls of the silver hollow cathode tube after only two hours of pulsed operation. The copper tube showed less plating even after days of continuous similar operation.

Figure 38. Time resolved line profile of the Ag(I) emission line at 328.0 nm in a commercial hollow cathode lamp. Pulse level = 200 mA, dc background level = 5.0 mA.

$R_f = 10^6$

$C_f = 5$ pf

SW = 1000 μm

PMT = 710 VDC

Scale = 0.2 V/inch

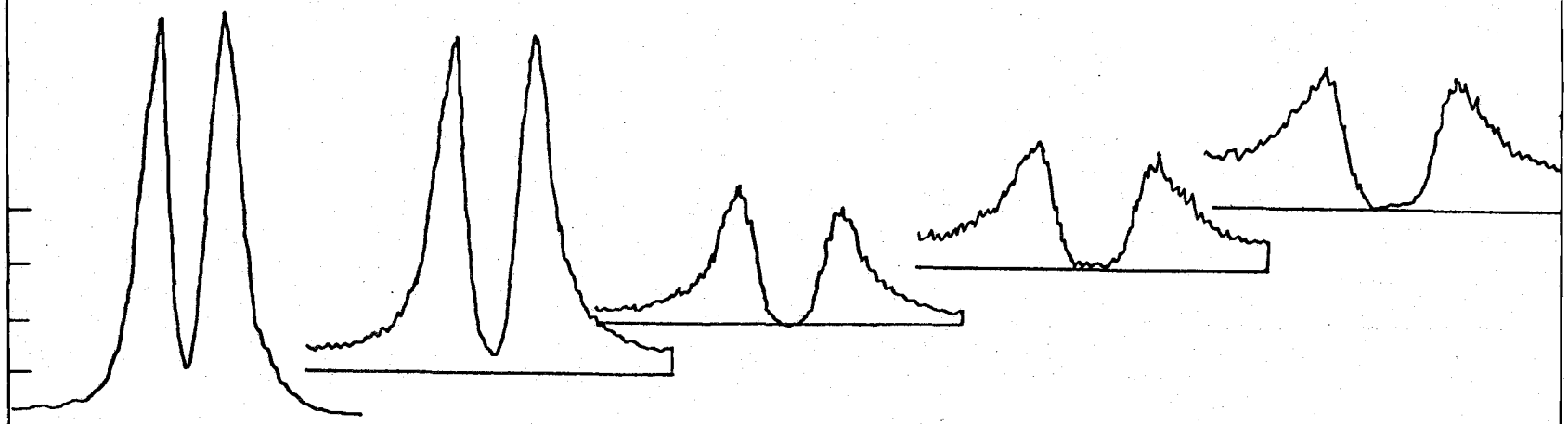

Demountable Hollow Cathode Lamp

The demountable hollow cathode lamp was used to study the effect of various electrode configurations and inert gas pressures on the 324.7 nm Cu(I) emission lines during pulsed operation. The electrodes, Figure 39 , were connected to tungsten support wires with crimp connectors fashioned from a one-half inch long piece of 1/8" OD, 1/16" ID copper tubing. The wire from the electrode was crimped into one end of the piece of tubing, and this assembly crimped onto the tungsten for good mechanical and electrical contact.

Electrode configurations which were used include parallel plate electrodes, point cathode and plate anode, and point electrodes. Little or no Cu emission was detected either in the region between the electrodes or at the surface of the electrodes under normal glow discharge conditions (10-20 mA dc). Under pulsed conditions (up to 200 mA pulses) there was no detectable Cu emission from the plate electrodes. Under pulsed conditions the point cathode produced a small, brilliant blue-white glow at the junction of the copper tubing and the copper wire forming the electrode (Figure 40 (a)). The Cu emission from this glow was found to be orders of magnitude greater than in any other part of the discharge. A second type of cathode, Figure 40 (b), was constructed by filing the point flat with the face of the copper tubing. It also formed a brilliant blue-white glow region under pulsed conditions (50 mA - 300 mA) at moderately high pressures (15-25 Torr). At lower pressures the glow was not seen, but was replaced with a normal glow. At higher pressures the discharge was extinguished as the sparking

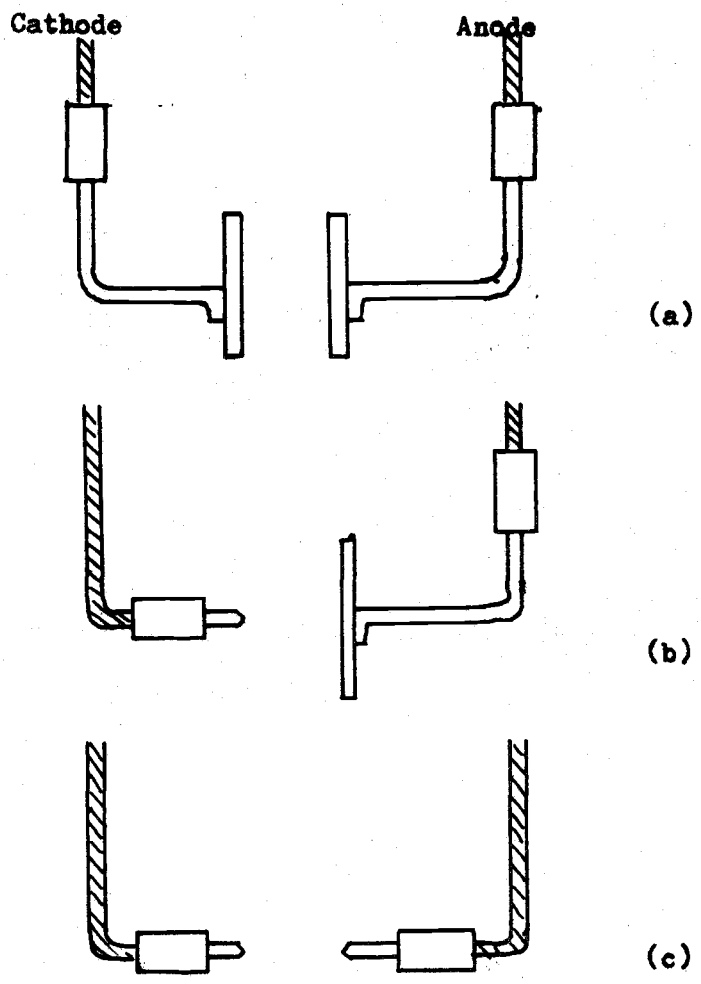

Figure 39. Electrode configurations first tried in the demountable hollow cathode lamp.

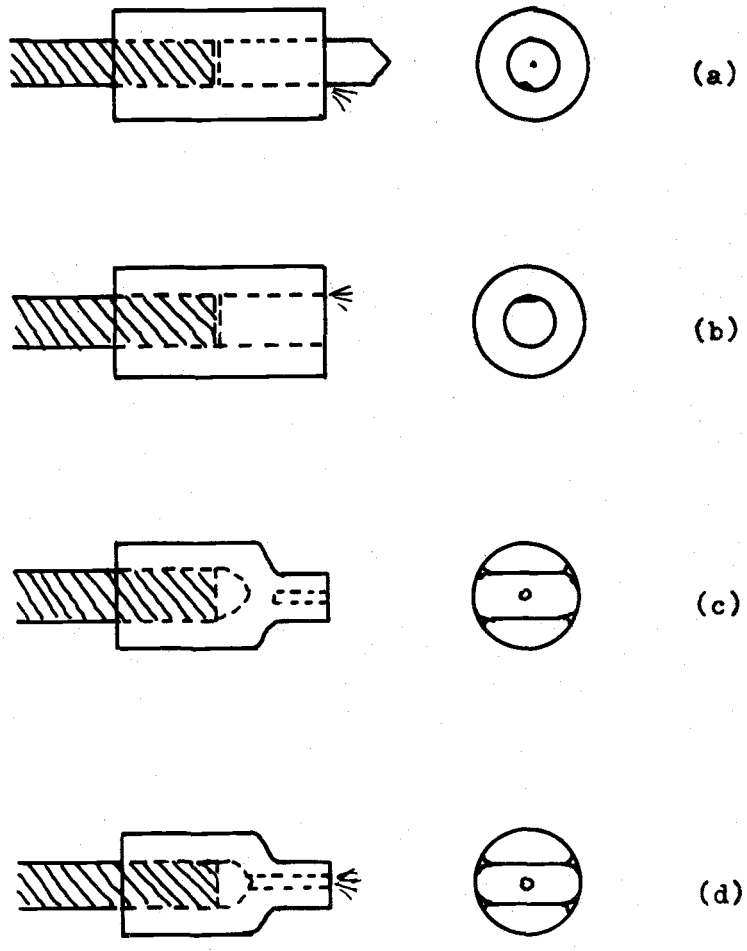

Figure 40. Cathode configurations for the arc-glow discharge.

potential (the potential at which the lamp fired) increased to a value greater than that which could be obtained with the power supply. At 15 Torr it was possible to visually follow the transition of the discharge from normal glow (at a 10 mA dc level) to the abnormal glow at moderate pulse levels (50 mA), and further to the blue-white arc-glow at high currents (100-300 mA). This transition was accomplished by changing only the pulse current (by changing the potential) to the lamp. Visually the normal glow was a pale blue glow covering the entire surface of the cathode, including the tungsten electrode. The abnormal glow showed its typical hot spots (refer to the section on the glow discharge) as light pink regions near the Cu cathode surface. As the pulse current was increased, these collapsed to form one glow region and the blue-white arc-glow was formed, indicating an arc or near arc condition.

Close inspection of the two cathodes which produced this arc-glow discharge led to the discovery of a small diameter crater at the tubing-wire junction in each electrode. By inserting a fine wire into the crater it was found that the opening went through the junction to the joint between the copper and the tungsten. A third electrode, Figure 40 (d), was then constructed by first mashing flat one end of the copper crimp tube and then drilling through to the tungsten wire lead a small diameter hole in the end of the cathode with a #80 drill bit. A similar cathode with the hole drilled only part way through was also constructed. It did not show the brilliant arc-glow under any conditions tried.

The cathode with the through-hole did produce the expected

blue-white arc-glow. With the cathode mounted so that the bore was facing the detection optics, the line profile observed on the oscilloscope for the arc-glow was extremely broad. The broad lines effectively filled the FSR of the interferometer and did not allow any resolution of the emission lines other than slight peaks. No time resolved data was taken for this arrangement.

All of the following data was taken with the axis of the arc-glow placed perpendicular to the optical path, giving a side view at the mouth of the discharge. A constant 1.0-mA dc background level was used throughout. Other dc levels made no difference in the intensities or profiles of the lines observed. A 0.3-mm diameter aperture was used on the monochromator entrance slit to allow spatial resolution.

Figure 41 shows the relative time and wavelength integrated intensity of the Cu(I) 324.75 emission line from the arc-glow and the commercial hollow cathode lamp vs pulse current. The pressure in the demountable lamp was 23.0 Torr. All instrumental conditions (aperture size, current pulses, PMT voltage, etc.) were identical for both lamps. At all currents the arc-glow exhibits higher integrated intensity.

Time resolved interferograms were produced for the demountable lamp and its arc-glow discharge. Instrumental parameters listed on the figures will help in comparison of line intensities. Figures 42 through 44 show the change in line shape of the two hyperfine lines of Cu near 324.7 nm with time. The Ar presure was 23.0 Torr with current pulse levels of 100 mA, 200 mA, and 300 mA used to excite the lamp. Note that there is little change in line shape or intensity during the

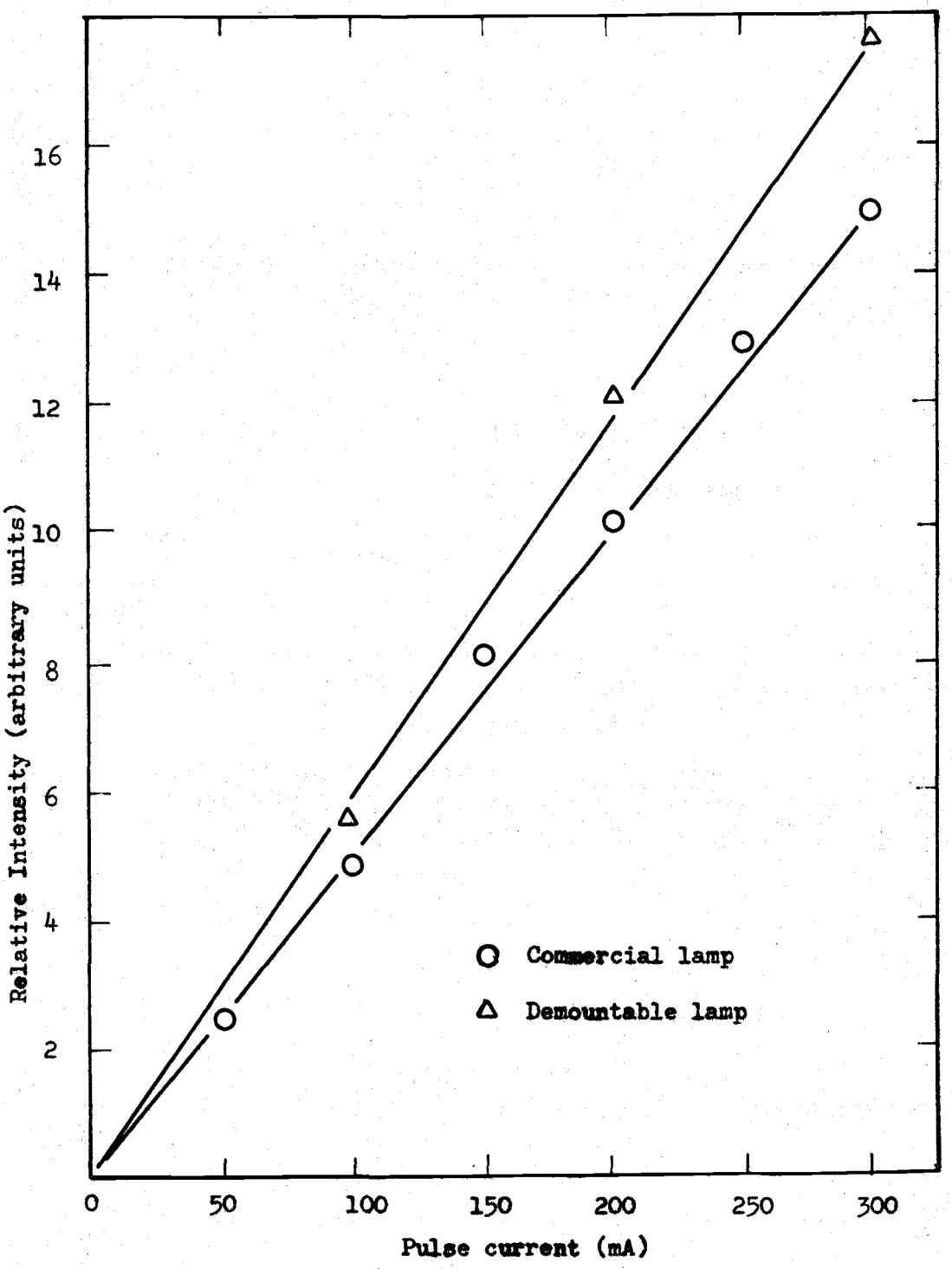

Figure 41. Relative integrated intensity of Cu emission for the commercial and demountable lamps at various pulse current levels. Background dc level in both lamps was 1.0 mA.

Figure 42. Time resolved line profiles of the Cu(I) 324.7 nm emission lines in the demountable hollow cathode lamp at an Argon pressure of 23.0 Torr. Pulse current = 100 mA.

$R_f = 10^5$

$C_f = 50$ pf

SW = 1000 μm

PMT = 670 VDC

Scale = 0.1 V/inch

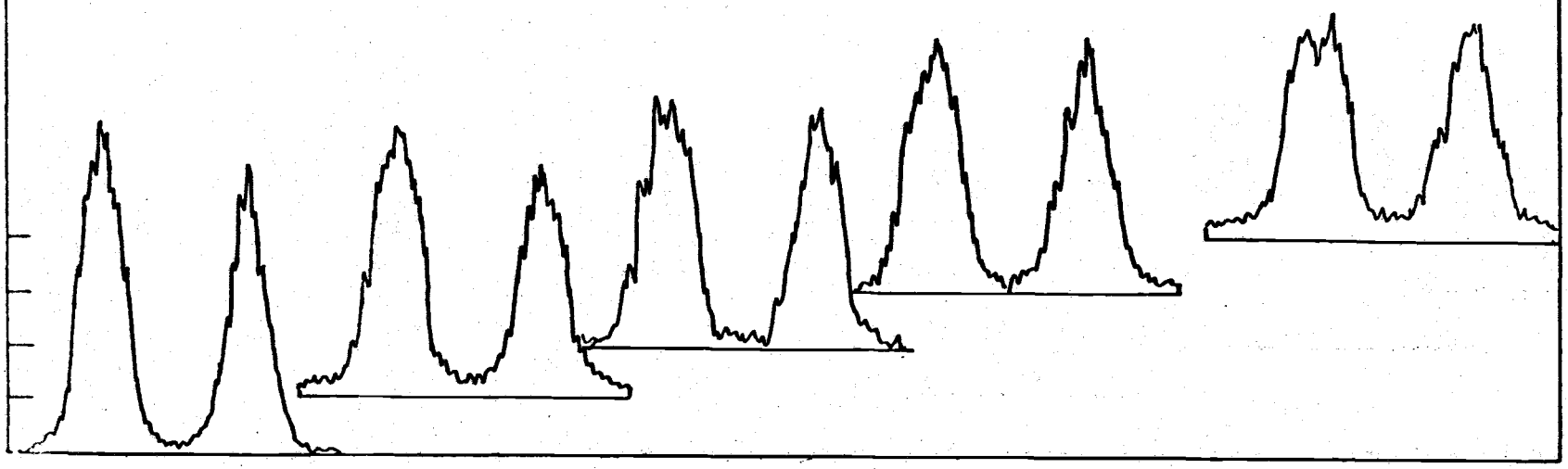

Figure 43. Time resolved line profiles of the Cu(I) 324.7 nm emission lines in the demountable hollow cathode lamp at an Argon pressure of 23.0 Torr. Pulse current = 200 mA.

$R_f = 10^5$

$C_f = 50$ pf

SW = 1000 μm

PMT = 670 VDC

Scale = 0.5 V/inch

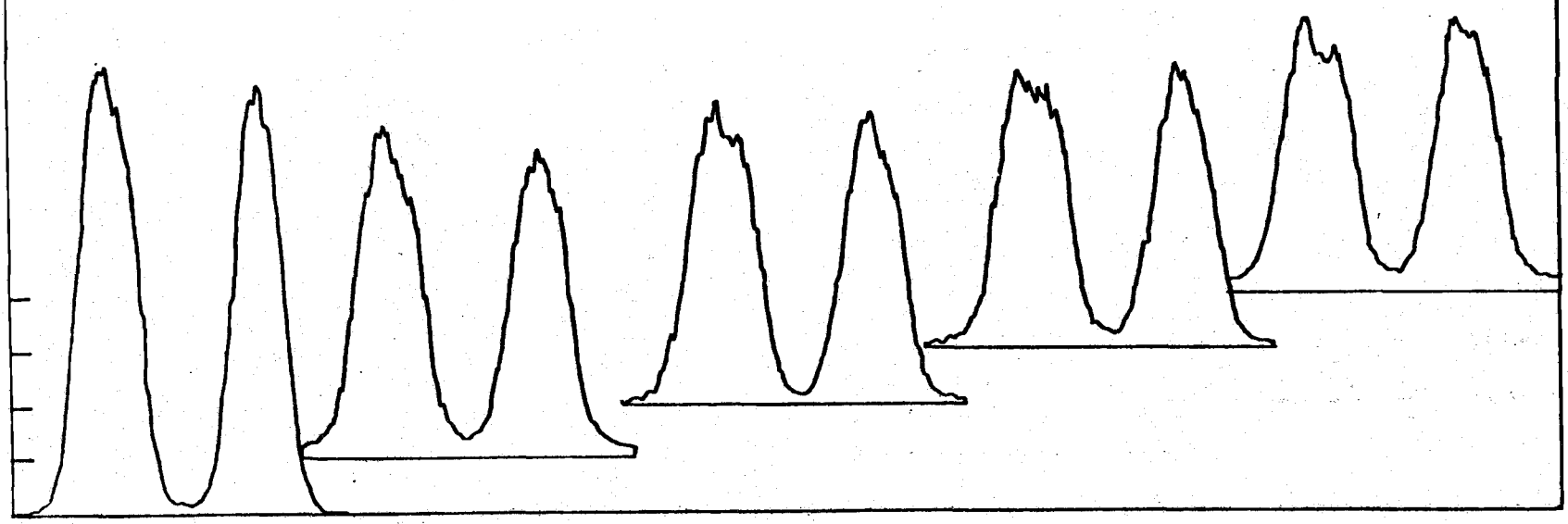

Figure 44. Time resolved line profiles of the Cu(I) 324.7 nm emission lines in the demountable hollow cathode lamp at an Argon pressure of 23.0 Torr. Pulse current = 300 mA.

$R_f = 10^5$

$C_f = 50$ pf

SW = 1000 μm

PMT = 670 VDC

Scale = 1.0 V/inch

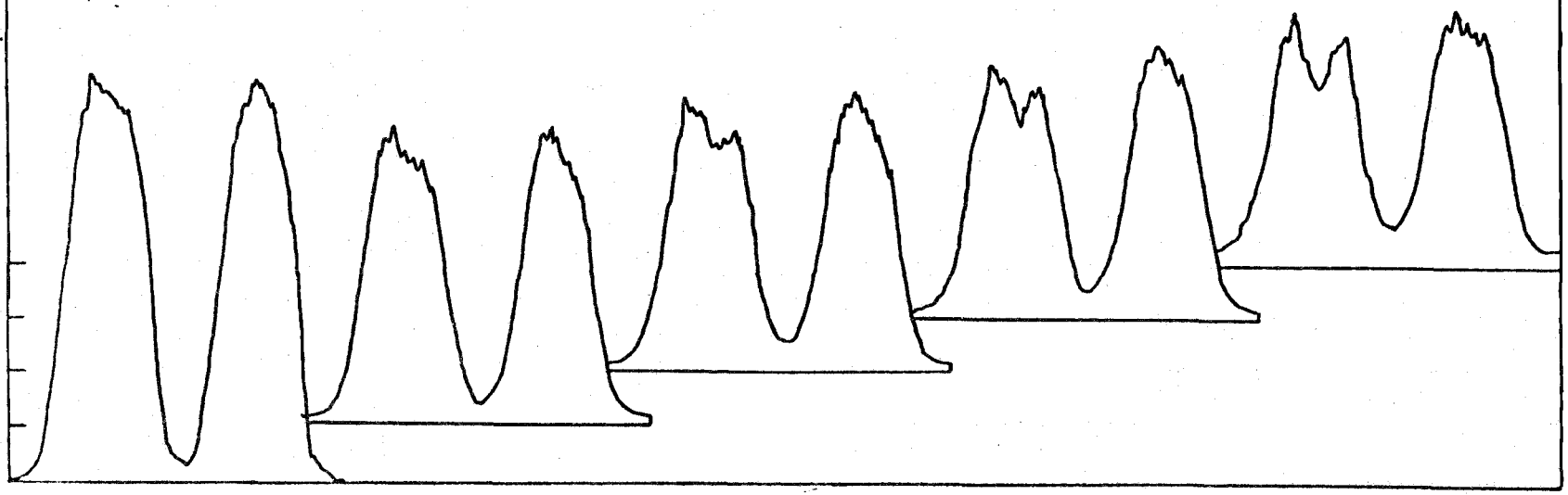

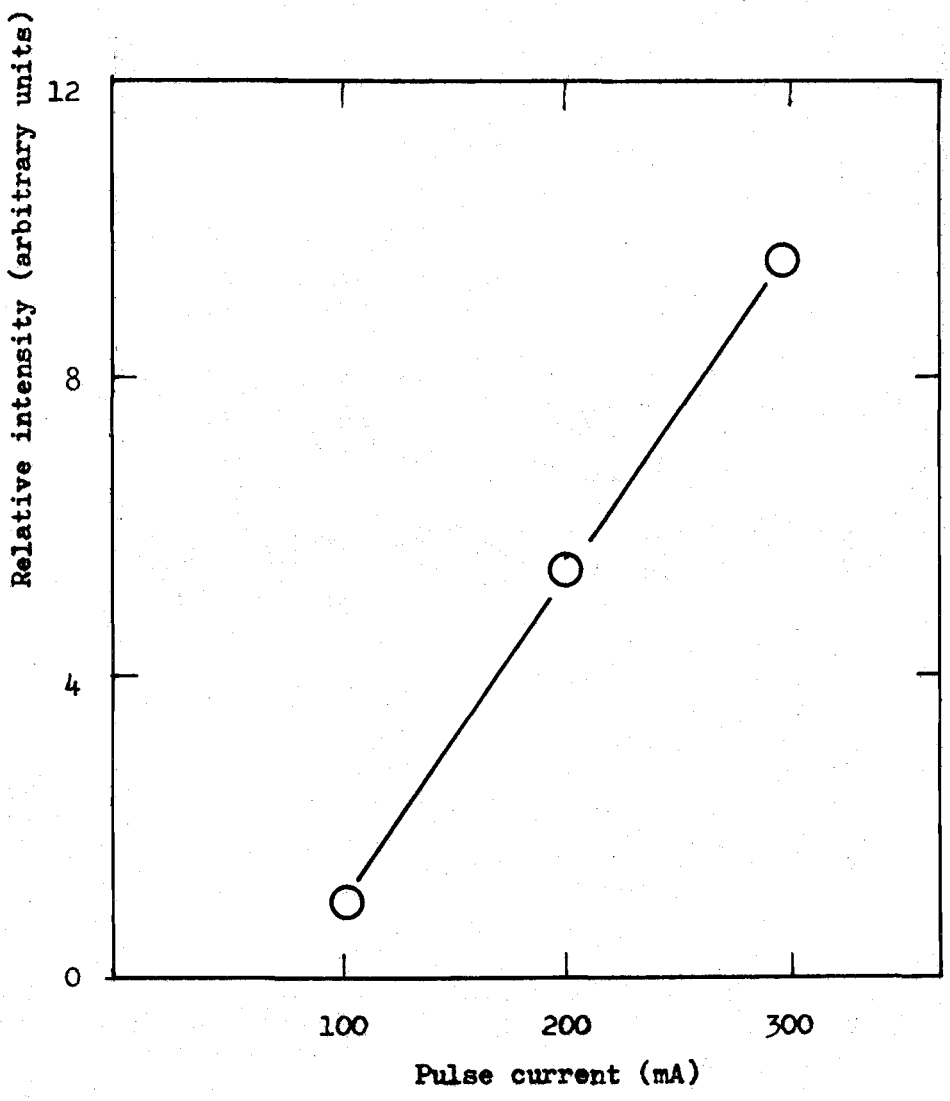

Figure 45. Relative peak intensity of the major emission line vs pulse current at 23.0 Torr Argon. Data from the first time period.

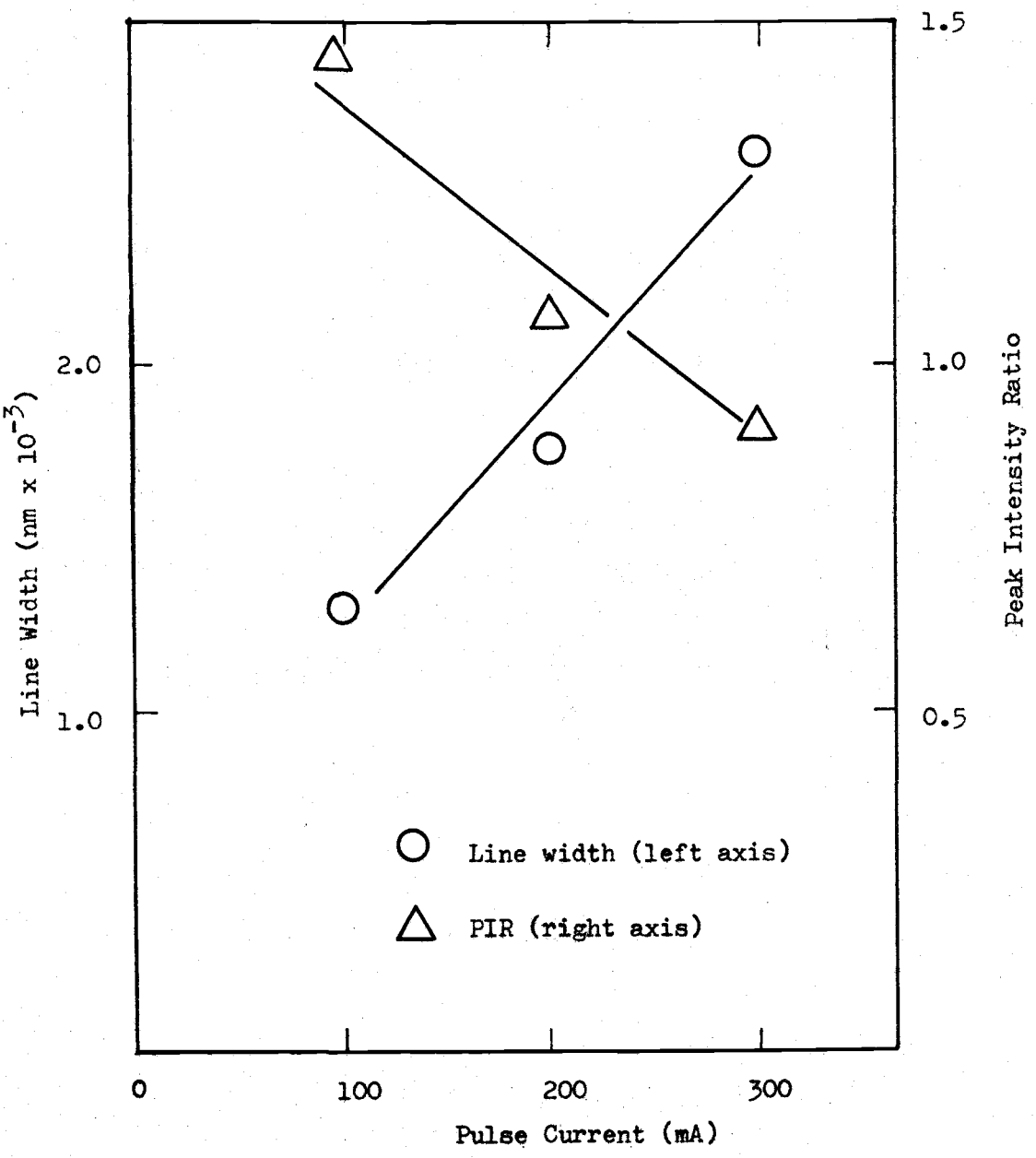

Figure 46. Line width (left axis) and peak intensity ratio (right axis) vs pulse current level for first 21 μseconds of the current pulse at Argon pressure of 23 Torr.

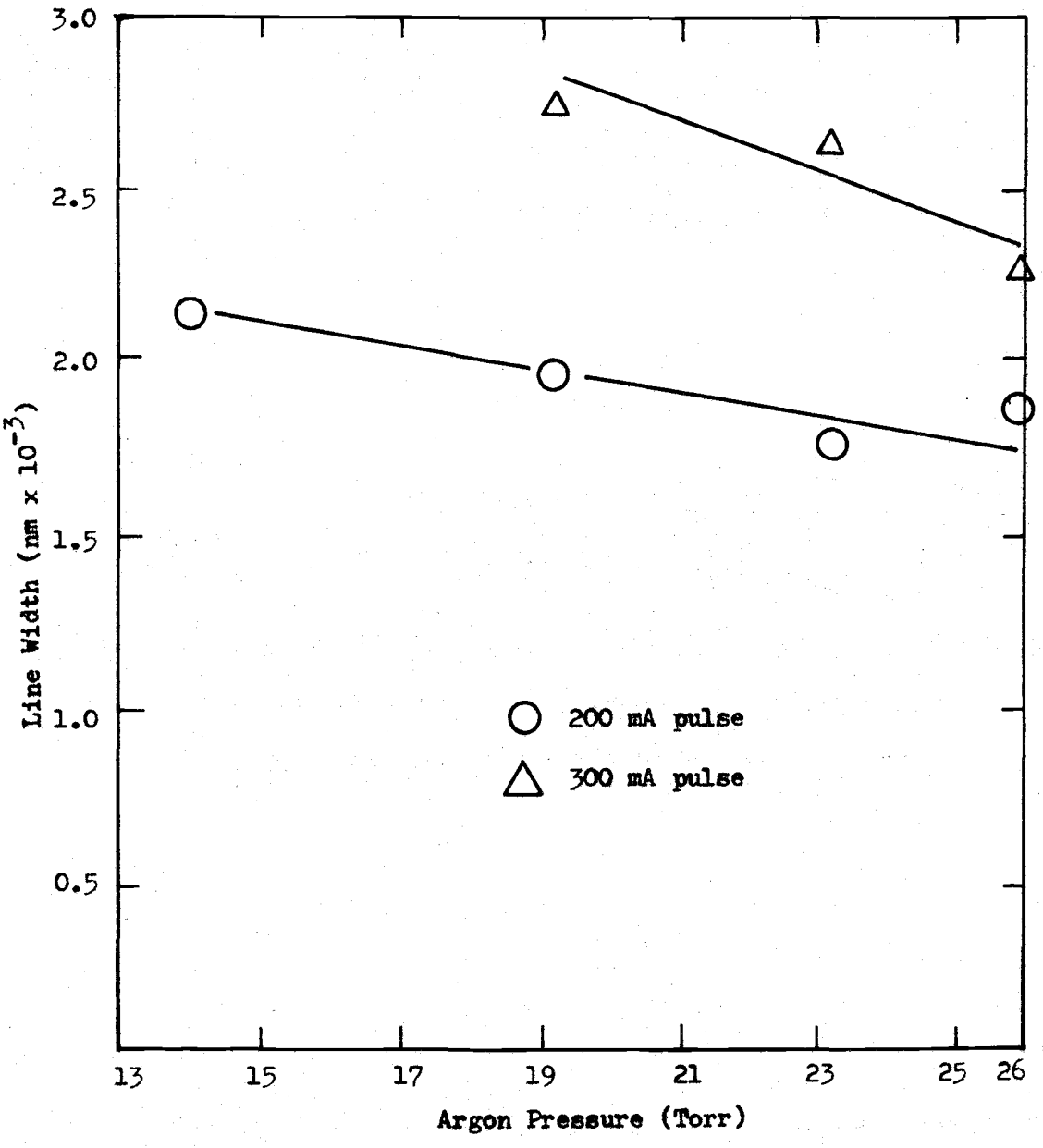

Figure 47. Line width for the first time period of the major 324.7 nm emission line in the demountable hollow cathode vs Argon pressure for 200 and 300 mA pulse currents.

third through fifth time periods when compared to the greater changes that occurred for the commercial lamp during those time periods, Figure 16. The last five time periods (6 through 10) are not included as virtually no change occurred during those time periods. Note that the third 21-μsecond time period shows only slight reversal even at the 300-mA pulse current level where the commercial lamp showed extreme self-reversal. Figure 45 shows the increase in peak intensity in the first 21-μsecond time period with pulse current, at a 1.0-mA background dc current level. The line width for the initial time period also increases with pulse current, as illustrated on the left axis of Figure 46. Note that these line widths ($1.3 - 2.6 \times 10^{-3}$ nm) are comparable to those obtained for the commercial lamp ($1.5 - 2.4 \times 10^{-3}$ nm). Peak hyperfine intensity ratios show a decrease as the pulse current increases. This ratio indicates that self-absorption is present to some degree at all pulse levels, although it is much greater at higher currents. Comparative PIR values for the commercial lamp can be seen in Figure 18 above.

Figure 47 indicates the relationship of the line width in the first time period to the inert gas pressure for two pulse current levels with a constant 1.0-mA dc background current. The line width at 200 mA is essentially independent of the pressure in the range used. The 300-mA pulse line width shows a moderate decrease with pressure. This indicates that there is little or no increase in the observed broadening as the pressure increases. The theoretical increase in pressure broadening (18) for this pressure increase would be ~ 0.0004 nm, which would

Figure 48. Time resolved line profiles of the Cu(I) 324.7 nm emission lines in the demountable hollow cathode lamp at an Argon pressure of 14.0 Torr. Pulse current = 200 mA.

$R_f = 10^5$

$C_f = 50$ pf

SW = 1000 μm

PMT = 700 VDC

Scale = 0.2 V/inch

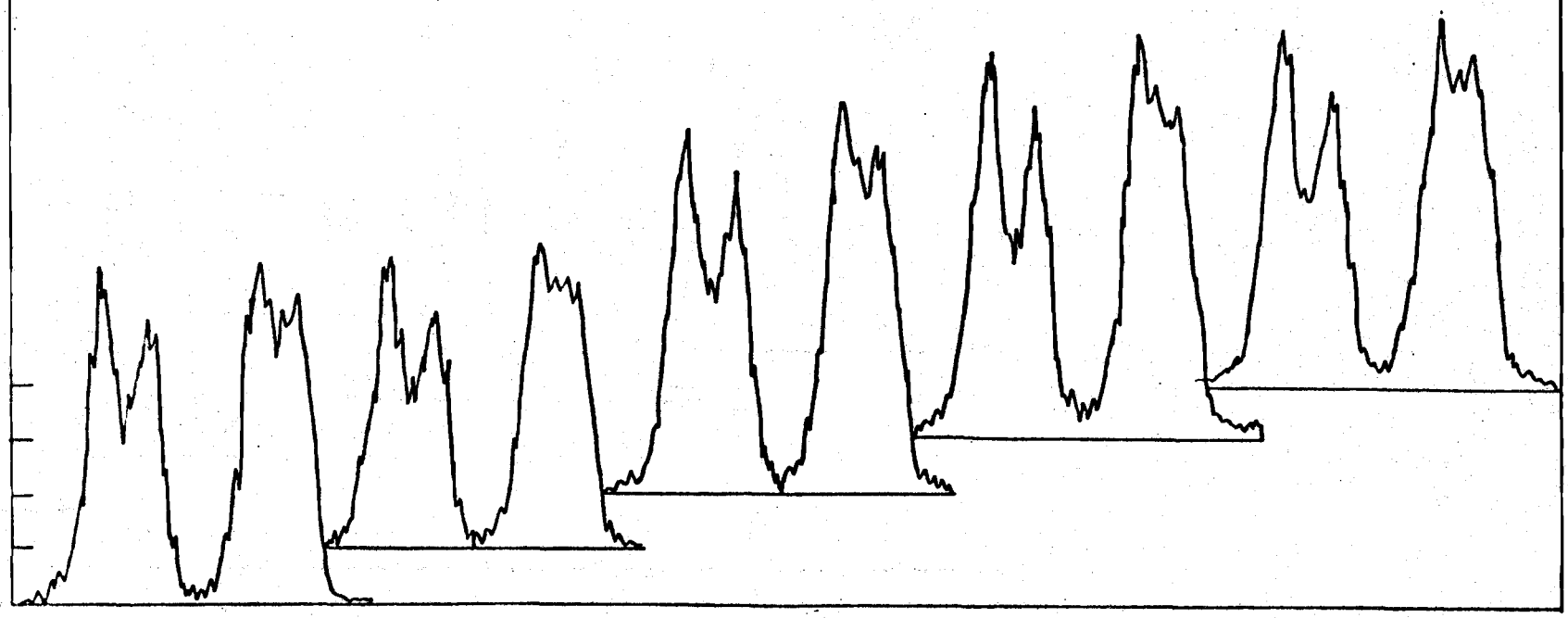

Figure 49. Time resolved line profiles of the Cu(I) 324.7 nm emission lines in the demountable hollow cathode lamp at an Argon pressure of 19.2 Torr. Pulse current = 300 mA.

$R_f = 10^5$

$C_f = 50$ pf

SW = 1000 µm

PMT = 670 VDC

Scale = 1.0 V/inch

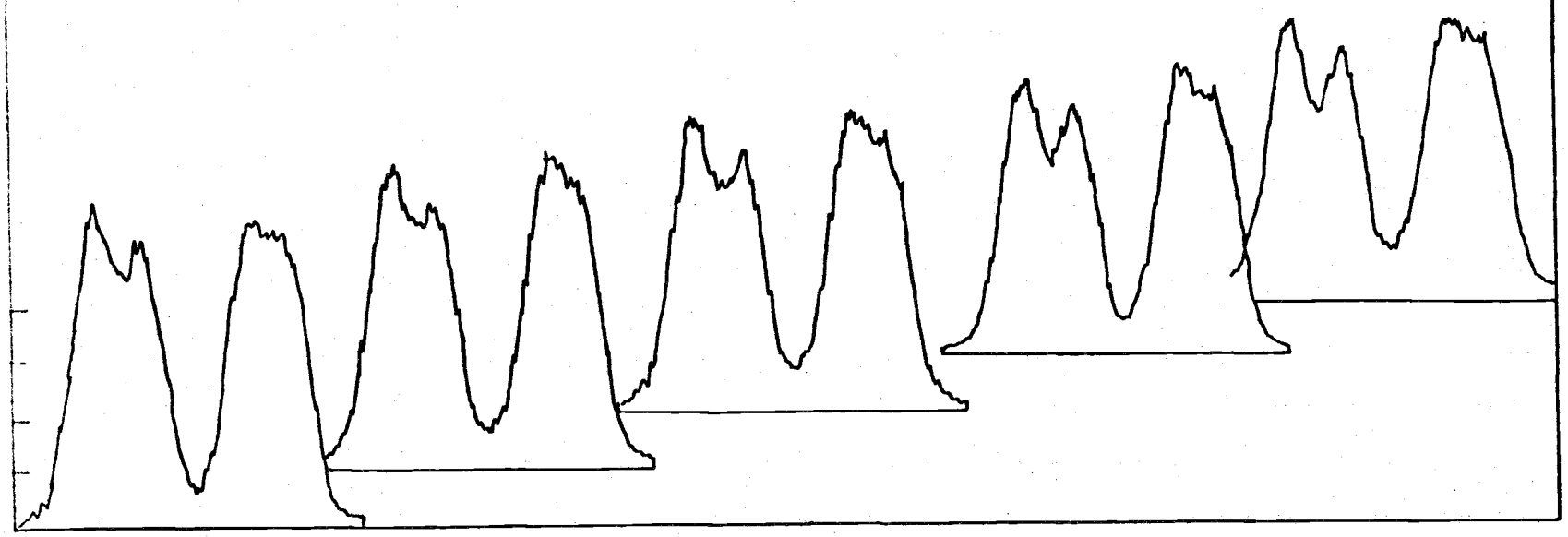

Figure 50. Time resolved line profiles of the Cu(I) 324.7 nm emission lines in the demountable hollow cathode lamp at an Argon pressure of 26.0 Torr. Pulse current = 300 mA.

$R_f = 10^5$

$C_f = 50$ pf

SW = 1000 μm

PMT = 670 VDC

Scale = 1.0 V/inch

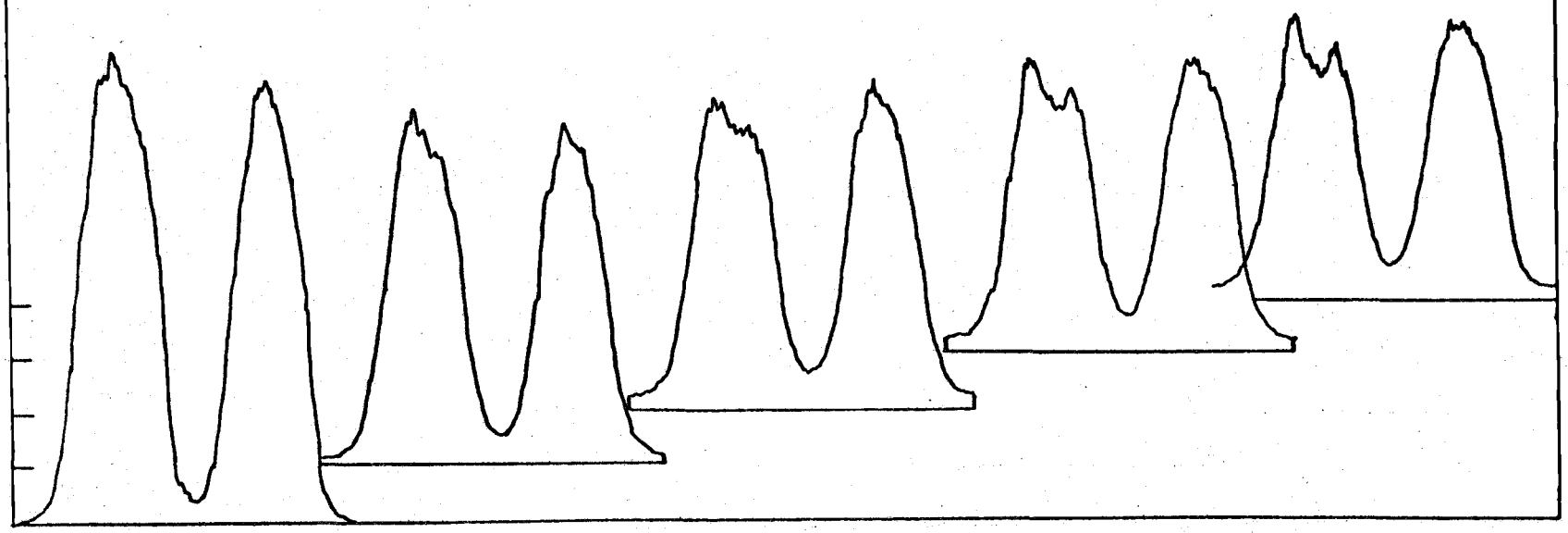

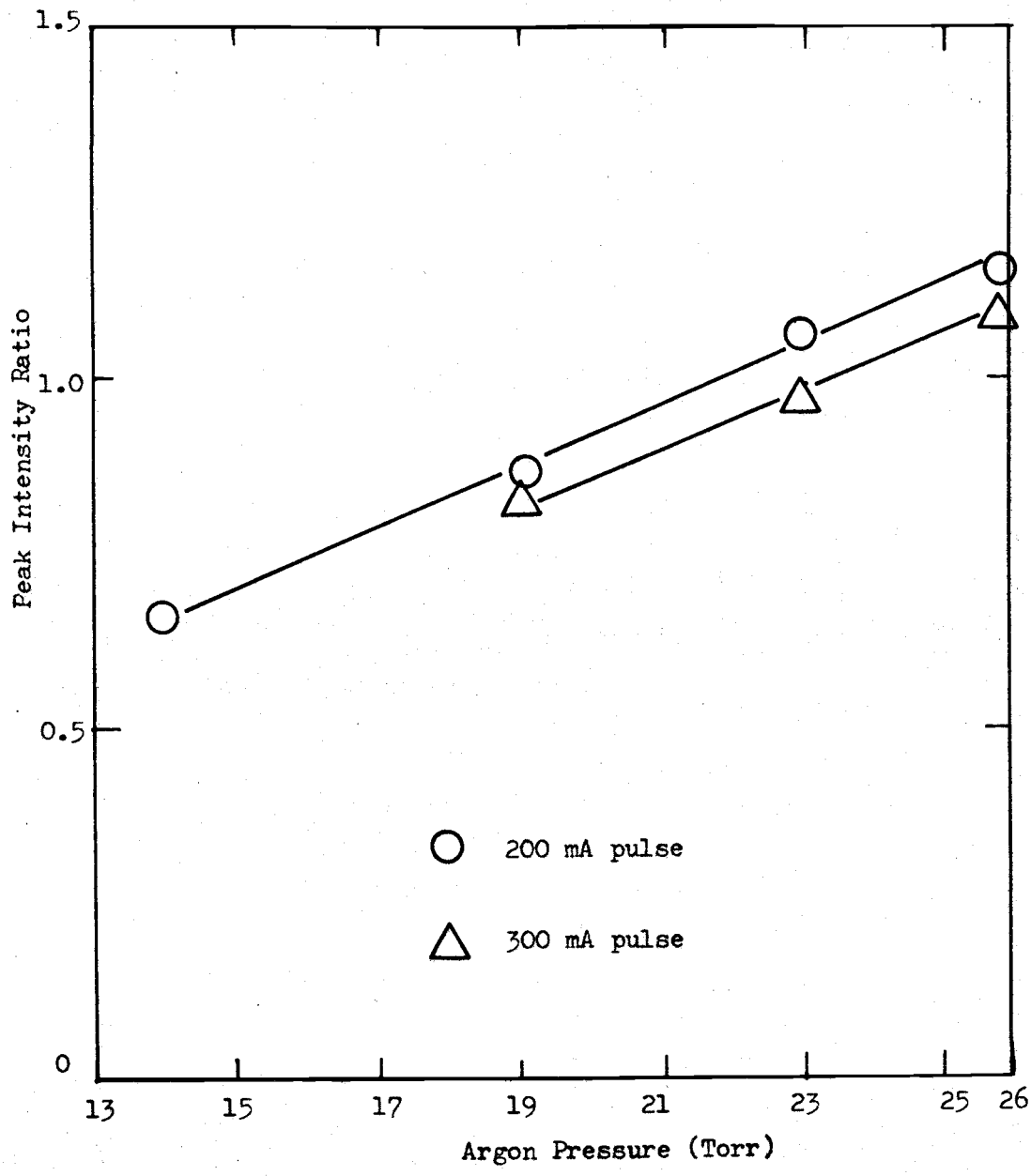

Figure 51. Peak intensity ratio vs Argon pressure in the demountable lamp for pulse current levels of 200 mA and 300 mA. Data for first time period.

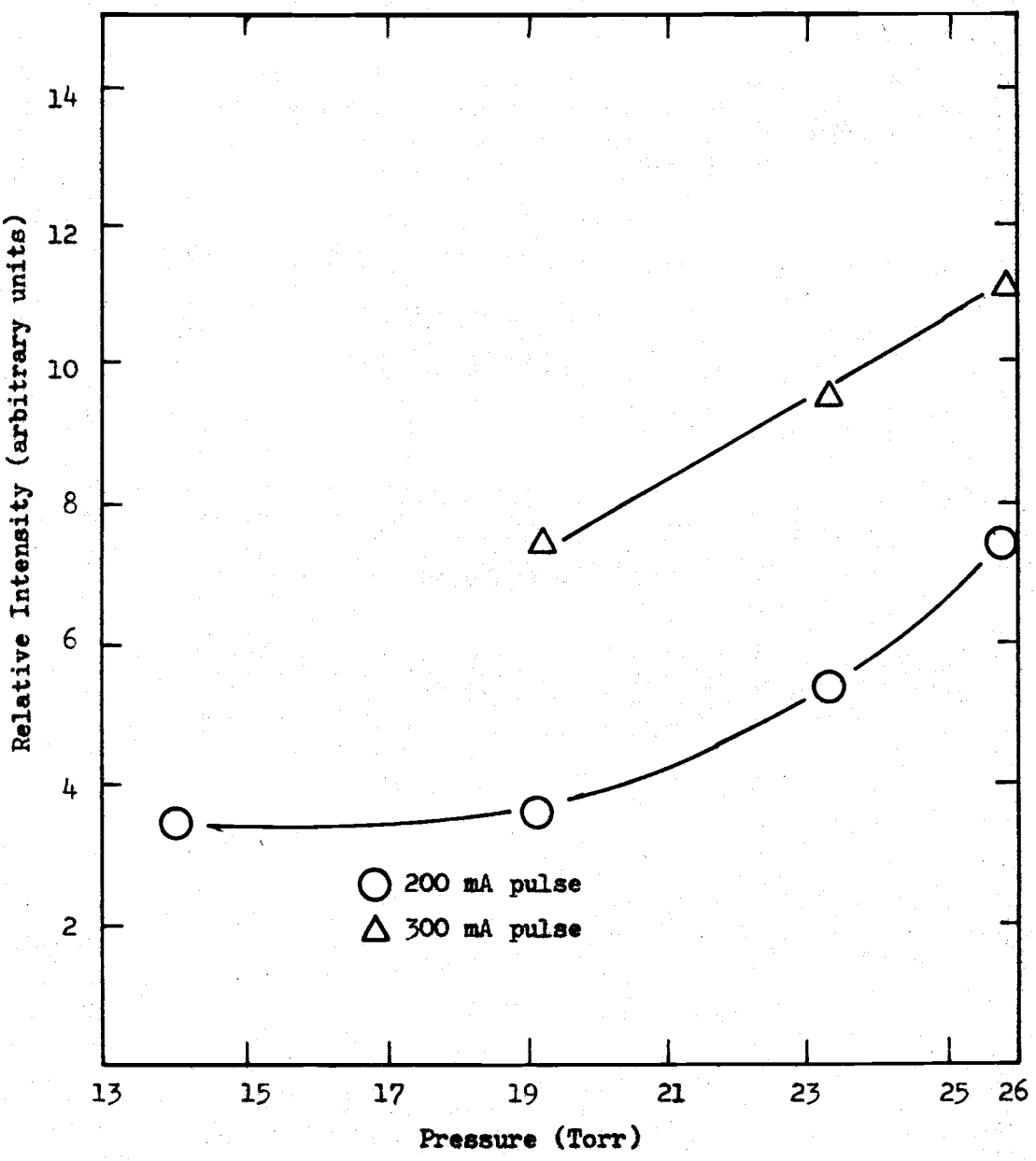

Figure 52. Relative peak intensity of the major 324.7 nm emission line vs Argon pressure for the first 21-μsecond time period for pulse currents of 200 mA and 300 mA.

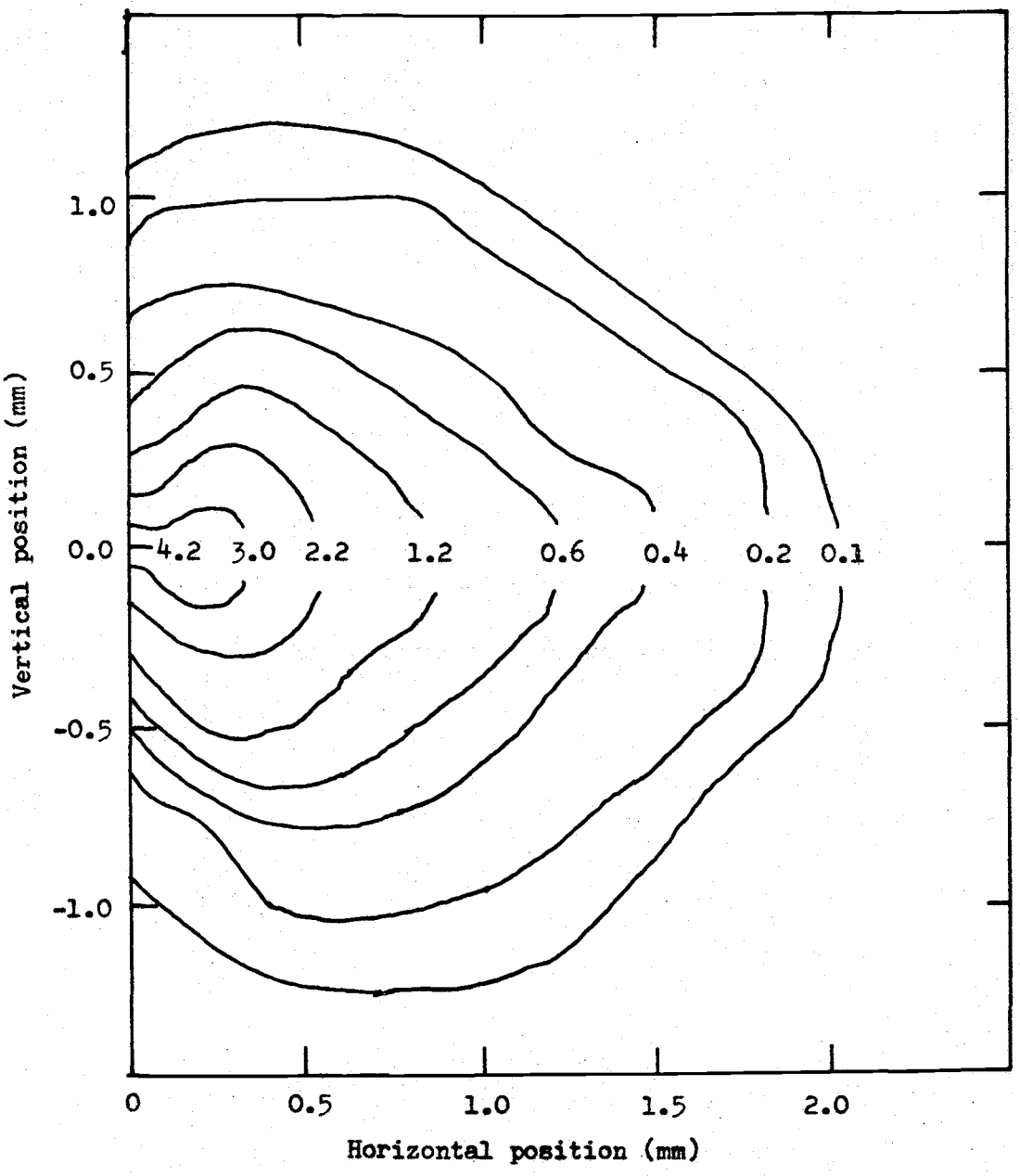

Figure 53. Isointensity lines for the Cu(I) emission lines in the arc-glow discharge of a 300 mA pulse at 26.0 Torr Argon pressure.

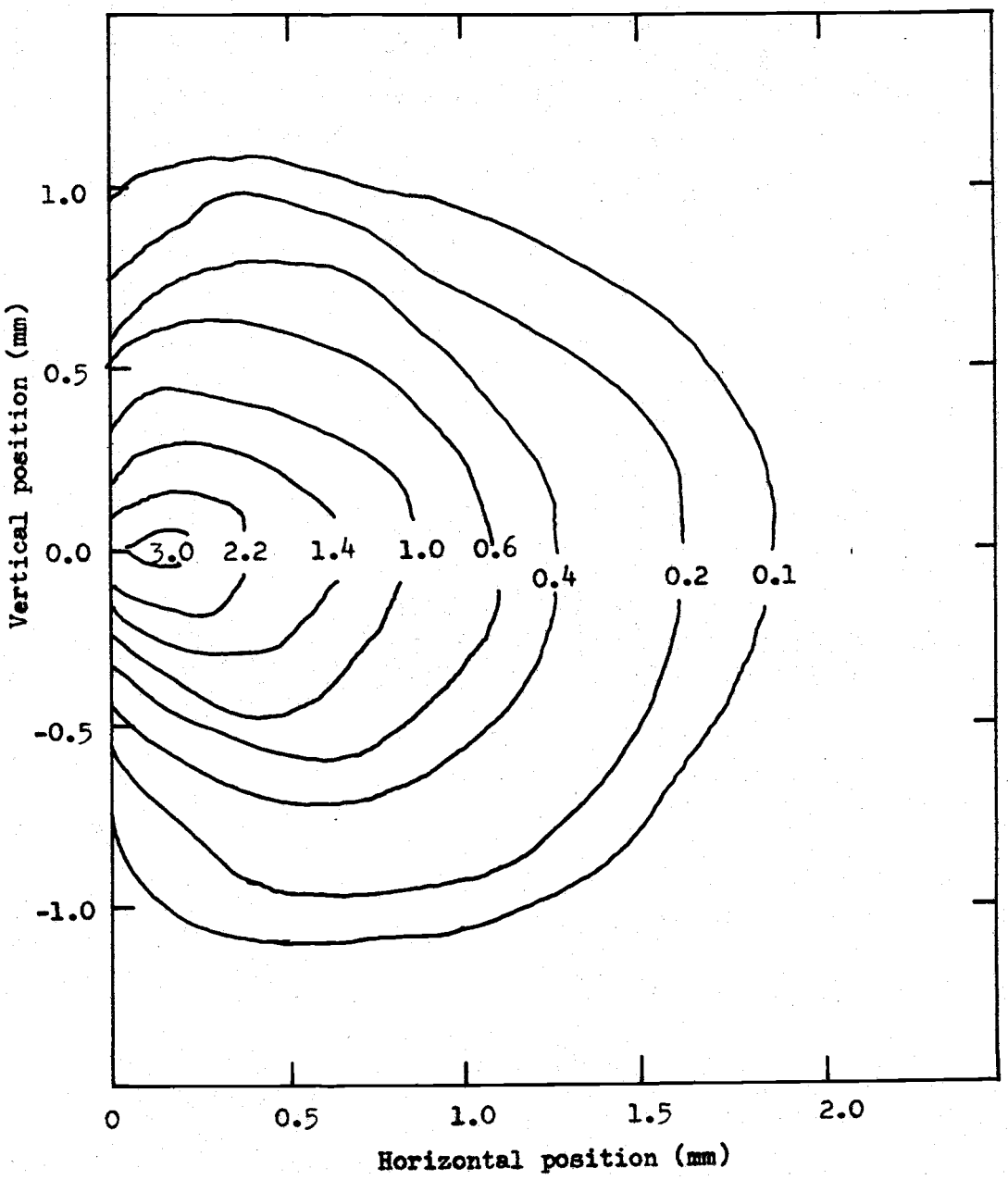

Figure 54. **Isointensity lines for the Cu(I) emission lines in the arc-glow discharge of a 300 mA pulse at 19.1 Torr Argon pressure.**

Figure 55. Time resolved line profiles of the Cu(I) 324.7 nm emission lines 0.5 mm out from the center of maximum intensity. Argon pressure = 26.0 Torr, pulse current = 300 mA.

$R_f = 10^5$

$C_f = 50$ pf

SW = 1000 μm

PMT = 670 VDC

Scale = 0.5 V/inch

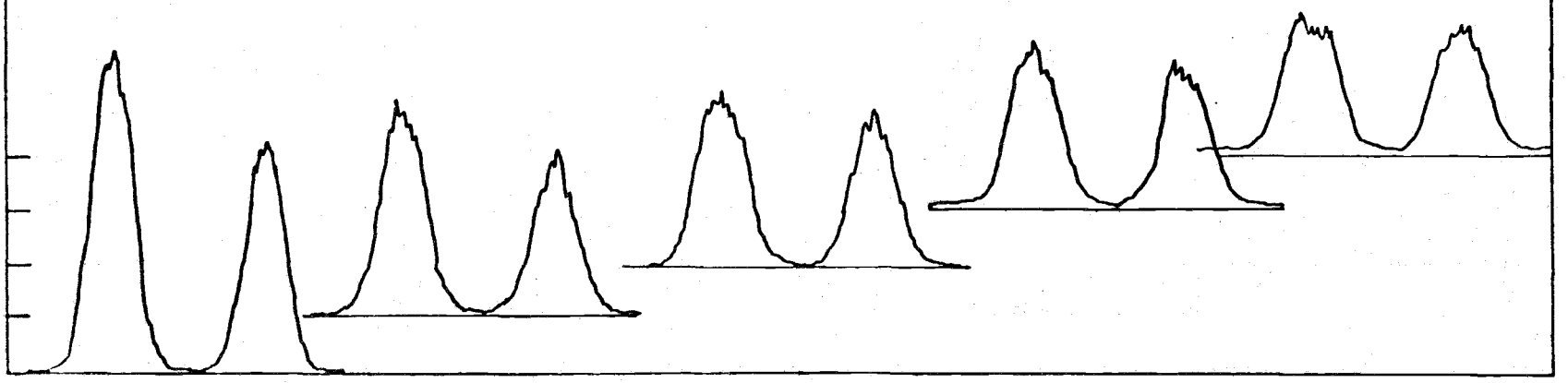

Figure 56. Time resolved line profiles of the Cu(I) 324.7 nm emission lines 1.00 out from the center of maximum intensity. Argon pressure = 26.0 Torr, pulse current = 300 mA.

$R_f = 10^5$

$C_f = 50$ pf

SW = 1000 μm

PMT = 670 VDC

Scale = 0.1 V/inch

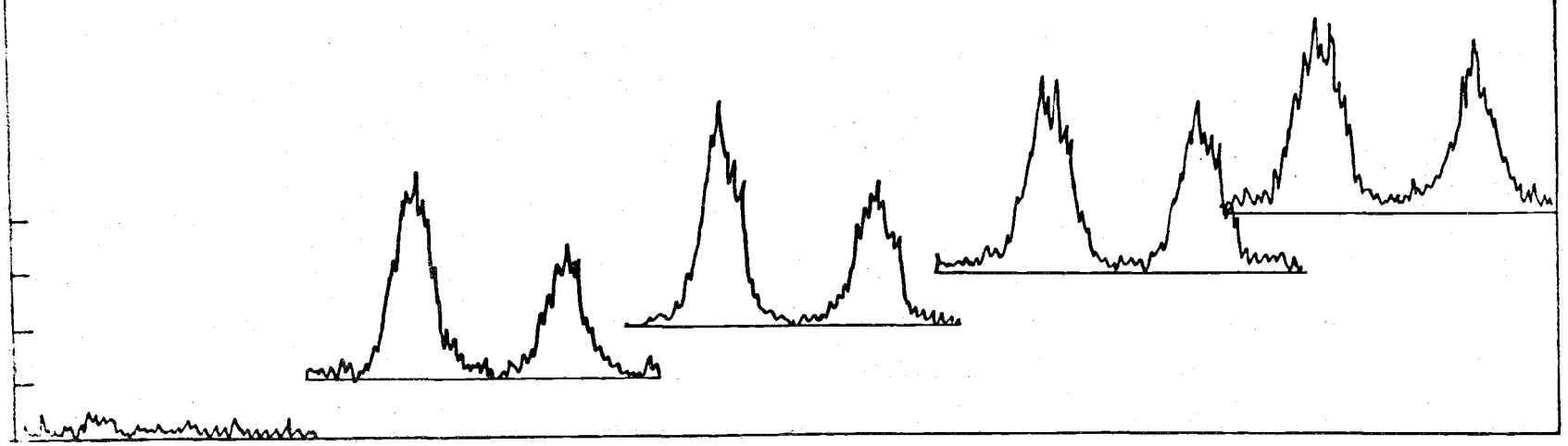

be barely detectable. Estimates of predicted changes in Doppler broadening would require temperature measurements which are not available. The decrease in line width is accompanied by a decrease in self-reversal, as shown in the profiles plotted in Figures 48, 49, 44 and 50, indicating that absorption is a major factor that influences the apparent line width. Figure 51 also indicates an increase in the PIR value with pressure for the 200-mA and 300-mA pulse current levels. This is also a good indicator of decreasing self-absorption of the Cu emission with inert gas pressure. The 300-mA pulse level shows slightly greater self-absorption than the 200-mA level. This is expected from the higher sampling rate of Cu with the higher current. The iso-intensity lines, Figures 53 and 54, were obtained by physically moving the entire demountable lamp through 2.0 mm of horizontal movement at 3.00 mm of vertical movement in 0.2-mm intervals. The zero position corresponds to the face of the cathode at the bore opening. The time-integrated peak intensities were monitored on an oscilloscope and recorded on a map in the position corresponding to the region of the observation. The outer boundary of the excitation region as indicated by the iso-intensity lines labeled 0.1 doesn'tchange greatly with pressure; however, the intensity near the mouth increases with pressure.

The Cu line shape and intensity also change as regions further from the region of maximum intensity are observed. Figures 55 and 56 show how the line shape and intensity change with time for regions 0.5 mm and 1.00 mm from the region of maximum intensity. The region at 0.5 mm shows some decrease in intensity and broadening with time.

The peak hyperfine intensity ratio changes dramatically from 1.4 in the first 21-μsecond time period to nearly 1.0 in the third time period. This is due to increased self absorption with time, with eventual reversal at 100 μseconds. The region at 1.00 mm shows no lines above the noise level initially and shows only slight line shape and intensity change after the emission starts. The peak hyperfine intensity ratio value for the first two time periods was about 1.5, dropping to 1.1 in the third time period and remaining there for the rest of the monitoring time. No further change was seen in the sixth-tenth time periods, and they are not shown.

The delay in the start of observable Cu emission at 1.00 mm from the mouth of the bore may indicate that the arc-glow region takes a few useconds of time to grow to its final size. The low amount of self-absorption compared to the results from the commercial hollow cathode lamp indicates a lower absorbing path length-copper concentration product for the path between the emitting discharge region and the detection system for this lamp.

Low inert gas pressures showed the most self-reversal for this arc-glow discharge, Figures 48 and 57. This increase in self absorption is caused by an increase in the Cu concentration-absorption path length product between the emitting region and the detector. Several factors could account for the increase in the product. One possibility is that the copper vapor in a sparser atmosphere diffuses further away from the cathode bore before vapor condensation or other vapor loss mechanisms become significant. The result would be an increase in path

Figure 57. Time resolved line profiles of the Cu(I) 324.7 nm emission lines in the demountable hollow cathode lamp at an Argon pressure of 26.0 Torr. Pulse current = 200 mA.

$R_f = 10^5$

$C_f = 50$ pf

SW = 1000 μm

PMT = 670 VDC

Scale = 0.5 V/inch

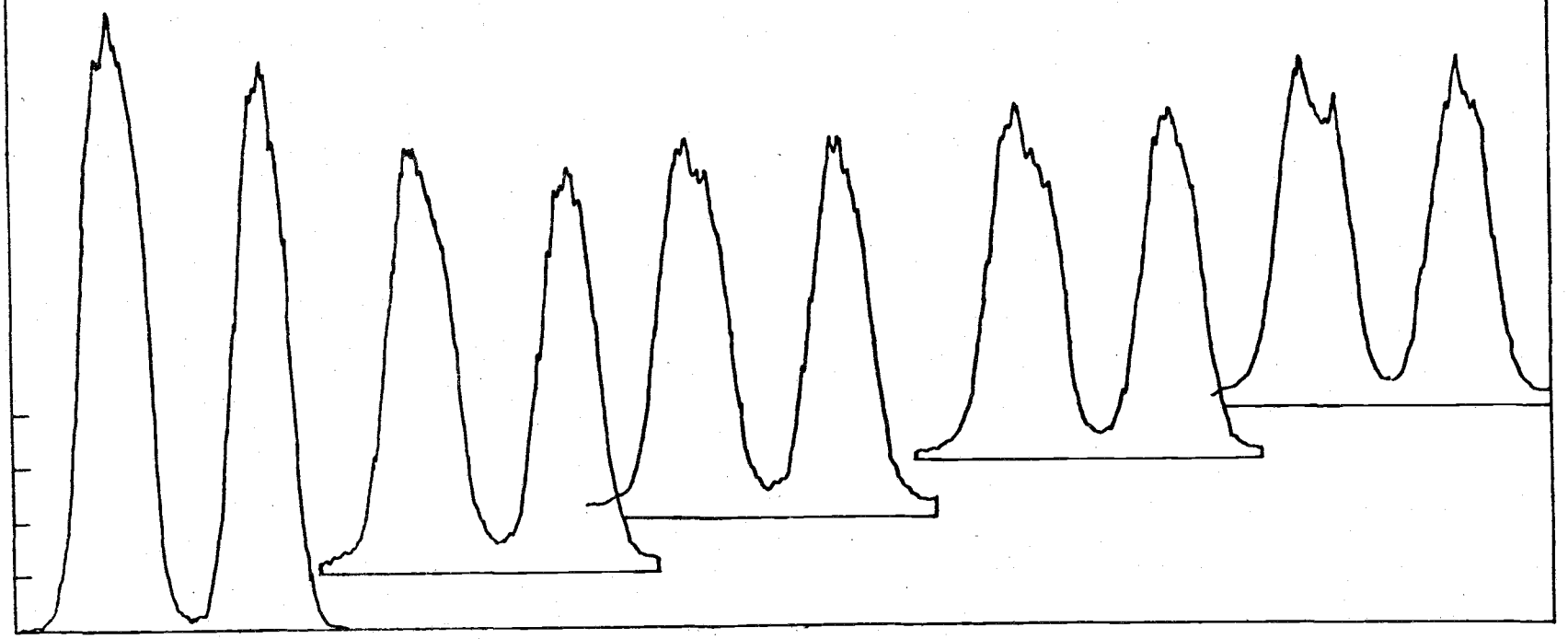

length. Also, at lower pressures sputtering of cathodic material increases. An increase in sputtering or other sampling mechanisms could cause an increase in the Cu concentration in the absorption path.

Sampling in this discharge may be of a different kind than in a typical low pressure hollow cathode discharge where sputtering is thought to be the principle means of obtaining Cu atoms in the excitation region. The blue-white arc-glow and the accompanying Cu emission is seen to sit directly in front of the through hole. The extreme broadening of the emission observed when viewing down the bore of the through-hole indicates high excitation temperatures within the bore. This is to be expected for an arc-type of discharge. At high temperatures, thermal bombardment of the walls by neutral and charged particles could be more important as a sampling mechanism than sputtering (bombardment by ions accelerated in an electric field), boiling the Cu atoms from the sides of the bore and allowing them to diffuse out into the observed arc-glow region.

The decreased self absorption found in this lamp is due to a lower path length-concentration product of Cu vapor in the region between the detector and the emitting region. This may be due to less Cu sampling by the discharge, lowering the total amount of Cu available in the lamp.

The observed intensity from the lamp is proportional to the mathematical product of (1) the concentration of the Cu in the excitation region, that is being viewed, (2) the path length of the excitation region and (3) the fraction of excited atoms within the excitation region. Increases in any of the factors associated with the excitation

region will lead to greater observed emission, while increases in factors (1) and (2) of the absorption region will tend to cause a decrease in the observed emission due to self absorption and eventually reversal. The arc-glow discharge could sample less total Cu but have nearly the same Cu concentration-path length product in the excitation region because of its much smaller size compared to the pulsed hollow cathode lamp, giving it similar intensity with less self absorption.

The fraction of excited atoms may also be significantly greater in the arc-glow lamp than in the commercial hollow cathode lamp. Calculations on a line with PIR of 1.4 in both lamps gave a Doppler (18) temperature of about 2600° K for the arc-glow and about 1700° K for the pulsed commercial hollow cathode lamp. This would allow a greater fraction (by 4 orders of magnitude) of the Cu atoms to be excited by thermal excitation in the arc-glow lamp and hence the high intensity even with less Cu present in the discharge.

The optimum conditions for greatest line intensity for the side viewed arc-glow are high current pulses (200-300 mA) at pressures of about 25 Torr. For the best PIR with good intensity, pulse currents of about 100 mA at 25 Torr seem to be the most advantageous. For a single bore it was not possible to drive the lamp much above 300 mA with a pulse. This current saturation did not seem to be limited by the power supply but by the lamp itself. Improvements in intensity could come from a double bore or multi-bore cathode and increased current which, if each bore would form the arc-glow, would increase the total radiant flux available of the lamp.

The intensity of the Cu-emission from the arc-glow also reached a saturation condition at the current maximum. Preliminary studies with a larger hole (5 x diameter) in the cathode, although giving less intensity and an arc-glow that did not fill the hole, showed that current saturation was not reached prior to reaching the current limitation of the power supply. This indicates that the current may be limited by the small size of the cathode bore, and shows that greater intensity cannot be achieved by simply increasing the current indefinitely.

CONCLUSIONS

The pulsed Cu hollow cathode lamp and the pulsed arc-glow of the demountable lamp both fulfill one of the goals of using a pulsed mode--that of increasing the integrated line intensity to decrease shot noise and allow measurements on a shorter time base required for some pulsed sampling systems. Total intensity enhancement for both of these types of lamps was about 100 when compared to a lamp at a 10-mA dc current level.

Line width and line profile for both lamps are similar for up to the first 20 to 40 μseconds after the initiation of the pulse. After this time the commercial lamp begins to show severe self-reversal of the emission lines. The arc-glow lamp, however, shows some increase in self-reversal with time but is not nearly so reversed as the output from the commercial lamp. Accordingly, the time integrated intensity at the wavelength center of the emission peak remains considerably greater (x 10) for the arc-glow discharge than for the commercial lamp during a 200 μsecond current pulse.

Both lamps show potential alignment problems when used in instrumental applications. The commercial hollow cathode lamp shows more severe self-reversal at the edge of the discharge than at the center for the first 60 μseconds of the discharge. If the measurement for which the lamp is used is taken in less than 60 μseconds after the start of the pulse, it would be best to use only the center portion of the discharge. For measurements taking longer, or taken after 60 μseconds, the entire cathode discharge region shows severe reversal.

The arc-glow lamp also needs critical alignment, with the region of greatest intensity being only 0.1 mm across, and the fall-off of intensity becoming rapid at distances of about 0.5 mm out from the region of highest intensity. Line profile is not so much of a problem, as the reversal is not severe even at conditions of maximum intensity (at 300 mA and 26.0 Torr), and the reversal decreases as regions further from the intensity maximum are reached.

Further comparison of the relative usefulness of the two lamps in the pulsed mode may be made by considering the absorption line profile of the atomic reservoir containing the sample atoms (for either atomic absorption or atomic fluorescence measurements) and comparing this to the emission profile obtained from the pulsed lamps.

Figure 58 shows the three basic emission profile types which are obtained from the lamps that were studied compared to a very broad absorption line, such as might be observed early in the plume of a laser sampling system. In this case all emission profiles are grouped near the center of the absorption peak. Very likely, all three emission sources would be expected to give similar results.

In contrast, Figure 59 shows a very narrow absorption line, as may occur late in the life of a laser plume or when using a hollow cathode discharge for the sampling system. Here the emission from a commercial lamp pulsed for a long time period would be nearly useless --there is very little emission at the absorption peak. Shorter pulses would help considerably, Figure 59 (C), but the best would be the emission profile obtained from a high pressure (26 Torr) arc-glow

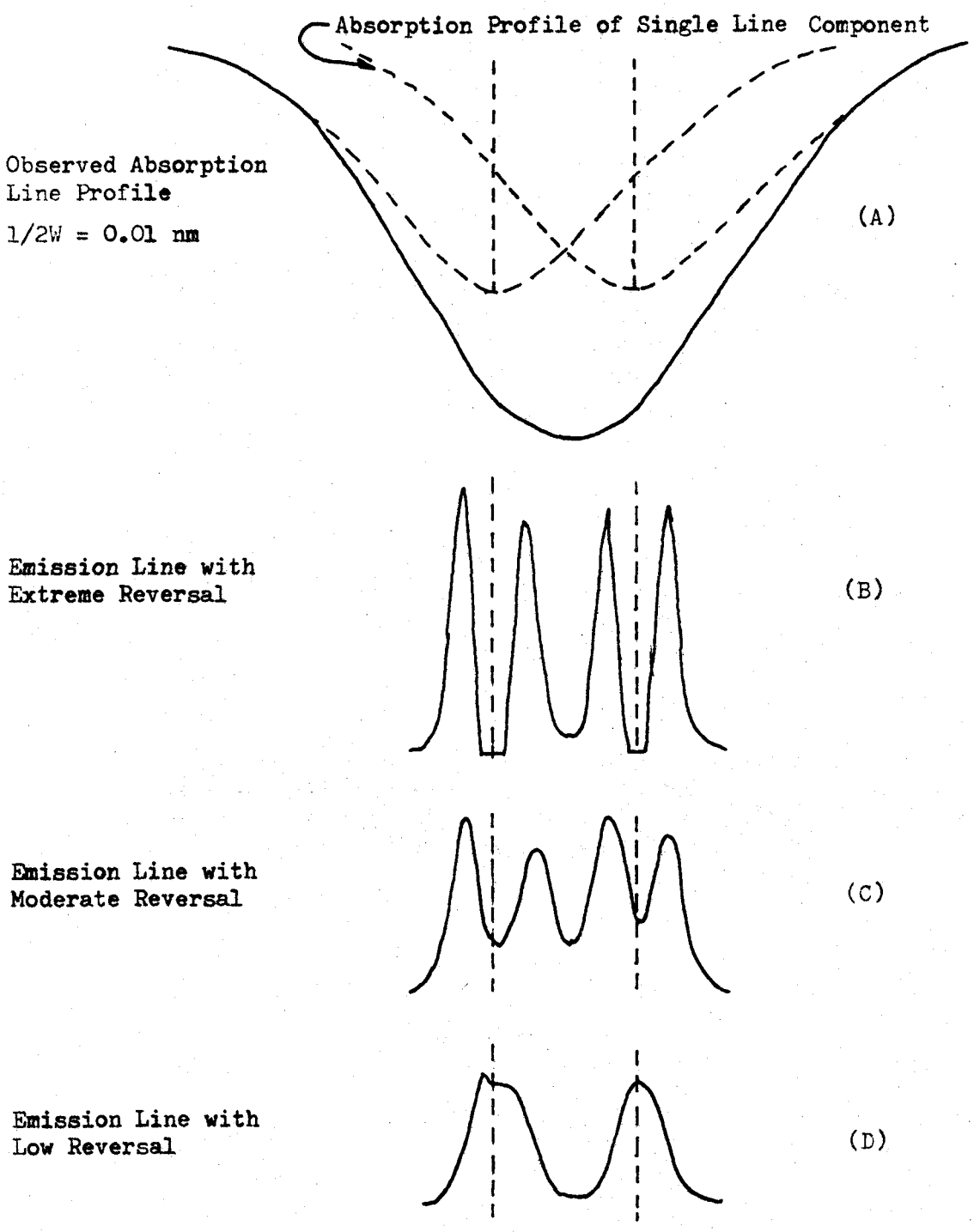

Figure 58. Emission line profiles for the commercial lamp with an 0.5-msecond long pulse (B), a 100-μsecond long pulse (C), and for the demountable lamp with a 100-μsecond long pulse (D) all compared to a broad absorption line profile.

Narrow Absorption
Line Profile

1/2W = 0.0008 nm

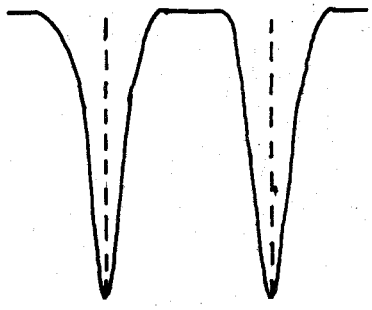

(A)

Emission Line with
Extreme Reversal

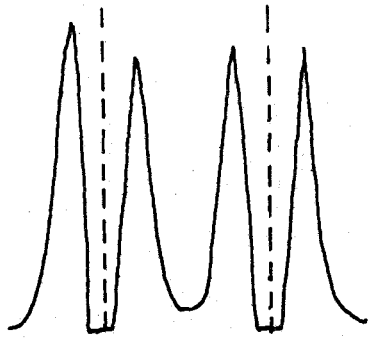

(B)

Emission Line with
Moderate Reversal

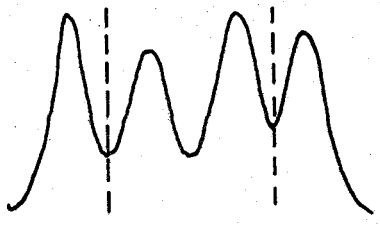

(C)

Emission Line with
Low Reversal

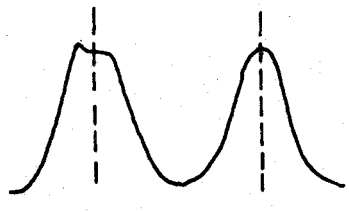

(D)

Figure 29. Emission line profiles for the commercial lamp with an 0.5-msecond long pulse (B), a 100-μsecond long pulse (C), and for the demountable lamp with a 100-μsecond long pulse (D) all compared to a narrow absorption line profile.

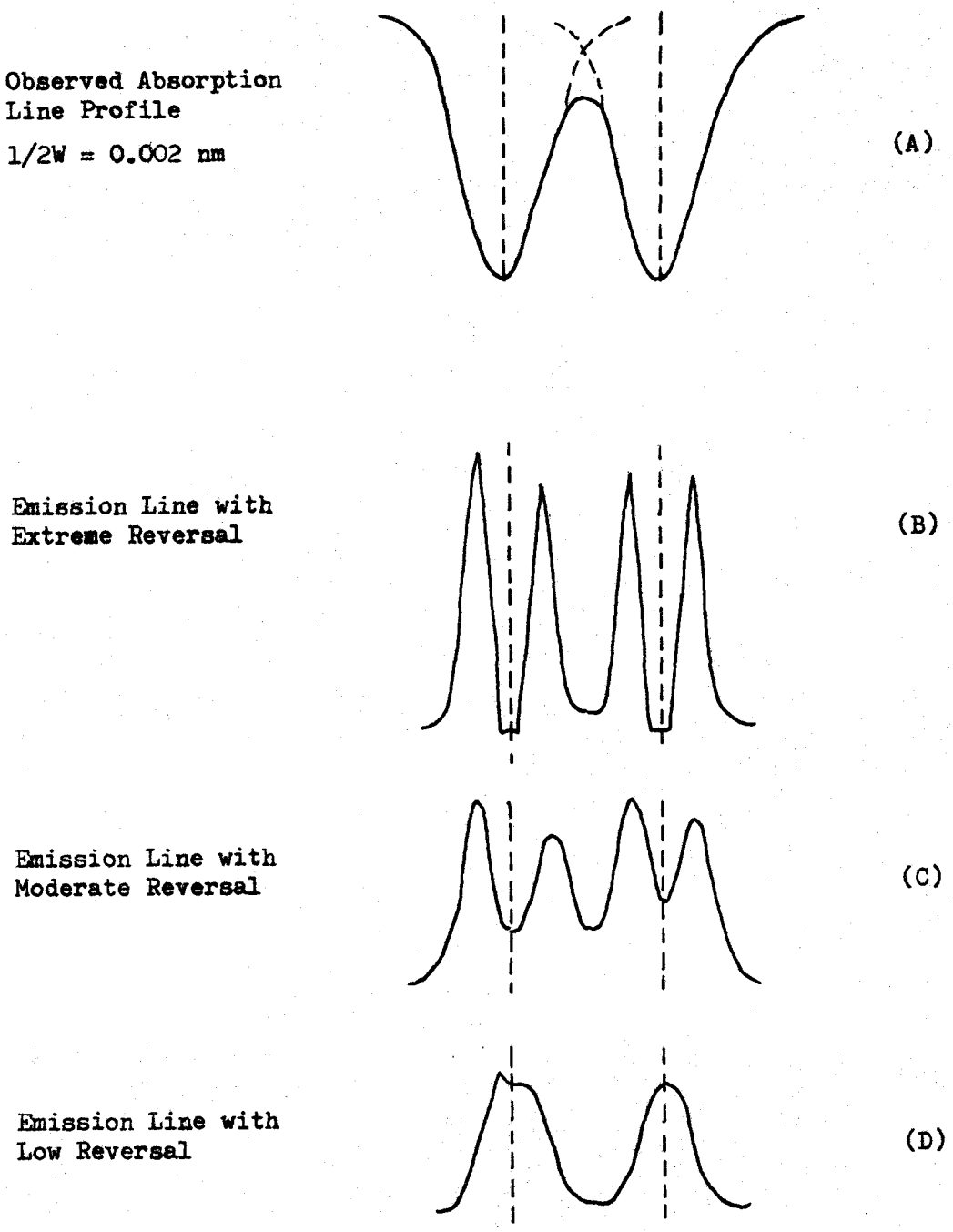

Figure 60. Emission line profiles for the commercial lamp with an 0.5-msecond long pulse (B), a 100-μsecond long pulse (C), and for the demountable lamp with a 100-μsecond long pulse (D) all compared to a typical (flame) absorption line profile.

discharge, Figure 59 (D). This would give the greatest overlap of emission intensity and absorption coefficient of the three available excitation types.

Figure 60 shows a moderate case, with an absorption profile of about the same width as the available emission profile. This absorption line width is typical of Cu vapor in analytical flames (14). Although all three types of emission sources would be useful, the best source would be (D), with the worst being (A).

Other considerations are important for routine work--problems such as cost ($100-$200 for a commercial lamp, much greater for the demountable lamp). Ease of use and speed of interchangeability of elements would be greater for the commercial lamp compared to the demountable lamp.

Another use of the demountable arc-glow lamp would be as a sampling source for bulk measurements of analytes in a metal. By forming a tube with a bore similar to that used in this research it may be possible to sample material from the bulk of the metal being analyzed (either by emission or absorption) rather than from the metal surface as occurs when sputtering is used as the sampling mechanism.

The arc-glow discharge lamp is a better emission source in pulsed systems than the pulsed hollow cathode lamp, and may also have a further use as a sampling system for bulk analysis of metal. Further work is needed on the use of other cathode materials and multi-bore configurations.

B I B L I O G R A P H Y

BIBLIOGRAPHY

1. P. W. J. M. Boumans. "Theory of Spectrochemical Excitation," Plenum Press, New York, N.Y. 1966, p. 90.

2. P. Brix and W. Humbach. Zeitschrift fur Physic, 128, 506 (1950).

3. C. F. Bruce and P. Hannaford. Spectrochimica Acta, 26B, 207 (1971).

4. J. Cooper and J. R. Greig. Journal of Scientific Instrumentation, 40, 433 (1963).

5. E. Cordos and H. V. Malmstadt. Analytical Chemistry, 45, 27 (1973).

6. L. deGalan and H. C. Wanenaap. Revue du GAMS, 3, 10 (1971).

7. D. K. Davies. Journal of Applied Physics, 38, 4713 (1967).

8. J. B. Dawson and D. J. Ellis. Spectrochimica Acta, 23A, 565 (1967)

9. G. F. Kirkbright and H. Sargent. Spectrochimica Acta, 25B, 577 (1970).

10. F. Llewellyn-Jones. "The Glow Discharge," Methuen & Co. LTD., London, 1966, pp. 6-13.

11. F. Llewellyn-Jones. "The Glow Discharge," Methuen & Co. LTD., London, 1966, p. 70.

12. H. V. Malmstadt and E. Cordos, American Laboratory, 4(8), 35 (1972).

13. D. G. Mitchell and A. Johansson, Spectrochimica Acta, 25B, 175 (1970).

14. M. L. Parsons, W. J. McCarthy and J. D. Winefordner. Applied Spectroscopy, 20, 223 (1966).

15. H. Prugger, R. Grosskopf and R. Torge. Spectrochimica Acta, 26B, 191 (1971).

16. J. V. Sullivan and A. Walsh. Spectrochimica Acta, 21, 721 (1965).

17. C. H. Townes. Physical Review, 65, 319 (1944).

18. J. D. Winefordner and T. J. Vickers. Analytical Chemistry, 36, 1947 (1964).

19. K. Yasuda, Analytical Chemistry, 38, 592 (1966).

A P P E N D I X

Appendix A

Flow Chart of Program

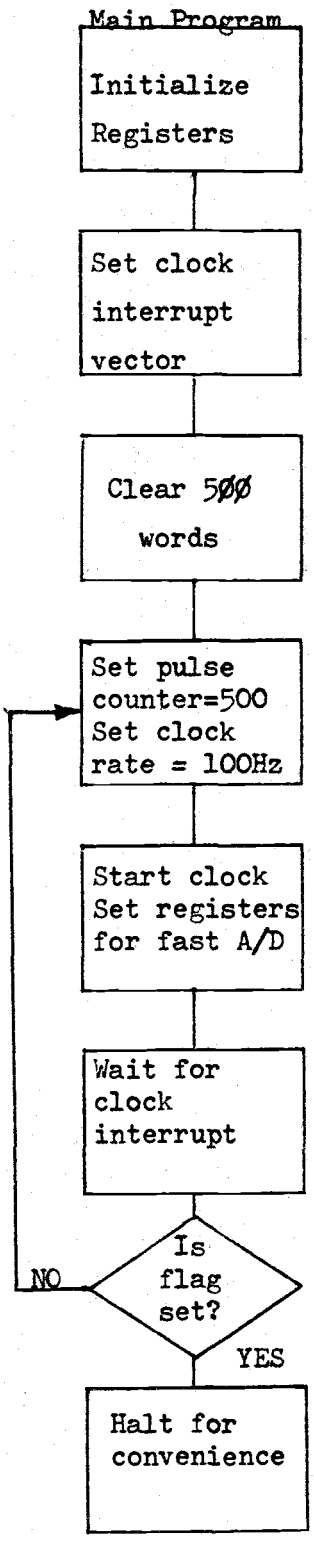

Binary data tape output commences when operator presses continue switch after the convenience halt has occurred.

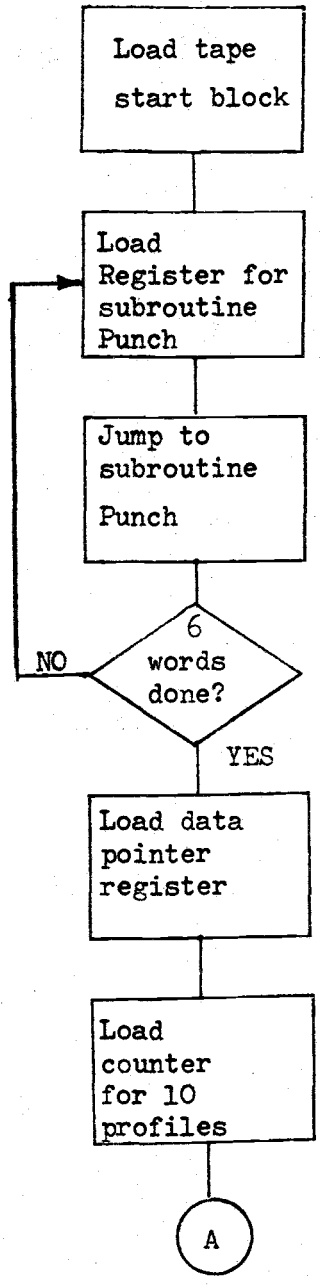

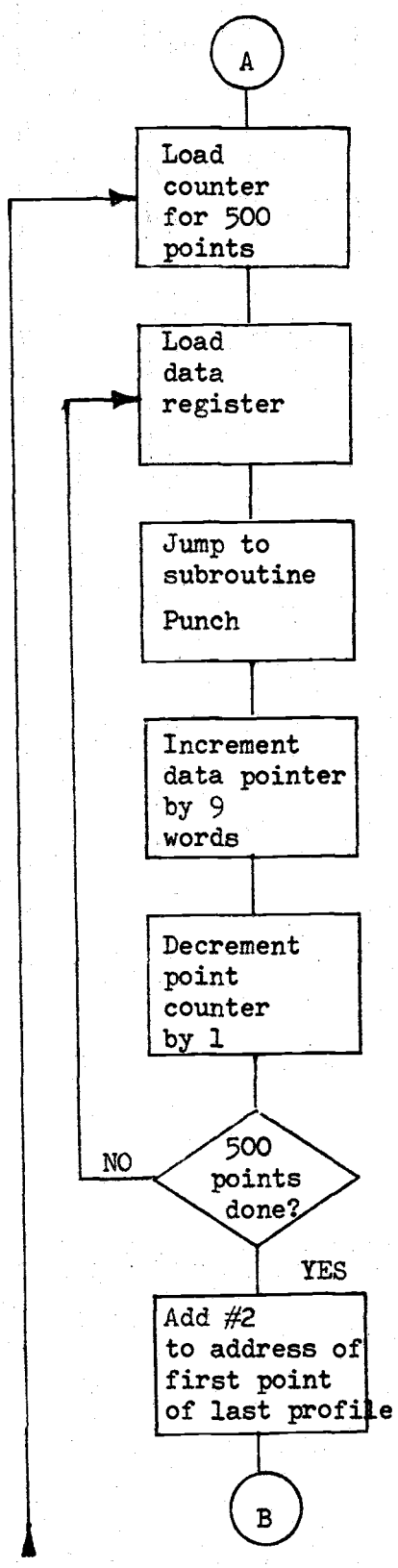
A
Load counter for 500 points
Load data register
Jump to subroutine Punch
Increment data pointer by 9 words
Decrement point counter by 1
NO
500 points done?
YES
Add #2 to address of first point of last profile
B

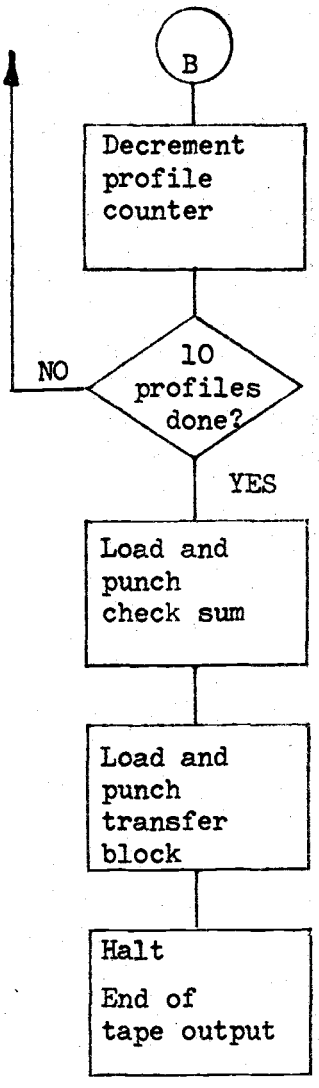
B
Decrement profile counter
NO
10 profiles done?
YES
Load and punch check sum
Load and punch transfer block
Halt
End of tape output

The clock interrupt service routine starts the lamp pulse and also starts A/D conversion. A subroutine loop is not used to take the 10 consecutive data points due to the slowness of such a loop. Considerable time is saved by using the sequential routines. The wait is a loop lasting 21 μseconds to give each A/D conversion time to come 98+% of its final value (normal A/D time is about 22 μseconds. Data taken before the A/D conversion is done.)

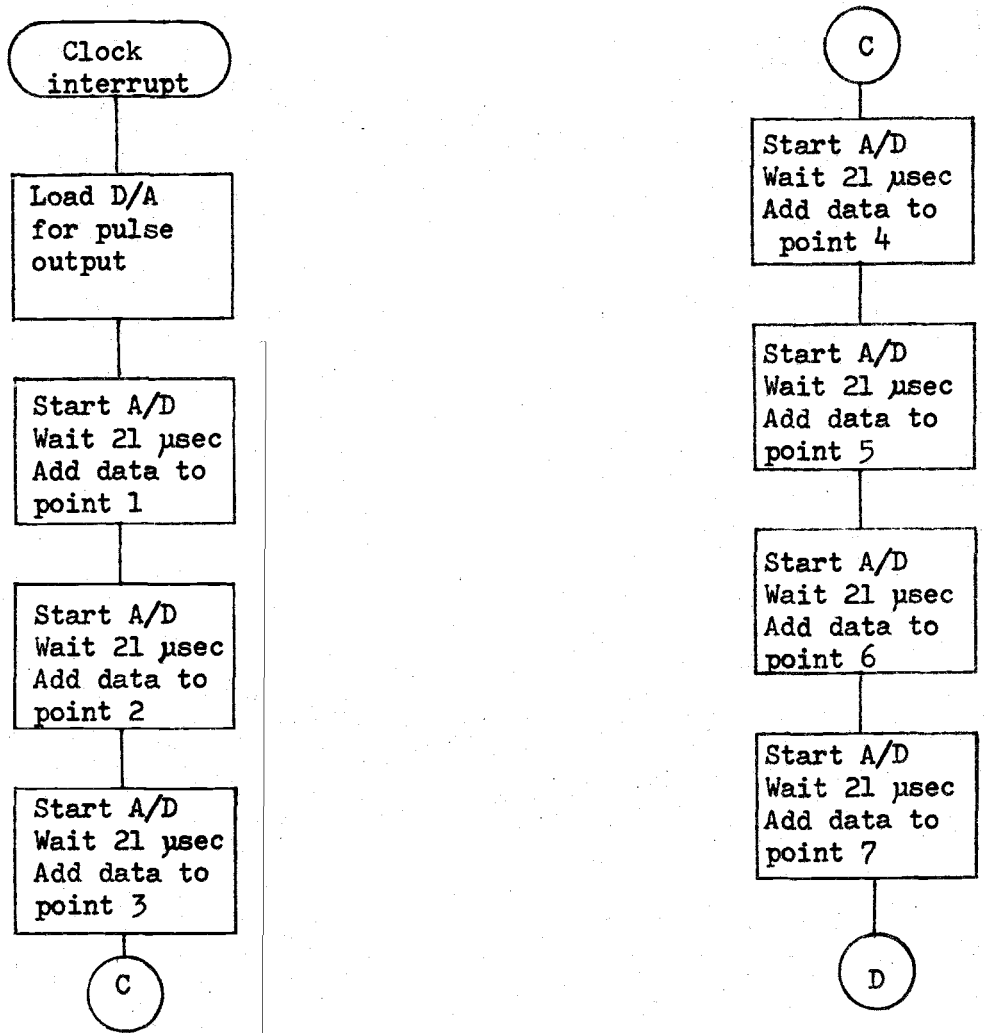

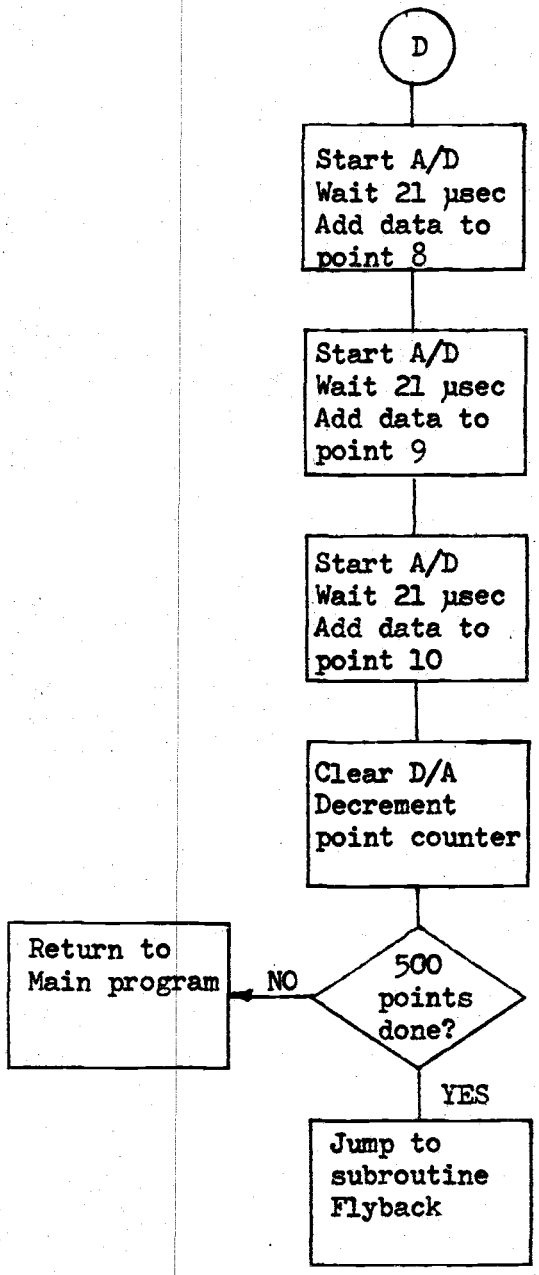
D
Start A/D
Wait 21 µsec
Add data to
point 8
Start A/D
Wait 21 µsec
Add data to
point 9
Start A/D
Wait 21 µsec
Add data to
point 10
Clear D/A
Decrement
point counter
500
points
done?
NO
Return to
Main program
YES
Jump to
subroutine
Flyback

Subroutine flyback is used to stop the clock and wait for the driving oscilloscope to finish its sweep and return to the triggerable ready state, and to count sweeps done and tell main program when 64 sweeps are done.

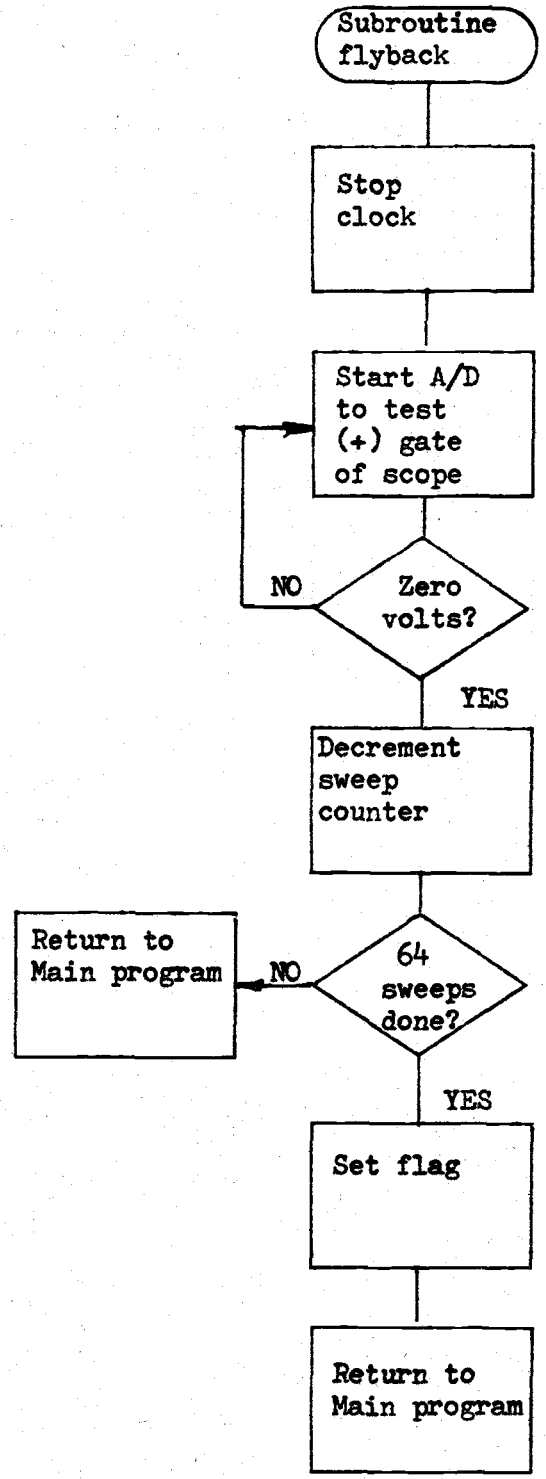

The punch subroutine is a short routine to take a binary integer in the data register and punch it out on paper tape.

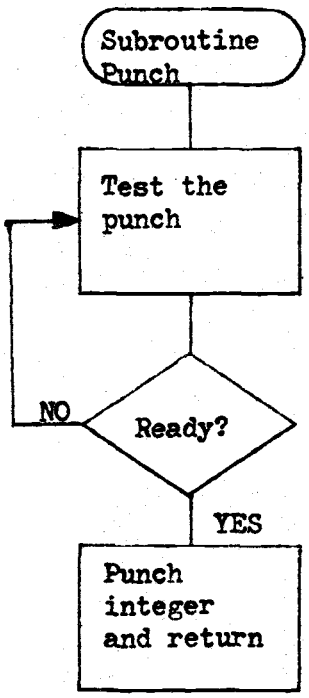

The Dummy subroutine is called in the A/D routine of the clock interrupt service routine and gives a variable delay time between each A/D conversion. The routine used is the shortest one possible and gives 21 useconds between each A/D conversion.

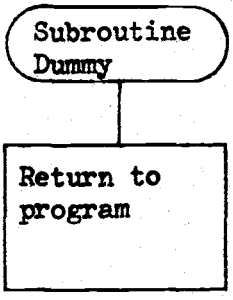

Appendix B

PAL 11-A Program for PDP 11/20

```
      RØ=%Ø
      R1=%1
      R2=%2
      R3=%3
      R4=%4
      R5=%5
      SP=%6
      PC=%7
      .=6ØØ
      MOV #6ØØ, SP
      MOV @#NSWP, SWEEP
      MOV #COLECT,@#1Ø4     ;LOAD CLK VECTOR
      MOV #34Ø, @#1Ø6      ;LOAD PSW
      MOV #2ØØØ, R1     ;LOC OF 1 ST DATA POINT
      MOV #5ØØØ., RØ
CLEAR:CLR (R1)+     ;CLEAR DATA LOCATIONS
      DEC RØ
      BNE CLEAR
INPUT:MOV #5ØØ., @#CNTR     ;START OF DATA INPUT
      MOV #2ØØØ, R1
      MOV #1ØØ., @#172542     ;1ØØ HZ PULSE RATE
      MOV #113, @#17254Ø     ;STRT CLK,INT MODE, 1ØR HZ
      MOV #176772, R2
      MOV #17677Ø, R3
      MOV #1Ø31, R4     ;A/D STRT CODE CHAN 2
PAUSE:TST R2     ;SET BY FLYBAK
      BEQ INPUT     ; DO ANOTHER SCAN
      TST R3
      BEQ DONE2     ;Ø IF ALL DONE, SET IN FLYBAK
      WAIT     ;FOR CLOCK INT
      JMP PAUSE     ;GO BACK AND WAIT FOR CLOCK
DONE2:HALT     ;CONVENIENCE HALT
      MOV #1, @#1772     ;START &NULL FRAMES
      MOV #1ØØØ6., @#1774     ;BYTE COUNT
      MOV #Ø, @#1776     ;START ADDRESS
      MOV #6, RØ
      MOV #1772, R2
START:MOVB (R2)+, R1     ;PUNCH OUT START BLOCK
      JSR PC, PUNCH
      ADD R1, @#CKSUM
      DEC RØ
      BNE START
      MOV #2ØØØ, R4     ;START ADD OF DATA
      MOV #1Ø, R3     ;TEN SETS OF DATA POINTS
DTAPE:MOV R4, R2     ;FOR TIME RES. INTERFERROGRAMS
      MOV #5ØØ., RØ     ;5ØØ POINTS PROFILE
```

```
POINT:MOVB (R2)+, R1      ;PUNCH IT
      JSR PC, PUNCH
      ADD R1, @#CKSUM
      MOVB (R2)+, R1
      JSR PC, PUNCH
      ADD R1, @#CKSUM
      ADD #18., R2
      DEC RØ
      BNE POINT
      ADD #2, R4      ;NEXT PROFILE
      DEC R3
      BNE DTAPE
      NEG @#CKSUM
      MOVB @#CKSUM, R1
      JSR PC, PUNCH
      MOV #1, @#2ØØØ+5ØØØ.+2     ;TRANSFER BLOCK
      MOV #6, @#2ØØØ+5ØØØ.+4     ;FOR END OF DATA TAPE
      MOV #Ø, @#2ØØØ+5ØØØ.+6     ;DATA IN BINARY INT FORM
      MOV #371, @#2ØØØ+5ØØØ.+1Ø
      MOV #8., RØ
      MOV #2ØØØ+5ØØØ.+2, R2
      MOVB (R2)+, R1
AGAIN:JSR PC, PUNCH
      DEC RØ
      BNE AGAIN-2
      HALT      ;END OF PROGRAM
COLECT:MOV #1777, @#176762    ;START OF INT ROUTINE
               ;START PULSE TO 114, 631,CHAN Y
   A1:MOV R4, (R3)      ;START A/D
      JSR PC, DUMMY      ;WAIT AROUND LOOP
      ADD (R2), (R1)+      ;TRANSFER DATA IN
   A2:MOV R4, (R3)      ;RESTART A/D
      JSR PC, DUMMY      ;DO IT ALL AGAIN
      ADD (R2), (R1)+
   A3:MOV R4, (R3)      ;AND AGAIN
      JSR PC, DUMMY
      ADD (R2), (R1)+
   A4:MOV R4, (R3)
      JSR PC, DUMMY
      ADD (R2), (R1)+
   A5:MOV R4, (R3)
      JSR PC, DUMMY
      ADD (R2), (R1)+
   A6:MOV R4, (R3)
      JSR PC, DUMMY
      ADD (R2), (R1)+
   A7:MOV R4, (R3)
      JSR PC, DUMMY
      ADD (R2), (R1)+
   A8:MOV R4, (R3)
```

```
        JSR PC, DUMMY
        ADD (R2), (R1)+
    A9:MOV R4, (R3)
        JSR PC, DUMMY
        ADD (R2), (R1)+
   A10:MOV R4, (R3)
        JSR PC, DUMMY
        ADD (R2), (R1)+
        CLR @#176762      ;CLEAR CHAN Y
        DEC @#CNTR       ;DONE 5ØØ YET?
        BNE RETURN       ;IF NOT DO IT SOME MORE
        JSR PC, FLYBAK      ;IF YES WAIT FOR DRIVE SCOPE
RETURN:RTI
FLYBAK:CLR @#172540      ;STOP CLOCK
 TEST1:MOV #1, @#176770      ;START A/D CHAN Ø
    B1:TSTB @#176770      ;DONE?
        BPL B1
        TST @#176772      ;FLYBACK DONE?
        BNE TEST1
        DEC @#SWEEP
        BEQ FINIS      ;ALL SWEEPS DONE?
        MOV #Ø, R2      ;IF NO START FROM THE TOP
        RTS PC
 FINIS:MOV #Ø, R3      ;IF YES TELL MAIN PROGRAM
        RTS PC      ;TO COOL IT!
 PLOTR:MOV #PLOT, @#1Ø4      ;START PLOT HERE, LOAD NEW CLK VECTOR
        MOV #5ØØ., @#172542      ;OUTPUT AT Ø.Ø5 SEC INTERVALS
        MOV #113, @#172540
        MOV #2ØØØ, R4
        CLR @#176762      ;CLEAR CHAN Y TO Ø RECORDER
        CLR @#176760      ;CLEAR CHAN X ON RECORDER
        MOV #1Ø., R3      ;1Ø PROFILES AGAIN
 PPLOT:MOV R4, CNTR
        MOV #5ØØ., RØ
AGAIN1:MOV @CNTR, R2
        MOV #5, R1
AGAIN2:ROR R2
        DEC R1
        BNE AGAIN2
        BIC #174ØØØ, R2
        MOV R2, R5
        WAIT
        ADD #2Ø., @#CNTR
        DEC RØ
        BNE AGAIN1
        ADD #2, R4
        HALT      ;SCAN OUTED; LIFT PEN & PRESS CONT
        CLR @#176760
        CLR @#176762
        HALT      ;LOWER PEN & PRESS CONT
```

```
      DEC R3      ;ALL PROFILES OUTED?
      BNE PPLOT
      CLR @#172540
      HALT      ;ENTIRE THING DONE !!!!!!!!!!
 PLOT:MOV R5, @#176762      ;NOTE ! PLOTS OUTED ON CHANNEL Y
      ADD #4, @#176760      ;INC CHAN X FOR TIME AXIS
      RTI      ;DON'T BLOW IT !
PUNCH:TSTB @#177554
      BPL PUNCH
      MOVB R1, @#177556
      RTS PC
DUMMY:RTS PC      ;THIS GIVES 20 US PER A/D CONV.
      CNTR:0
      CDOUT:0
      DPNT:0
      CKSUM:0
      SWEEP:0
      NSWP:64.
     .END
```